Muropeptide recycling in *Bacillus subtilis*: β-*N*-acetylglucosaminidase NagZ operates by a unique Asp-His catalytic dyad mechanism

DISSERTATION

Zur Erlangung des akademischen Grades des
Doktors der Naturwissenschaften
(Dr. rer. nat.)
an der Universität Konstanz
Fachbereich Biologie

vorgelegt von
Dipl. Biol. Silke Litzinger

September 2009
Konstanz

Tag der mündlichen Prüfung: 06.11.2009

Referenten: Prof. Dr. Winfried Boos, Universität Konstanz
Prof. Dr. Iwona Adamska, Universität Konstanz

“In all science error precedes the truth,
but it is better it should go first than last.”
Horace Walpole (1717-97)

„Irrtümer haben ihren Wert;
jedoch nur hie und da.
Nicht jeder, der nach Indien fährt,
entdeckt Amerika.“
Erich Kästner (1899-1974)

Dedicated to my parents

TABLE OF CONTENTS

ZUSAMMENFASSUNG

Die meisten Bakterien sind von einem rigiden Exoskelett, dem Murein Sacculus, umhüllt; dies ermöglicht den Zellen dem intrazellulären osmotischen Druck (Turgor) standzuhalten und die Zellform aufrecht zu halten. Das Murein (Peptidoglykan) ist ein Heteropolymer bestehend aus Glykansträngen, die über kurze Peptidketten quervernetzt sind. Während des Wachstums der Bakterien wird der Murein Sacculus kontinuierlich von zelleigenen lytischen Enzymen (Autolysinen) abgebaut um die Insertion von neuem Peptidoglykan zu gewährleisten. Wir haben einen Abbauweg in *Bacillus subtilis* identifiziert, über den *N*-Acetylglukosamin-*N*-Acetylmuramisäure-Peptide (Muropeptide), freigesetzt aus dem Peptidoglykan während des Wachstums, regeneriert werden. Dieser Abbauweg beinhaltet Orthologe zu Enzymen des Stoffwechsels von MurNAc sowie des Recyclings von Murein in *E. coli*: die MurNAc-6-Phosphat Etherase (MurQ), den MurNAc-6-Phosphat-spezifischen transkriptionellen Repressor (MurR) und das MurNAc-spezifische Phosphotransferase-System (MurP).

In dieser Arbeit wurden zwei weitere Enzyme untersucht, deren Gene mit den Genen der oben genannten Enzyme in einem möglichen Operon organisiert sind. Es wurde gezeigt, dass das erste Gen, *nagZ* (früher *ybbD*), für eine β-*N*-Acetylglukosaminidase kodiert, die in den frühen 70er Jahren beschrieben wurde, jedoch konnte ihr zu jenem Zeitpunkt noch kein Gen zugeordnet werden. Wir haben anhand von fluorophore-assisted carbohydrate electrophoresis (FACE) und reversed-phase high performance liquid chromatography (RP-HPLC) gezeigt, dass NagZ das endständige nicht-reduzierende *N*-Acetylglukosamin (GlcNAc) aus Muropeptiden freisetzt. Weiterhin hydrolysiert es die glykosidische Bindung des chromogenen Substrates 4-nitrophenyl-β-*N*-acetyl-D-glucosaminide (pNP-β-GlcNAc) sowie des fluorogenen Substrates 4-methylumbelliferyl-β-*N*-acetyl-D-glucosaminide (4-Mu-β-GlcNAc). K_M Werte von jeweils 172 und 110 µM sowie k_{cat} Werte von jeweils 9.9 und 6,4 s^{-1} für pNP-β-GlcNAc und 4-Mu-β-GlcNAc wurden bestimmt. Das pH-Optimum liegt in einem Bereich von 5,8 bis 6,2. NagZ wird sekretiert, ist nicht-kovalent an die Zellwand gebunden und kann von partikulärem Material durch hohe Salzkonzentrationen freigesetzt werden. NagZ wird in der späten exponentiellen Wachstumsphase exprimiert und erreicht eine 6-fach höhere Aktivität in der stationären bzw. Autolyse-Phase und ist zudem die wichtigste exo-β-*N*-Acetylglukosaminidase von *B. subtilis*. Das zweite Enzym, AmiE, wird ebenfalls sekretiert und wurde als neue Amidase identifiziert, die die *N*-Acetylmuramyl-L-Alanin Bindung von

MurNAc-Peptiden spaltet, nicht aber von Muropeptiden. Daher benötigt das Enzym die Aktivität von NagZ, so dass MurNAc von Muropeptiden durch sequentielle Hydrolyse beider Enzyme gemeinsam freigesetzt wird.

Der in dieser Arbeit beschriebene Muropeptidabbauweg ist der erste Hinweis auf ein Murein-Recycling in *B. subtilis*, das im Gegensatz zu *E. coli* im Zellwandkompartiment stattfindet. Ein Modell bezüglich des Recyclings in *B. subtilis* lässt sich aus den Ergebnissen dieser Arbeit folgendermaßen darstellen: GlcNAc-MurNAc-Peptid Turnover Produkte werden durch NagZ im Periplasma gespalten. GlcNAc wird über das spezifische Phosphotransferase-System NagE ins Zytoplasma transportiert und weiter verstoffwechselt. Die Peptide werden von MurNAc durch AmiE abgespalten und durch eine unbekannte Permease ins Zytoplasma aufgenommen. MurNAc wird über Phosphotransferase-System MurP ins Zytoplasma transportiert und gleichzeitig phosphoryliert. Das so entstandene MurNAc-6-P wird anschließend durch die Etherase MurQ zu GlcNAc-6-P umgesetzt.

Die β-*N*-Acetylglukosaminidase NagZ aus *B. subtilis* gehört zur Familie 3 der Glykosid-Hydrolasen. Die Familie 3 der Glykosid-Hydrolasen besteht hauptsächlich aus β-Glukosidasen und exo-Glukanasen, die die Hydrolyse der glykosidischen Bindung ihrer Substrate unter Retention ihrer anomerischen Konfiguration durch einen Zwei-Stufen-Mechanismus katalysieren. Im Allgemeinen besitzen Glykosidasen, die unter Retention arbeiten, im aktiven Zentrum je zwei Carboxyl-Gruppen, die als Nukleophil und Säure/Base-Katalysator fungieren. Das katalytische Nukleophil, ein Aspartat, ist innerhalb aller Familie-3-Glykosidasen konserviert, während der allgemeine Säure/Base-Katalysator, ein Glutamat, nur für die β-Glukosidasen identifiziert wurde, nicht aber in den β-*N*-Acetylglukosaminidasen. Die β-*N*-Acetylglukosaminidasen bilden eine Untergruppe innerhalb dieser Familie, die durch das konservierte D-(ST)-H-Motiv charakterisiert ist.

In dieser Arbeit wurde die erste Struktur einer β-*N*-Acetylglukosaminidase mit zwei Domänen der Familie-3-Glykosidasen, NagZ, gelöst. Die Struktur wurde sowohl mit als auch ohne gebundenen Übergangszustand-Inhibitor PUGNAc (*O*-(2-Acetamido-2-deoxy-D-glucopyranosylidene) amino-*N*-phenylcarbamate) im aktiven Zentrum mit einer Auflösung von jeweils 1,7 und 1,4 Å gelöst. Die Struktur zeigte eine *N*-terminale $(\alpha/\beta)_8$-TIM-Barrel- und eine *C*-terminale αβα-Sandwich-Domäne. Die Struktur und kinetische Analysen zeigten, dass eine Asp-His-Diade in der Hydrolyse *O*-glykosidischer Bindungen involviert ist. Mutationen dieser Reste bestätigten, dass His234 der Diade als Säure/Base-Katalysator fungiert, der durch Asp232 koordiniert wird. Der Austausch des Restes His234 oder Asp232 durch Glycin

reduzierte die Geschwindigkeit der Hydrolyse des fluorogenen Substrates 4-Mu-β-GlcNAc und beeinträchtigte das pH-Aktivitätsprofil übereinstimmend mit der Rolle als Säure/Base-Katalysator. Darüberhinaus akkumulierte das Glykosyl-Enzym-Zwischenprodukt in der His234Gly Mutante. Die Asp-His-Diade ist in allen β-*N*-Acetylglukosaminidasen konserviert, während in den β-Glukosidasen anstelle der Diade ein konservierter Glutamat-Rest lokalisiert ist, der von der zweiten Domäne in das aktive Zentrum ragt. Die Funktion der *C*-terminalen αβα-Sandwich Domäne in NagZ konnte nicht geklärt werden. NagZ von *B. subtilis* ist das erste Enzym, bei dem eine Asp-His-Diade an der Hydrolyse *O*-glykosidischer Bindungen beteiligt ist und zudem der katalytischen Asp-His-Ser-Triade von Serinproteasen ähnelt.

SUMMARY

Nearly all bacteria are surrounded by a rigid bag-shaped exoskeleton, the murein sacculus, which protects the cells from rupture by osmotic pressure and maintains the cell's characteristic shape. The murein (peptidoglycan) is a heteropolymer made up of glycan strands that are cross-linked by short peptides. During growth of the bacteria the existing murein is continuously degraded by specific lytic enzymes (autolysins) to enable the insertion of new peptidoglycan. We identified a pathway in *B. subtilis* which recovers the *N*-acetylglucosamine-*N*-acetylmuramic acid-peptides (muropeptides) derived from the peptidoglycan during growth. This pathway involves orthologs of enzymes involved in MurNAc dissimilation and murein recycling in *E. coli*: the MurNAc-6-phosphate etherase (MurQ), the MurNAc-6-phosphate-specific transcriptional repressor (MurR) and the MurNAc-specific phosphotransferase system (MurP).

In this thesis two further enzymes of this pathway were investigated whose genes are organized in a putative operon along with genes encoding the above mentioned enzymes. The first gene, *nagZ* (formerly *ybbD*), was shown to encode a β-*N*-acetylglucosaminidase that is identical to an enzyme which was described in the early 1970s, but the corresponding gene was not identified at that time. We showed that the enzyme hydrolyzes the terminal non-reducing *N*-acetylglucosamine (GlcNAc) of muropeptides as analyzed by fluorophore-assisted carbohydrate electrophoresis (FACE) and reversed-phase high performance liquid chromatography (RP-HPLC). It also hydrolyzes the glycosidic bond of the chromogenic substrate 4-nitrophenyl-β-*N*-acetyl-β-D-glucosaminide (pNP-β-GlcNAc) and the fluorogenic substrate 4-methylumbelliferyl-β-*N*-acetyl-D-glucosaminide (4-Mu-β-GlcNAc). K_M values of 172 and 110 μM and k_{cat} values of 9.9 and 6.4 s^{-1} for pNP-β-GlcNAc and 4-Mu-β-GlcNAc, respectively, were determined. The optimum pH ranges between pH 5.8 and 6.2. NagZ is secreted and non-covalently bound to the cell wall and can be released from particulate material by high concentrations of salt. NagZ is expressed in the late exponential growth phase and reaches 6-fold higher activity in the stationary or autolysis phase and beside that it is the major exo-β-*N*-acetylglucosaminidase of *B. subtilis*. The second enzyme, AmiE, is also secreted and was identified as a novel amidase that hydrolyzes the *N*-acetylmuramyl-L-alanine bond of MurNAc-peptides but not of muropeptides. Therefore the enzyme requires the activity of NagZ and together the enzymes liberate MurNAc from muropeptides by sequential hydrolysis.

The muropeptide catabolic pathway presented in this thesis is the first evidence for murein recycling in *B. subtilis* which proceeds distinct from *E. coli* in the cell wall compartment. Including the results presented in this thesis the following model of recycling in *B. subtilis* could be generated: GlcNAc-MurNAc-peptide turnover products are cleaved by NagZ in the periplasm. GlcNAc is imported into the cytoplasm by the specific phosphotransferase system NagE and further metabolized. The peptides are released from MurNAc by AmiE and are imported into the cytoplasm by an unknown permease. MurNAc is phosphorylated and imported into the cytoplasm by phosphotransferase system MurP and the product MurNAc-6-P is converted to GlcNAc-6-P by MurQ.

The β-*N*-acetylglucosaminidase NagZ of *B. subtilis* belongs to family 3 of glycoside hydrolases. Family 3 of glycoside hydrolases primarily consists of β-glucosidases and exo-glucanases which catalyze the hydrolysis of the glycosidic linkages of their substrates via a two-step double-displacement mechanism under retention of their anomeric configuration. In general retaining glycosidases harbour two carboxyl groups in the active site functioning as nucleophile and general acid/base catalyst. The catalytic nucleophile, an aspartate, is conserved within all family 3 glycosidases, whereas the general acid/base catalyst, a glutamate, was only identified for the β-glucosidases, but is absent in the β-*N*-acetylglucosaminidases. The β-*N*-acetylglucosaminidases generate a sub-group within this family and are characterized by the conserved D-(ST)-H motif.

In this thesis the first three-dimensional structure of a two domain β-*N*-acetylglucosaminidase of family 3 glycosidases, NagZ, was determined with and without the transition state inhibitor *O*-(2-Acetamido-2-deoxy-d-glucopyranosylidene) amino-*N*-phenylcarbamate (PUGNAc) bound to the active site with a resolution of 1.7 and 1.4 Å, respectively. The structure revealed an *N*-terminal $(\alpha/\beta)_8$-TIM-barrel and a *C*-terminal αβα-sandwich domain. From the structure and kinetic analyses an Asp-His dyad was shown to be involved in hydrolysis of *O*-glycosidic linkages. Mutational studies further confirmed that His234 of the dyad functions as general acid/base catalyst and is coordinated by Asp232. Replacement of the residues His234 or Asp232 with glycine reduced the rate of hydrolysis of the fluorogenic substrate 4-Mu-β-GlcNAc and affected the pH activity profile consistent with the role as acid/base catalyst. Furthermore the glycosyl-enzyme intermediate accumulated in the His234Gly mutant. The Asp-His dyad is conserved in all β-*N*-acetylglucosaminidases, whereas in β-glucosidases a conserved glutamate is located at the position of the dyad and protrudes from the second domain into the active site. The function of the *C*-terminal αβα-sandwich domain in NagZ could not yet be identified. NagZ of *B. subtilis* is the first enzyme in which an Asp-His dyad is involved in hydrolysis of *O*-glycosidic bonds resembling the catalytic Asp-His-Ser triad of serine proteases.

GENERAL INTRODUCTION

The cell wall of Gram-positive and Gram-negative bacteria

The architecture of the cell wall of bacteria was first visualized by electron microscopy and later, in the mid-1950s, by transmission electron microscopy (TEM) (Beveridge, 2006) showing fundamental differences between Gram-positive and Gram-negative bacteria. Whereas Gram-negative bacteria possess an inner and an outer membrane encompassing the thin murein sacculus (also known as peptidoglycan) within the periplasmic space, Gram-positive bacteria do not contain an outer membrane and are only surrounded by a thick murein layer covering the cytoplasmic membrane (Fig. 1). In both cases the murein is the stabilizing macromolecular component of the cell wall that is missing in only very few bacterial groups such as mycoplasma (mollicutes) and planctomycetes. It constitutes a single macromolecule that encases the entire cell (Koch, 2006; Seltmann and Holst, 2002). Bacteria developed this exoskeleton-like structure to withstand the increasing turgor that is caused by accumulation of high concentrations of nutrients inside the cell and can reach 2 to 5 atmospheres in Gram-negative and up to 50 atmospheres in Gram-positive bacteria (Archibald et al., 1993; Seltmann and Holst, 2002). The murein sacculus stabilizes the fragile cytoplasmic membrane and the cytoplasm within, protects the cells from the changing conditions of the environment and moreover determines the cells characteristic shape. The murein sacculi can be isolated in their intact shape reflecting the length and diameter of a cell.

In Gram-negative bacteria the murein sacculus represents only approximately 2% of the whole cell mass with 75 to 80% being monolayered and the rest being triple-layered in *Escherichia coli* (Labischinski et al., 1991). Moreover in *E. coli* the murein is attached to the outer membrane via lipoprotein (Lpp; Braun's lipoprotein) which is covalently linked to the peptidoglycan by a peptide bond between the ε-amino group of its *C*-terminal lysine and the L-carboxyl group of *meso*-diaminopimelic acid (*m*-DAP) in the murein peptide (Braun, 1975). Gram-positive bacteria like *Bacillus subtilis*, which lack an outer membrane, are surrounded by a peptidoglycan layer 10- to 20-fold thicker compared to Gram-negative bacteria representing 20 to 70% of the cells' dry weight (Archibald et al., 1993; Foster and Popham, 2002; Rogers et al., 1974; Shockman and Barrett, 1983).

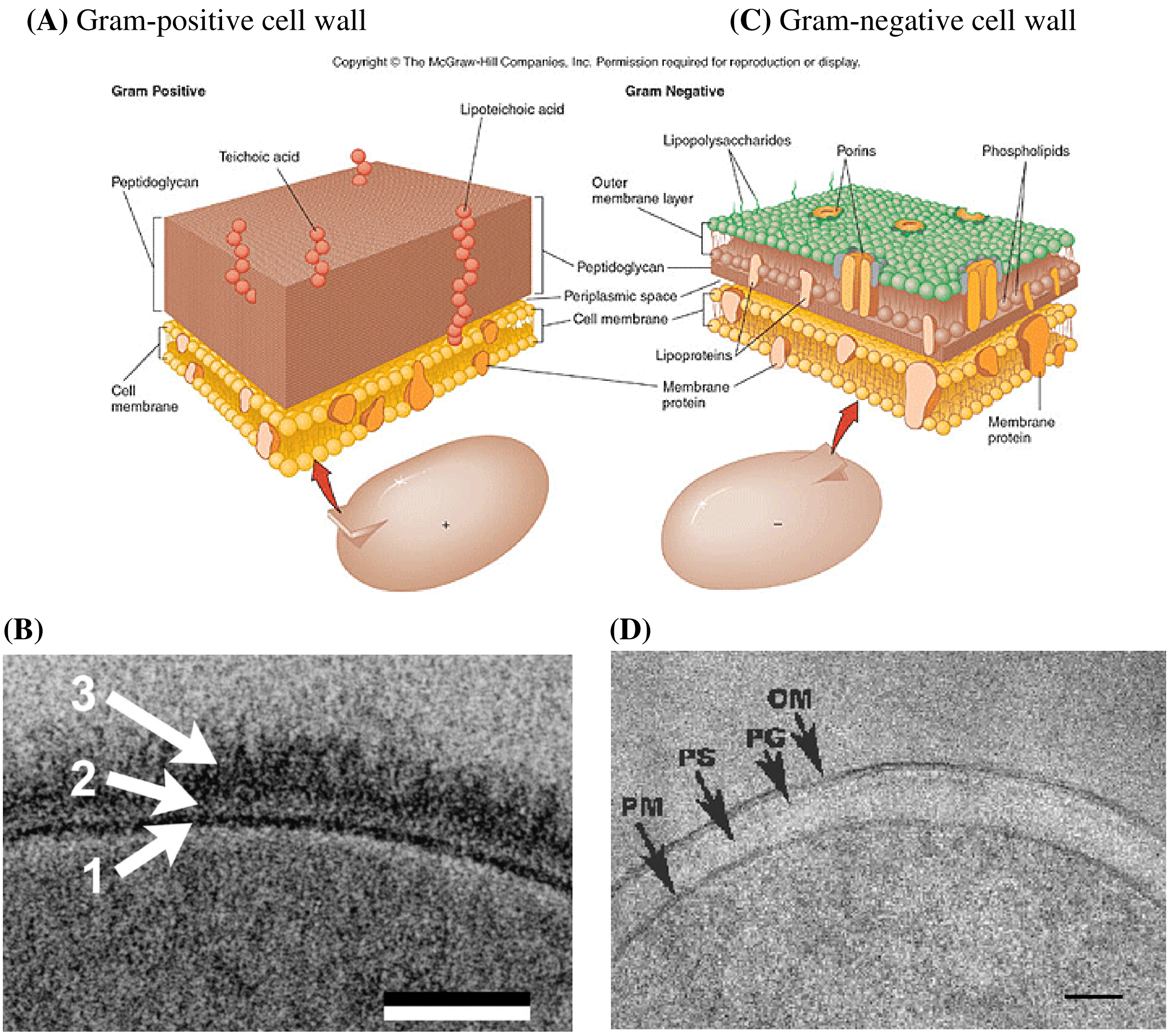

(A) Gram-positive cell wall

(C) Gram-negative cell wall

(B)

(D)

Figure 1: Overview of the cell wall of Gram-positive and Gram-negative bacteria. **(A)** Gram-positive bacteria lack an outer membrane and are surrounded by a 10 to 20 layer thick murein sacculus. (**B)** The murein sacculus of *B. subtilis* reveals three regions of peptidoglycan as visualized by electron microccopy (EM) of thin sections of freeze-substituted cells. The innermost region (1) consists of unstressed peptidoglycan, the region above (2) is greatly stressed and the outermost region (3) is subject to autolysins that degrade the older peptidoglycan. (**C/D)** By contrast Gram-negative bacteria possess an inner plasma membrane (PM) and an outer membrane (OM) flanking the monolayered peptidoglycan (PG) within the periplasm (PS). Scale bar, 50 nm. Figure A and C were taken from the homepage: http://water.me.vccs.edu/courses/ENV108/Lesson5_print.htm. Figure B and D were taken from Beveridge, 2006.

Additionally the cell wall of Gram-positive bacteria contains anionic polymers, such as teichoic, teichuronic and lipoteichoic acids (Foster and Popham, 2002; Navarre and Schneewind, 1999). Under non-phosphate-limiting conditions, the predominant teichoic acid types are poly-glycerol-phosphate (GroP) in *B. subtilis* strain 168 and poly-ribitol-phosphate (RboP) in strain W23 (Fig. 2) (Bhavsar et al., 2004). The teichoic main chain contains approximately 40 repeating phosphate units that are linked C1 to C3. The hydroxyl group on C2 is often substituted by a glucose or a D-alanine residue. A linkage unit connects the main chain to the peptidoglycan. It consists of one to three glycerol-phosphate (GroP) residues and the disaccharide *N*-acetylmannosamine-β-1,4-*N*-acetylglucosamine-1-phosphate which links the peptidoglycan to an *N*-acetylmuramic acid residue (Araki and Ito, 1989; Foster and Popham, 2002; Yokoyama et al., 1986).

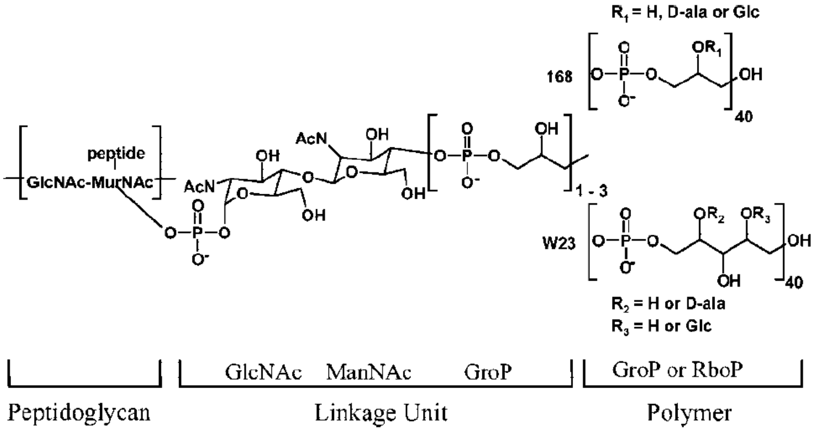

Figure 2: Chemical structure of the two types of teichoic acid in *B. subtilis*. Strain 168 contains poly-glycerol-phosphate (GroP), whereas strain W-23 contains poly-ribitol-phosphate (RboP). The peptidoglycan linkage unit consists of one to three glycerol-phosphate monomers and the disaccharide ManNAc-β-1,4-GlcNAc, which is 1,6-phosphodiester linked to MurNAc within the glycan strands of the murein sacculus. Hydroxyl groups on the main chain are often glucosylated or D-alanylated. Gro-P, glycerol-phosphate; RboP, ribitol-phosphate; GlcNAc, *N*-acetylglucosamine; ManNAc, *N*-acetylmannosamine; Glc, glucose; MurNAc, *N*-acetylmuramic acid. The figure was taken from Bhavsar *et al.*, 2004.

Under phosphate-limiting conditions, teichuronic acids predominate in the peptidoglycan of *B. subtilis*. Teichuronic acid is a phosphate-free carbohydrate polymer containing glucuronic acid and *N*-acetylgalactosamine and is attached directly to a muramic residue of the peptidoglycan via a phosphodiester bond (Wright and Heckels, 1975). *B. subtilis* also contains lipoteichoic acid (LTA), which is a polymer of glycerol-phosphate 24 to 33 units long, anchored to the cytoplasmic membrane via a 3-gentiobiosyl diglyceride and extends through the peptidoglycan. 40 to 60% of the glycerol-phosphates are substituted with glucosyl or *N*-acetylglucosamine residues. The remaining glycerol-phosphates carry D-alanine substitutions (Foster and Popham, 2002).

The chemical composition of the murein sacculus is very similar in bacteria. Therefore the peptidoglycan structure and pathways of the rod-shaped model organisms *E. coli* (Gram-negative) as well as *B. subtilis* (Gram-positive) presented in this thesis are representative for all bacteria.

Murein is made up of linear glycan strands interlinked by short peptides and hence it is also called peptidoglycan (Fig. 3). The glycan strands consist of alternating units of *N*-acetylglucosamine (GlcNAc) and its 3-*O*-lactyl ether derivative *N*-acetylmuramic acid (MurNAc; 2-amino-3-*O*-[(R)-1-carboxyethyl]-D-glucopyranose) linked by β-1,4-glycosidic bonds (Fig. 3). In *E. coli* all glycan strands terminate with GlcNAc at the non-reducing end and 1,6-anhydromuramic acid (anhMurNAc) at the formally reducing end (Höltje et al., 1975). In *B. subtilis* glycan strands generally have *N*-acetylmuramic acid (MurNAc) at the reducing terminus, but anhMurNAc was also found as chain terminator (Atrih et al., 1999b). Furthermore mature glycan strands of *B. subtilis* also can have MurNAc aside from GlcNAc at the non-reducing terminus (Atrih et al., 1999a). The length-distributions of the glycan strands can vary to some extent. An average length of 21 disaccharide units was found for *E. coli* murein (Vollmer and Höltje, 2004), whereas the length was estimated to range from 54 to 96 disaccharide units in the murein of *B. subtilis* (Ward, 1973). In contrast, recently, Hayhurst *et al.* isolated glycan strands from *B. subtilis* murein with a length of up to 5 µm which is equal to 5000 disaccharide units and determined an average length of approximately 1.3 µm which corresponds to glycans of 1300 disaccharids (Hayhurst et al., 2008).

The glycan strands show only few variations among different bacteria such as *O*-acetylation (at C6 of MurNAc) and *N*-de-acetylation (of GlcNAc as well as MurNAc) which are absent in *E. coli*. *B. subtilis* lacks *O*-acetylation of the murein, but contains *N*-de-acetylated amino sugars. Two *B. subtilis* laboratory strains (W23 and 168) differ in the degree of *N*-de-acetylation (Vollmer, 2008). In *B. subtilis* W23 only the GlcNAc residues (16%) are de-acetylated, whereas in *B. subtilis* 168 GlcNAc as well as MurNAc are partially de-acetylated (19% and 33%, respectively).

Short peptides are attached by a D,L-amide bond to the carboxyl group of the D-lactyl residue of MurNAc and contain unusual non-codogenic D-amino acids (D-Glu, D-Ala) besides L-amino acids (L-Ala) and the di-basic amino acid (*meso*-diaminopimelic acid, *m*-DAP). In *E. coli* and *B. subtilis* the stem peptides that are attached to the carboxyl group of MurNAc usually consist of L-alanine-γ-D-glutamate-(L)-***meso*-diaminopimelic acid**-D-alanine-(D-alanine) (L-Ala-γ-D-Glu-***m*-DAP**-D-Ala-(D-Ala)). The fifth amino acid, D-Ala, is used to perform the transpeptidase reaction cross-linking the stem-peptides (described in “Peptidoglycan biosynthesis”).

The composition of the stem peptides varies significantly in bacteria; in particular, the third position of the di-basic amino acid (Quintela et al., 1995; Schleifer and Kandler, 1972; Vollmer, 2008; Vollmer et al., 2008). The di-basic amino acid *m*-DAP (an intermediate of the biosynthetic pathway leading to lysine) is present in Gram-negative bacteria and some Bacilli, but substituted by L-lysine (L-Lys) in most Gram-positive bacteria or L-ornithine (L-Orn) in Spirochetes, *Bifidobacterium globosum* and *Thermus thermophilus* (Vollmer et al., 2008). In *B. subtilis* about 99% of the *m*-DAP are amidated on at least one free carboxylic group (Foster and Popham, 2002).

Neighbouring glycan strands within the murein are connected by the peptide side chains which are interlinked by the amino group of the di-basic amino acid of one peptide chain and the carboxyl group of another peptide chain to form a net-like structure. In *E. coli* and *B. subtilis* the cross-links are mainly from the D,D-type formed between the ε-amino group at the D-center of *m*-DAP at position 3 of one peptide and the carbonyl amide group of D-Ala at position 4 of a neighbouring glycan strand (Glauner et al., 1988). A small extent of L,D-cross-links also exists between the L-center of *m*-DAP of one peptide and the D-center of *m*-DAP of another peptide. Besides the dimeric peptide cross-links a lower number of trimeric and tetrameric structures containing three or four cross-links occur (Glauner et al., 1988). Depending on the strain and growth conditions, 40 to 60% and 56 to 63% of the peptides in *E. coli* and *B. subtilis*, respectively, cross-link neighbouring glycan strands to form a net-like structure (Atrih et al., 1999a; Glauner et al., 1988).

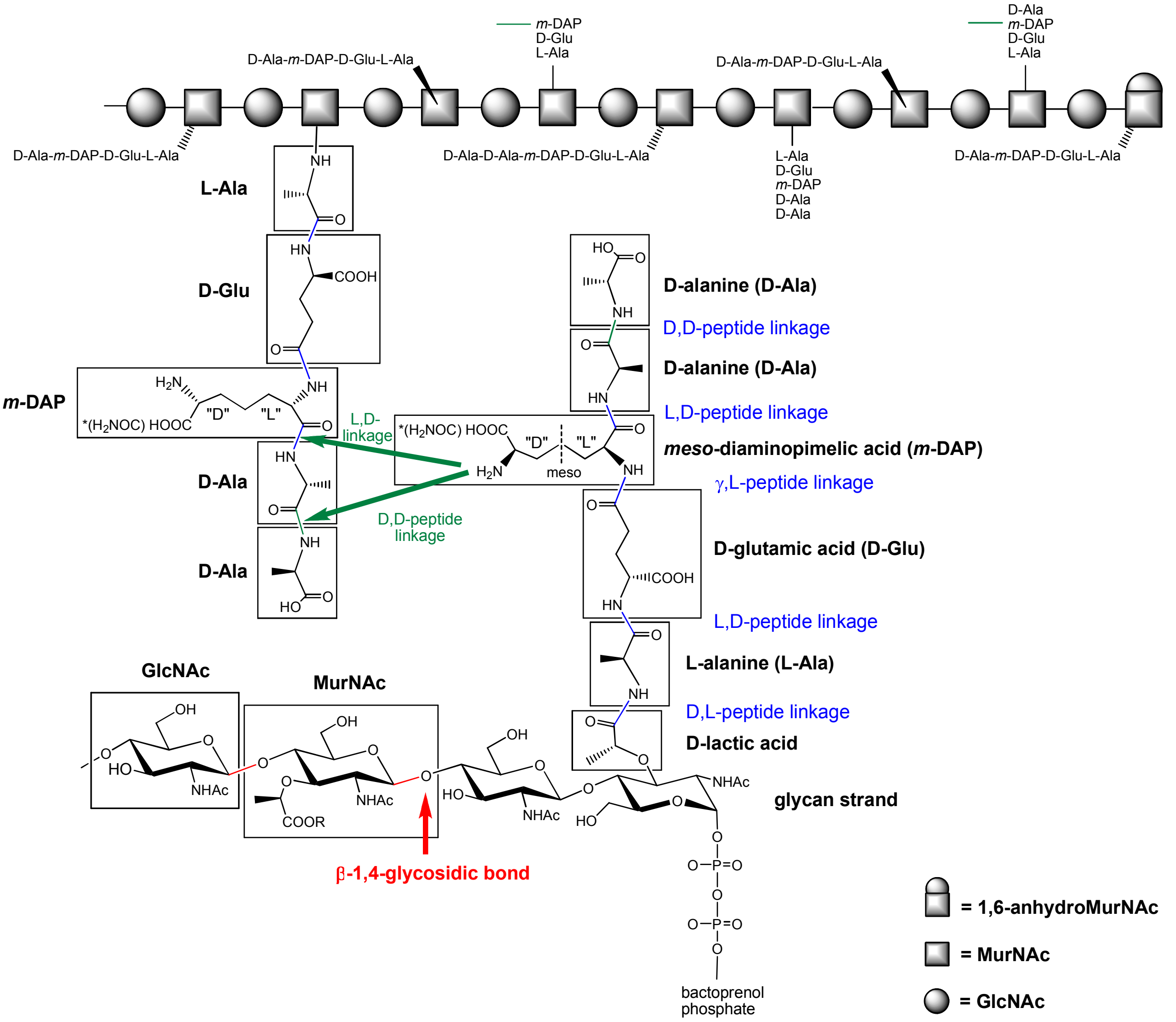

Figure 3: Peptidoglycan structure of the model organisms *E. coli* and *B. subtilis*. The amino sugars *N*-acetylglucosamine (GlcNAc) and *N*-acetylmuramic acid (MurNAc) are connected by β-1,4-glycosidic bonds. The peptides are connected via a D,L-amide bond to the ether-linked D-lactic acid substituent of MurNAc. Neighbouring glycan strands are mainly connected via a D,D-peptide cross-link between the amino group at the D-center of *m*-DAP and the carbonyl amide group of the fourth amino acid (D-Ala). In addition, a small number of L,D-cross-links between two *m*-DAP residues is present. In *B. subtilis* about 99% of the D-carboxylate of *m*-DAP are amidated *($CONH_2$) and the amino sugars are partially *N*-de-acetylated. GlcNAc, *N*-acetylglucosamine; MurNAc, *N*-acetylmuramic acid; 1,6-anhydroMurNAc, MurNAc with an intramolecular 1,6-glycosidic bond terminating the reducing end of a glycan strand in *E. coli*. For definition of the used symbols see figure insert.

The murein sacculus is quite elastic and can reversibly expand and shrink dependent on the cell's turgor (Ghuysen, 1968; Höltje, 1998). This phenomenon is mediated mainly by the flexibility of the peptide part due to its alternating D-L-D-L-sequence (beginning with the D-lactyl group of MurNAc and including the L-center of *m*-DAP) which prevents the formation of α-helical structures (Barnickel et al., 1979), whereas the glycan strands are rather rigid (Labischinski et al., 1979). It has been estimated that the elasticity and thus the surface area of the murein sacculus can reversibly increase threefold without rupture (Koch and Woeste, 1992). In contrast to the cell wall polysaccharides of plants (cellulose) and arthropods (chitin) the glycan strands within the murein are α-helically twisted due to the presence of the bulky lactyl group at MurNAc allowing less rotation. Presumably four disaccharide units generate one turn with the stem peptides protruding in all four directions in space (Labischinski et al., 1985; Leps et al., 1987; Meroueh et al., 2006). A recent NMR structure of a small muropeptide suggests a threefold symmetry (Kern et al., 2008). The three-dimensional arrangement of the glycan strands is still unknown due to the lack of a suitable method to determine its structure. Two different models of the arrangement of the glycan strands exist. In the classical "horizontal model" it is presumed that the glycan strands in the murein layer are arranged parallel to the cell membrane along the short axis with the peptides running in the direction of the long axis of the murein sacculus (Fig. 4, 5A) (Vollmer and Höltje, 2001; Weidel and Pelzer, 1964). Every second stem peptide is thought to be cross-linked to the neighbouring glycan strands thereby generating in stress-bearing murein hexagonal pores like a honeycomb (so-called tessera), the smallest formed by two glycan strands and two peptide cross-links (Fig. 4) (Demchick and Koch, 1996; Koch, 1998).

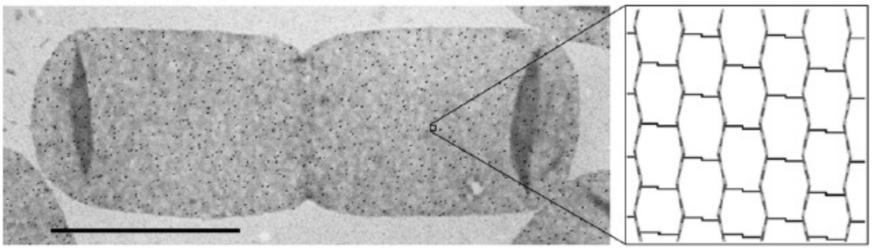

Figure 4: Electron micrograph of a murein sacculus of a dividing *E. coli* cell (left side). Scale bar, 1µm. The right side shows the "horizontal-model" of the murein layer of approximately 30 x 30 nm. The glycan strands (zigzag lines) are arranged perpendicular to the long axis, whereas the peptides (thin lines) are running in the direction of the long axis of the murein sacculus. The smallest hexagonal unit is formed by two glycan strands and termed "tessera". The picture was taken from Vollmer and Bertsche, 2008.

Recently a new model was proposed, the so-called “scaffold-model”, in which the glycan strands protrude perpendicular from the cytoplasmic membrane and grow outward in a linear instead of a layered fashion (Fig. 5B) (Dmitriev et al., 1999; Dmitriev et al., 2000; Dmitriev et al., 2004; Dmitriev et al., 2003). As argued by Vollmer and Höltje this model is not in accordance with many experimental data such as thickness of the murein sacculus, length of the glycan strands, degree of the cross-linkages and the elasticity of *E. coli* (Vollmer and Höltje, 2004).

Very recently the inner surfaces of *B. subtilis* were visualized by a novel technique, atomic force microscopy (AFM), indicating thick, 50 nm wide peptidoglycan cables running across the short axis of the bacterial cell different from the current models of the layered murein (Fig. 5C) (Hayhurst et al., 2008).

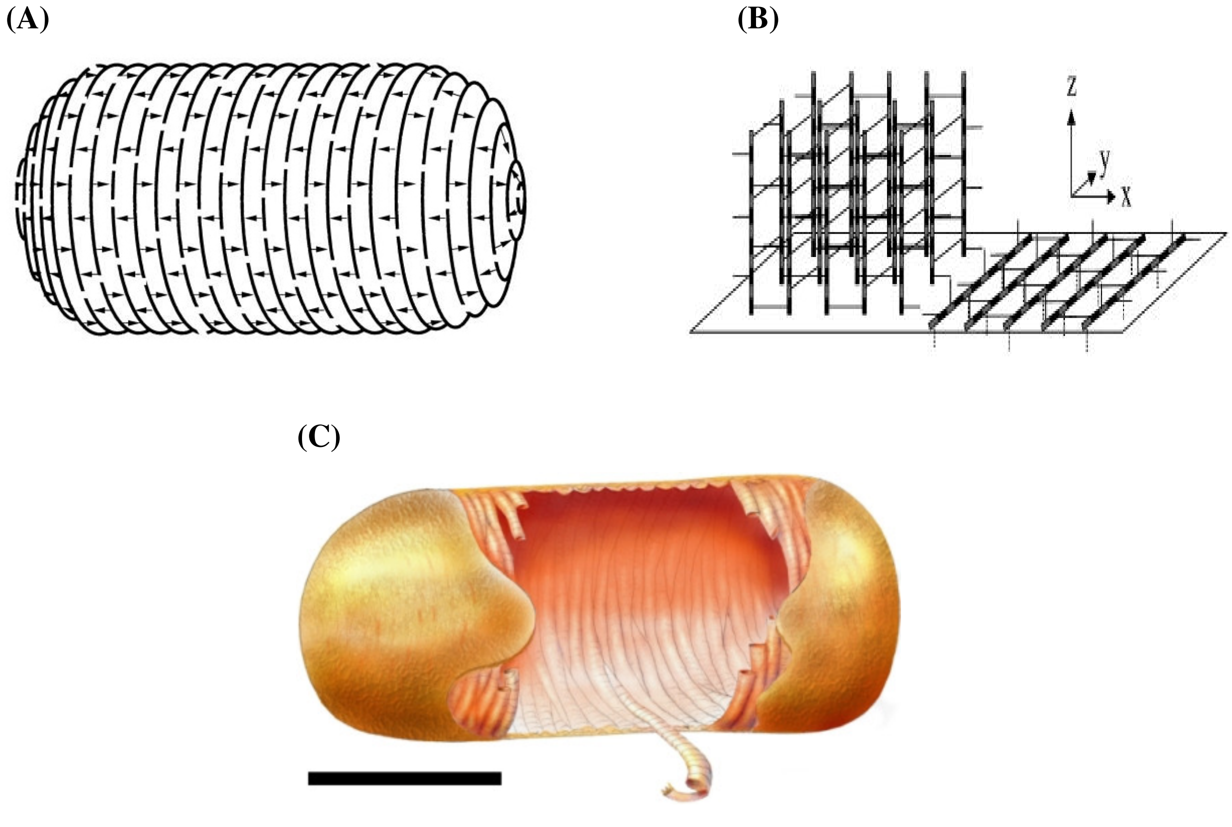

Figure 5: Structural models of the murein sacculus. (A) In the “horizontal layer model” the glycan strands are arranged along the short axis and parallel to the cell membrane whereas **(B)** in the “scaffold model” the glycan strands are arranged perpendicular from the cell membrane. **(C)** Recently, Hayhurst *et al.* visualized by atomic force microscopy (AFM) the architecture of *B. subtilis* peptidoglycan indicating thick cables running across the short axis of the cell (Scale bar, 1 µm). The figures were taken from Höltje, 1998 (A); Vollmer and Höltje, 2004 (B) and Hayhurst *et al.*, 2008 (C).

Peptidoglycan biosynthesis

The peptidoglycan biosynthesis of Gram-positive and Gram-negative bacteria is almost identical and occurs in a complex three-stage process in three different cellular compartments. In the first stage the soluble nucleotide precursors UDP-GlcNAc and UDP-MurNAc-peptides, also known as “Park’s nucleotides”, are synthesized in the cytoplasm. The second stage takes place on the inner side of the cytoplasmic membrane, where the lipid-linked intermediates (lipid I and lipid II) are generated and translocated (lipid II) across the membrane to the outer surface. The last stage terminates in the periplasmic compartment with the insertion of the disaccharide-peptide units of lipid II by polymerization and cross-linking into the existing murein sacculus as reviewed by different authors (Fig. 6) (Archibald et al., 1993; Barreteau et al., 2008; Bouhss et al., 2008; Höltje, 1998; Litzinger and Mayer, 2009; Sauvage et al., 2008; van Heijenoort, 1998; van Heijenoort, 2001a; van Heijenoort, 2001b; van Heijenoort, 2007; Vollmer and Bertsche, 2008).

The assembly of the peptidoglycan disaccharide-peptide units proceeds in four stages of reactions beginning with the synthesis of UDP-GlcNAc from fructose-6-phosphate catalyzed by the enzymes GlmS (aminotransferase) (Badet et al., 1988), GlmM (mutase) (Jolly et al., 1999; Mengin-Lecreulx and van Heijenoort, 1996) and GlmU (bifunctional transferase) (Brown et al., 1999; Hove-Jensen, 1992; Mengin-Lecreulx and van Heijenoort, 1993; Mengin-Lecreulx and van Heijenoort, 1994) using L-glutamine as nitrogen source for the amino group. Subsequently UDP-MurNAc is formed in a two-step mechanism by the enzymes MurA and MurB (Barreteau et al., 2008; van Heijenoort, 2001b). The transfer of enolpyruvate from phosphoenolpyruvate (PEP) to the 3’hydroxyl group of GlcNAc yielding UDP-GlcNAc-enolpyruvate is catalyzed by transferase MurA. Thereafter the reductase MurB converts the enolpyruvate substituent to D-lactyl with UDP-MurNAc as final product. MurA and MurB are essential in *E. coli*, while Gram-positive bacteria usually have two paralogs of MurA (MurA1 and MurA2).

The production of UDP-MurNAc-pentapeptide proceeds by adding the peptides stepwise onto the D-lactyl group of UDP-MurNAc with concomitant ATP hydrolysis catalyzed by three Mur ligases (MurC, D, and E) (Barreteau et al., 2008; van Heijenoort, 2001b; Vollmer and Bertsche, 2008). In *B. subtilis* most of the *m*-DAP residues are amidated on their free carboxyl group by an unknown mechanism (Mengin-Lecreulx and van Heijenoort, 1994). In the last step the dipeptide D-Ala-D-Ala moiety is attached by ligase MurF to position 4 and 5 important for cross-linkage reaction catalyzed by transpeptidases (Healy et al., 2000).

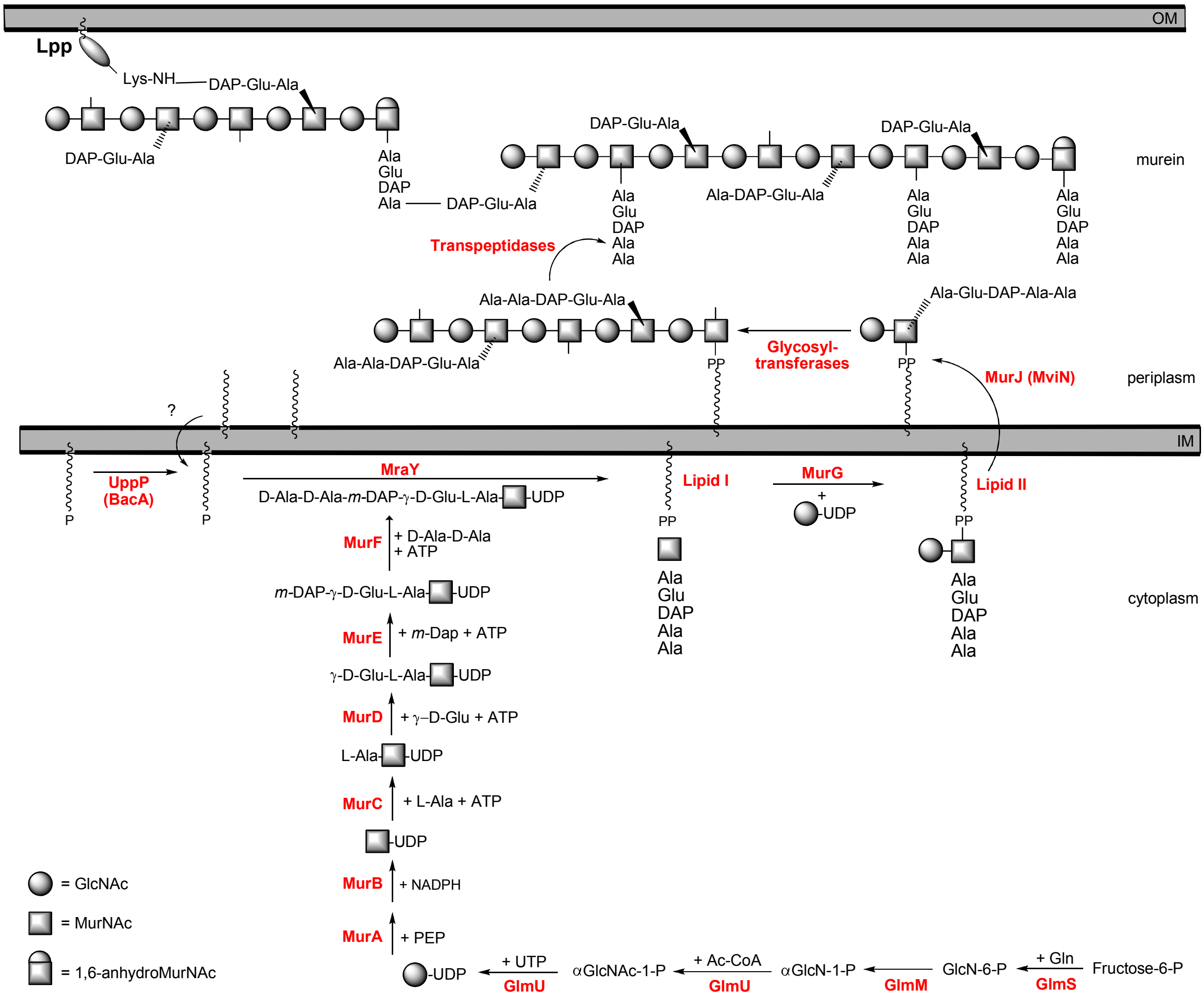

Figure 6: Biosynthesis of peptidoglycan in *E. coli*. The amino sugars of the glycan strands are shown in symbols; for definition of the used symbols see figure insert. The peptides L-Ala-γ-D-Glu-*m*-DAP-D-Ala-D-Ala are abbreviated with Ala-Glu-DAP-Ala-Ala. For a detailed description see the text.

The first membrane step is catalyzed by the transferase MraY on the inner side of the cytoplasmic membrane which transfers the phospho-MurNAc-pentapeptide moiety of the cytoplasmic UDP-MurNAc-pentapeptide to the membrane acceptor undecaprenyl-phosphate (C55-P, also known as bactoprenol phosphate) yielding MurNAc-pentapeptide-pyrophosphoryl undecaprenol (lipid I) (Anderson et al., 1965; Barreteau et al., 2008; Bouhss et al., 2008; van Heijenoort, 2007). Thereafter transferase MurG catalyzes the addition of *N*-acetylglucosamine (GlcNAc) from UDP-GlcNAc to lipid I generating the final disaccharide-muropeptide precursor undecaprenyl-pyrophosphoryl-MurNAc-pentapeptide-GlcNAc (lipid II). The hydrophilic lipid II is then translocated across the hydrophobic environment of the cytoplasmic membrane by a yet unknown mechanism, probably by a hypothetical flippase (van Dam et al., 2007). Recently MurJ (MviN) was identified as a lipid II flippase of *E. coli* essential for murein biosynthesis since deletion of the corresponding gene causes accumulation of lipid II and the cells show morphological defects and eventually burst (Ruiz, 2008).

The last stage of peptidoglycan biosynthesis, the polymerization of lipid II and incorporation into the pre-existing murein sacculus, occurs at the outer side of the cytoplasmic membrane within the periplasmic space and is catalyzed by murein synthases. In Gram-negative bacteria murein synthases are monofunctional glycosyl transferases (GTs), bifunctional transferases/transpeptidases (GTs/TPs) or monofunctional transpeptidases (TPs) (Di Berardino et al., 1996; Park and Matsuhashi, 1984). MtgA, the monofunctional GT of *E. coli*, is capable to polymerize glycan strands but not to cross-link the peptides (Di Berardino et al., 1996; Vollmer and Bertsche, 2008). In *B. subtilis* monofunctional GTs do not exist (Foster and Popham, 2002), hence bifunctional GTs/TPs polymerize glycan strands.

GTs transfer the growing, lipid-linked peptidoglycan strand with its reducing end of MurNAc (C1) (donor) onto the C4-carbon of the GlcNAc residue of lipid II (acceptor) (Archibald et al., 1993). Therefore the peptidoglycan chain grows at the reducing end, but protrudes to the cell wall with its non-reducing end (Lovering et al., 2007; Yuan et al., 2007). The β-1,4-glycosidic linked glycan strands that have been polymerized by GTs are cross-linked and incorporated into the existing murein sacculus by TPs which catalyze the cross-linking between the stem peptides (Archibald et al., 1993; Foster and Popham, 2002; Höltje, 1998; Navarre and Schneewind, 1999; Scheffers and Pinho, 2005; van Heijenoort, 2001b). During this reaction undecaprenyl-pyrophosphate is released and regenerated by dephosphorylation yielding the lipid carrier bactoprenol which can again serve as lipid II carrier (El Ghachi et al., 2005; van Heijenoort, 2007). The transpeptidation reaction is a two-step mechanism for cross-linking the glycan strands by two peptides. In Gram-negative bacteria and Bacilli the glycan strands are cross-linked by direct cross-bridges. This reaction is energized by the hydrolysis of the D-Ala-D-Ala bond with formation of an enzyme-substrate intermediate and concomitant release of the terminal D-Ala. Thereafter the tetrapeptidyl group is transferred to the acceptor which is the non-alpha amino group of the di-basic amino acid *m*-DAP in a second stem peptide.

Enzymes with D,D-TP activity are also known as penicillin-binding proteins (PBPs) due to their ability to bind penicillin and other β-lactam antibiotics which mimic the structure of the dipeptide D-Ala-D-Ala. PBPs can be divided into two classes: high-molecular weight (HMW)

PBPs and low-molecular weight (LMW) PBPs (Ghuysen, 1991; Goffin and Ghuysen, 1998). HMW-PBPs consist of two domains located in the periplasm, a *C*-terminal penicillin binding domain catalyzing the peptide cross-linkages and an *N*-terminal domain with different catalytic activities. Depending on the catalytic activity of the *N*-terminal domain HMW-PBPs are further divided into class A and class B (Goffin and Ghuysen, 1998). Class A HMW-PBPs are bifunctional enzymes due to the GT acivity of their *N*-terminal domain allowing them to polymerize the glycan strands and to form peptide cross-linkages. By contrast class B HMW-PBPs are monofunctional TPs since they have an *N*-terminal domain whose function is unknown, presumably it is involved in interactions with membrane proteins (Anderson et al., 1965; Terrak et al., 1999).

LMW-PBPs are monofunctional D,D-peptidases generally involved in peptidoglycan maturation. Most of these act as D,D-carboxypeptidases cleaving the terminal D-Ala-D-Ala peptide bond of a stem peptide which prevents cross-linking of these peptides (Ghuysen, 1991; Massova and Mobashery, 1998).

Growth and turnover of the murein sacculus

Cell wall growth and division do not only depend on the synthesis of new peptidoglycan but also on the hydrolysis of the covalent bonds of the existing murein sacculus to enable the insertion of the new material. This creates the problem of a safe enlargement and division maintaining the structural integrity during these processes. Already in 1964, Pelzer and Weidel proposed an enzymatic balance model for the growth of the sacculus, in which autolysins and murein synthases function in a balanced interplay, with the autolysins introducing nicks into the murein sacculus and the synthases inserting new material at these sites (Weidel and Pelzer, 1964). Different models have been proposed for Gram-positive and Gram-negative bacteria since the former have a thick, multilayered murein sacculus compared to the monolayered sacculus of the latter.

Koch proposed in his “make-before-break” strategy that covalent bonds have to be formed prior to hydrolysis (Koch, 1988; Koch and Doyle, 1985) and argued in his “surface stress theory” that the newly synthesized glycan strands are then automatically inserted into the layer of the murein sacculus due to the existing tension in the surface (Koch, 1985; Koch et al., 1981; Koch et al., 1982). This strategy is realized in the “inside-to-outside” growth model for Gram-positive bacteria (Fig. 7). According to the “surface-stress-theory” newly synthesized peptidoglycan is cross-linked to the existing murein sacculus at the inner side of the cell wall in an unextended form. As subsequent additions of peptidoglycan occur the wall is pushed outwards, becomes stretched and bears the stress due to hydrostatic pressure (Koch and Doyle, 1985). The activity of autolysins is expected to be greater in the more stressed (external) layers. The addition of new polymers at many sites along the cylindrical wall and the stretching of these polymers as they are displaced towards the murein sacculus' outermost periphery allow the cell to elongate. During cell division a greater proportion of the murein synthases must be directed towards the production of the septum (Foster and Popham, 2002). PBP3 and PBP4a are localized specifically to the lateral sacculus, whereas PBP1 and PBP2b are localized specifically to the septum. All other PBPs localized to both, the septum and the cylindrical murein sacculus (Scheffers and Errington, 2004). Therefore in this growth model the murein sacculus is never weakened because new layers are formed before the older and outer ones are degraded and released into the growth medium as turnover products (Koch and Doyle, 1985).

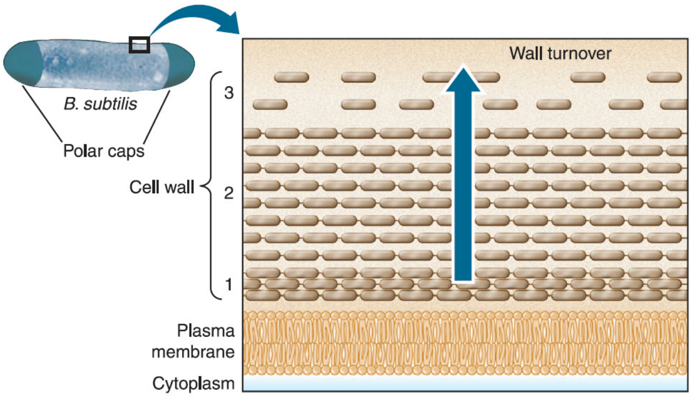

Figure 7: "Inside-to-outside" growth of the murein sacculus of Gram-positive bacteria. Shown are the three regions of the peptidoglycan of *B. subtilis*, determined from images like those in Fig. 1B. In region 1, the newly synthesized glycan strands are found; region 2 consists of older, less densed peptidoglycan that is stretched by the cell's turgor pressure. Region 3 contains the oldest peptidoglycan layers that are hydrolyzed by autolysins. The peptidogylcan turnover processes from the inside to the outside. The figure was taken from Beveridge, 2006.

For Gram-negative bacteria the more elaborated "three-for-one" model was proposed by Höltje, 1998. It is in agreement with the "make-before-break" theory since the new glycan strands are made and inserted in the murein sacculus before the old material is removed and therefore the risk of autolysis is avoided. Beyond that it explains the massive turnover observed in *E. coli* during growth and division (Höltje, 1996a; Höltje, 1996b; Höltje, 1998; Höltje and Heidrich, 2001; Vollmer and Höltje, 2001). As shown in Fig. 8 the model suggests that three new glycan strands are synthesized, are cross-linked to each other and are attached in a relaxed conformation below the intact murein sacculus which is under osmotic pressure.

Simultaneously upon removal of the so-called “old” docking strand, the triplet is inserted into the murein sacculus. It is obvious that this mechanism requires the coordination, temporarily and spatially, of autolysins and murein synthases. Therefore according to the “three-for-one” model, the formation of a multienzyme complex was proposed combining murein synthases and murein hydrolases to ensure that the hydrolases are only active at the sites of synthesis to allow safe insertion of new material into the growing murein sacculus. Indeed protein-protein interaction studies by affinity chromatography demonstrated that murein hydrolases and synthases do interact with each other (Höltje, 1998; Romeis and Höltje, 1994b; Vollmer and Bertsche, 2008; Vollmer et al., 1999; von Rechenberg et al., 1996). As illustrated in Fig. 8B a dimer of a bifunctional PBP (PBP1A or PBP1B) (Bertsche et al., 2005; Born et al., 2006; Spratt and Jobanputra, 1977; Suzuki et al., 1978) cross-links each new glycan strand to its neighbour forming a triplet which is then attached to the existing murein sacculus by a dimer of transpeptidases (PBP2 or PBP3). It is known that PBP1A and PBP2 are primarily involved in cell elongation while PBP1B and PBP3 are responsible for cell division in *E. coli* (Spratt, 1975). Thereafter the central docking strand is removed by the concerned action of a dimer of an endopeptidase (PBP4 or PBP7) (Romeis and Höltje, 1994a) splitting the cross-linkages to the left and right side of the old strand and by a monomer of a lytic transglycosylase (e.g. Slt70, MltA or MltB) (Ehlert et al., 1995; Höltje et al., 1975; Lommatzsch et al., 1997) depolymerising the glycan strand and thus releasing the turnover products which are recycled by the cell (see below). The cell turgor pulls the three new glycan strands into the murein layer. Since cell constriction and division occurs with simultaneous insertion of multiple strands, the murein-multienzyme-complex responsible for cell constriction may synthesize a murein triplet in one step. Therefore it is postulated that the division-multienzyme-complex contains an additional monofunctional glycosyl transferase (GT) synthesizing the middle strand of the triplet (Höltje, 1998). The cell constriction is the result of the repeated addition of murein triplets, each followed by the release of the middle strand. This is accomplished by a mechanical device, the contracting FtsZ-ring that pulls the membrane-anchored murein-synthesizing enzymes inward and therefore prohibits the insertion of the newly added triplets into the surface of the cylindrical part of the sacculus. As a result a cleavage furrow is formed (Höltje, 1998).

In contrast the thicker peptidoglycan and the “inside-to-outside” growth mechanism of Gram-positive species abolish the close coupling of murein synthetic and degradative activities and a clear evidence of PBP-autolysin complex formation has not been provided (Foster and Popham, 2002).

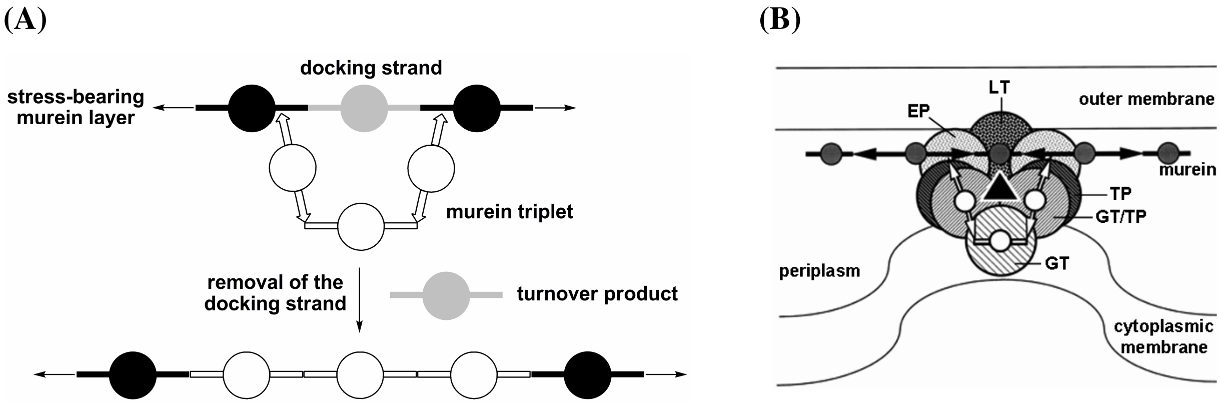

Figure 8. Model of insertion of new peptidoglycan in Gram-negative bacteria. (A) "Three-for-one" growth model. Three newly synthesized, cross-linked glycan strands in relaxed state (white circles) are covalently attached to the free amino groups of *m*-DAP present in the donor peptides of the cross-links on both sides of a strand, called the docking strand (grey circle). Specific cleavage of the pre-existing cross-links results in the replacement of the docking strand by the murein triplet. **(B) Multienzyme complex combining murein synthases and murein hydrolases.** The small black circles represent the stress-bearing murein sacculus, whereas the small white circles represent the newly synthesized cross-linked glycan strand triplet which must be inserted into the existing murein sacculus upon removal of the docking strand (black circle above the tip of the triangle). The large circles represent the multienzyme complex with the single components indicated from the front to the background as follows: a monomer of a glycosyl transferase (GT), a dimer of a bifunctional glycosyl transferase/transpeptidase (GT/TP), a dimer of a transpeptidase (TP), a dimer of a D,D-endopeptidase (EP), a monomer of a lytic transglycosylase (LT). The structural protein MipA (triangle) mediates the assembly of the enzymes into a complex. Figure (A) is an adaptation from Höltje, 1998 and figure (B) was taken from Vollmer *et al.* with modifications.

The assembly of the murein sacculus is directed by interactions of cytoskeletal elements which function as scaffolds for the murein synthesis machinery. In rod-shaped bacteria, like *E. coli* and *B. subtilis*, the longitudinal growth (elongation) depends on a multienzyme complex named elongase that inserts murein at discrete sites. The actin-like cytoskeletal elements MreB (Gram-negative rods) and Mbl (Gram-positive rods) are essential for murein synthesis along the lateral wall. As visualized by fluorescence microscopy using GFP-fusions they form helical structures just beneath the cytoplasmic membrane extending from pole to pole (Daniel and Errington, 2003; Errington et al., 2003; Jones et al., 2001). Further they co-localize with other morphogenetic proteins and cell wall synthesizing enzymes (Cabeen and Jacobs-Wagner, 2005; Cabeen and Jacobs-Wagner, 2007; Scheffers and Pinho, 2005).

Upon initiation of cell division a switch from dispersed to localized murein synthesis in the middle of the cell occurs. The accumulation of the tubulin-homolog FtsZ at the cell center initiates the assembly of a multienzyme complex of division, the divisome. FtsZ polymerizes in a GTP-dependent fashion and forms a contractile ring structure in the middle of the cell that pulls inwards both: the synthesis of murein and the invagination of the membrane generating a septum that maturates into new cell poles (Bi and Lutkenhaus, 1991; den Blaauwen et al., 2008; Goehring and Beckwith, 2005; Höltje, 1998; Rothfield and Justice, 1997).

During cell growth and division of bacteria a loss of peptidoglycan components from the cell wall was observed in both, Gram-negative (Goodell, 1985; Goodell and Schwarz, 1983; Goodell and Schwarz, 1985) and Gram-positive (De Boer et al., 1981; Mauck et al., 1971; Mauck and Glaser, 1970; Pooley, 1976) bacteria. This process was termed peptidoglycan turnover.

Lysis of the peptidoglycan (turnover) proceeds by specific hydrolases which target almost every covalent linkage of the peptidoglycan. These enzymes can be classified as muramidases (or lytic transglycosylases), glucosaminidases, *N*-acetylmuramyl-L-alanine amidases endopeptidases and carboxypeptidases, depending on the specific bond cleaved by the enzyme (Fig. 9). Besides a role in growth of the murein sacculus, peptidoglycan hydrolases have been proposed to be involved in other processes such as cell separation after division, cell wall turnover and muropeptide recycling or sporulation of Gram-positive bacteria (Scheffers and Pinho, 2005). Hence despite being a rigid, stabilizing structure, the murein sacculus is a highly dynamic compartment that is continuously remodelled, degraded and resynthesized (Litzinger and Mayer, 2009).

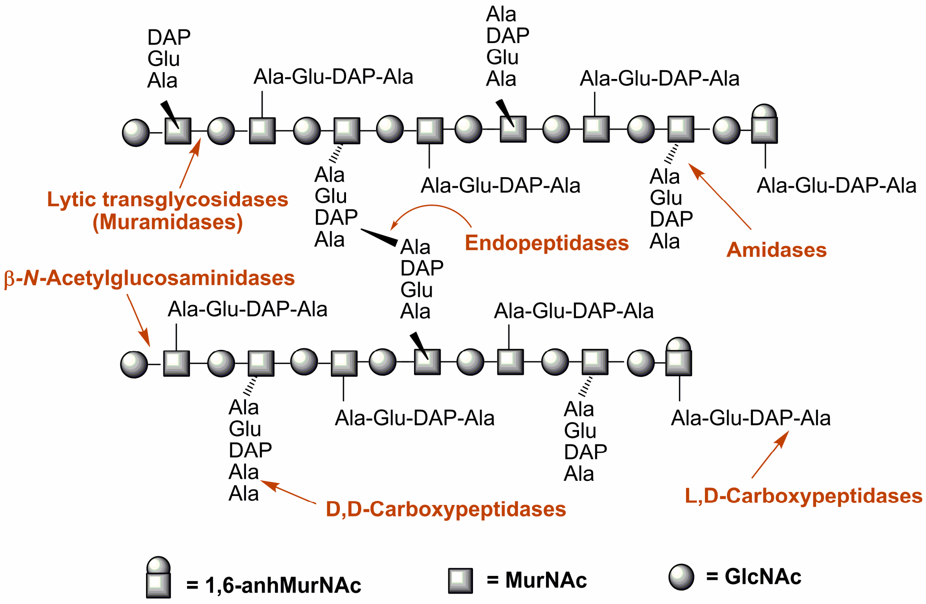

Figure 9: Peptidoglycan hydrolyzing enzymes (autolysins) of *E. coli* and their sites of cleavage. The arrows indicate the specific cleavage sites of the different hydrolases (autolysins). The glycan strands are degraded by lytic transglycosylases and β-*N*-acetylglucosaminidases yielding 1,6-anhydro-disaccharides and GlcNAc. Amidases release peptides from the intact murein sacculus during septation or from the GlcNAc-1,6-anhydroMurNAc muropeptides during recycling. The peptides L-Ala-γ-D-Glu-*m*-DAP-D-Ala-D-Ala are abbreviated with Ala-Glu-DAP-Ala-Ala.

In *E. coli* peptidoglycan turnover was long overseen since the turnover products are efficiently recycled as described below (Goodell, 1985; Goodell and Schwarz, 1983; Park, 1993). During growth and division *E. coli* releases about 50% of its existing peptidoglycan in one generation by the activity of different hydrolases (autolysins) like lytic transglycosylases, amidases and endopeptidases (Goodell and Schwarz, 1985; Jacobs et al., 1994). The turnover products released during growth are processed by the concerned action of lytic transglycosylases and endopeptidases and are mainly GlcNAc-1,6-anhydroMurNAc-tetrapeptides (Höltje et al., 1975). Endopeptidases (PBP4, PBP7 and MepA) cleave the peptide cross-links between *m*-DAP at position 3 of one glycan strand and D-Ala at position 4 of a neighbouring strand. MepA hydrolyzes both, the D,D- and L,D-crosslinks (Vollmer and Bertsche, 2008). Endopeptidases alone would not release peptidoglycan fragments into the periplasm and therefore glycosidases must exist. In Gram-negative bacteria lytic transglycosylases are the major murein glycosidases. In contrast to lysozyme, lytic transglycosylases cleave the β-1,4-glycosidic bond between carbon 1 of MurNAc and carbon 4 of GlcNAc while simultaneously forming a 1,6-anhydro ring at the MurNAc residue by an intramolecular transglycosylation reaction (Fig. 10) (Höltje et al., 1975).

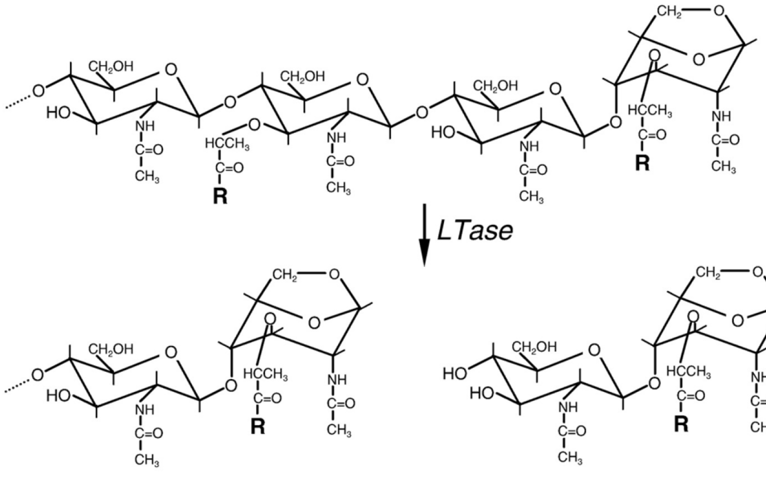

Figure 10: The turnover product GlcNAc-1,6-anhydroMurNAc-tetrapeptide released during growth of *E. coli* by lytic transglycosylases. R, peptide. Lytic transglycosylases cleave the β-1,4-glycosidic bond between carbon 1 of MurNAc and carbon 4 of GlcNAc while simultaneously forming a 1,6-anhydro ring at the MurNAc residue by an intramolecular transglycosylation reaction. The figure was taken from Vollmer and Bertsche, 2008.

The principal lytic transglycosylase responsible for turnover of peptidoglycan is the soluble Slt70 (SltY) found in the periplasm and acting as exo-enzyme from the end of the glycan strands. In addition *E. coli* has multiple membrane-bound lytic transglycosylases (MltA, B, C, D, E (EmtA)). Some of them are presumably involved in special functions such as cell wall remodelling, e.g. providing space for flagellum insertion (Dijkstra and Keck, 1996; Koraimann, 2003; Scheurwater et al., 2008; Zahrl et al., 2005).

Another class of enzymes that cleave bonds in the intact murein sacculus includes the periplasmic MurNAc-L-Ala amidases AmiA, AmiB and AmiC which cleave the bond between MurNAc and the stem peptide and were shown to participate in cell separation (Heidrich et al., 2001; Heidrich et al., 2002; Priyadarshini et al., 2006). A further amidase, AmiD, is linked as lipoprotein to the inner side of the outer membrane (Park and Uehara, 2008; Uehara and Park, 2007). In addition to the lytic enzymes D,D-carboxypeptidases (PBP5, PBP6, PBP6B) or L,D-carboxypeptidases convert stem pentapeptides to stem tetra- or tripeptides by removing the *C*-terminal D-Ala residues (Höltje, 1998).

It has been observed that *B. subtilis* also turns over approximately 50% of its peptidoglycan but releases the turnover products in the growth medium during logarithmic growth (Mauck and Glaser, 1970). The candidates for peptidoglycan hydrolases in the *B. subtilis* genome were identified by performing amino acid sequence similarity searches via the *SubtiList* genome sequence with representatives of all known classes of autolysins (Kunst et al., 1997; Smith et al., 2000). Altogether, at least 35 candidate peptidoglycan hydrolases were identified (Table 1) (Smith et al., 2000). Some peptidoglycan hydrolases were characterized enzymatically but most were only classified on bases of sequence identity as *N*-acetylmuramidases, *N*-acetylglucosaminidases, *N*-acetylmuramyl-L-alanine amidases (amidases), D,L-endopeptidases (digesting D-Glu-*m*-DAP linkages) and L,D-endopeptidases (digesting L-Ala-D-Glu linkages) (Foster and Popham, 2002; Fukushima et al., 2008; Fukushima et al., 2007; Smith et al., 2000). In contrast to *E. coli* D,D-endopeptidases digesting the cross-linked D-Ala-*m*-DAP linkage have not yet been identified in *B. subtilis*. Interestingly the groups of muramidases and lytic transglycosylases in *B. subtilis* are not fully characterized and it remains unclear whether the turnover products are released by the activity of lytic transglycosylases or muramidases. Already in 1973, in crude enzyme preparations Del Rio *et al.* discovered an exo-muramidase which was able to cleave the disaccharide MurNAc-GlcNAc, but neither the responsible enzyme nor the corresponding gene have been identified yet (Del Rio et al., 1973). Recently Fukushima *et al.* identified a bifunctional D,L-endopeptidase/muramidase, CwlT (YddH). The *C*-terminal domain of CwlT acts as a D,L-endopeptidase hydrolyzing the linkage of D-γ-glutamyl-*m*-DAP of peptidoglycan and the *N*-terminal domain functions as an *N*-acetylmuramidase releasing tetra-, hexa- and octasaccharides and only a very low amounts of disaccharide (GlcNAc-MurNAc) from purified glycan strands of peptidoglycan of *B. subtilis* (Fukushima et al., 2008).

The two major vegetative autolysins of *B. subtilis*, LytC, a 50 kDa *N*-acetylmuramyl-L-alanine amidase and LytD, a 90 kDa endo-β-*N*-acetylglucosaminidase, are responsible for about 95% of the autolytic activity of the cell (Blackman et al., 1998; Herbold and Glaser, 1975; Kuroda and Sekiguchi, 1991; Margot and Karamata, 1992; Margot et al., 1994; Rashid et al., 1995; Rogers et al., 1984). They participate in cell separation along with the two D,L-endopeptidases LytE and LytF and the putative autolysin YwbG (Smith et al., 2000).

According to the "inside-to-outside" growth mechanism of *B. subtilis*, autolysins are necessary for the hydrolysis of older peptidoglycan in the outermost layers to allow the newly synthesized peptidoglycan to expand and become stressed as the cell elongates (cell wall turnover). Surprisingly, so far, no association between autolytic activity and growth of the bacterial cell has been shown. Neither single nor multiple inactivations of different autolysins did affect cell growth. Despite this, the exogenous addition of an autolysin preparation accelerated the growth of *Bacillus* cultures (Fan and Beckman, 1971). It remains inexplicable how cell growth takes place without selected disconnection of covalent bonds within the murein sacculus to permit peptidoglycan expansion (Smith et al., 2000). Alternatively the expansion of the cell may cause such great stress forces in the outer layers of the murein sacculus that critical covalent bonds are fractured without the need for enzyme-catalyzed hydrolysis (Archibald et al., 1993; Smith et al., 2000).

Although there was no association between autolytic activity and cell growth, peptidoglycan turnover was investigated in exponentially growing cells by pulse-chase experiments with *N*-acetyl-D-[1-^{14}C]glucosamine labelled peptidoglycan (Blackman et al., 1998). It was shown that the major vegetative amidase LytC is important in this process. In one study it was shown that inactivation of *lytC* delayed the release of radiolabelled peptidoglycan material without affecting the turnover rate (Margot and Karamata, 1992). In contrast in another study, carried out by Blackman *et al.*, *lytC* inactivation caused thickening of the peptidoglycan and a large decrease in the rate of turnover (Blackman et al., 1998). Inactivation of *lytD* alone did not affect peptidoglycan turnover but a greater reduction in peptidoglycan turnover was observed in a *lytC lytD* double mutant (Margot et al., 1994).

Most of the autolysins of *B. subtilis* have functional redundancy and perform more than one role in the cell and can phenotypically compensate for the lack of each other (Foster, 1991). Therefore it is necessary to characterize the total complement of the autolysins to determine their individual and combined roles in the cellular processes (Blackman et al., 1998).

Table 1: Proposed peptidoglycan hydrolase complement of *B. subtilis*

Family/ Protein	Location	Expression	Activity	Function	Reference
LytC amidase family (LytC of *B. subtilis*, aa 322-496)					
LytC (CwlB)	Cell wall	Vegetative (σ^A and σ^D); remains active during sporulation	Amidase	Cell separation, motility, wall turnover, cell lysis, mother cell lysis	(Blackman et al., 1998; Chen et al., 2009; Kuroda and Sekiguchi, 1991; Lazarevic et al., 1992; Margot and Karamata, 1992; Smith and Foster, 1995)
YqiI					
CwlC	Mother cell wall		Amidase	Mother cell lysis	(Kuroda et al., 1993; Smith and Foster, 1995)
CwlD		Sporulation (σ^E, σ^G)	Amidase ?	Spore germination; formation of muramic δ-lactam structure in spore cortex	(Atrih et al., 1996; Popham et al., 1996; Sekiguchi et al., 1995)
YrvJ					
LytD glucosaminidase family (LytD of *B. subtilis*, aa 569-880)					
LytD (CwlG)	Cell wall	Vegetative, primarily σ^D	Glucosaminidase	Cell separation	(Blackman et al., 1998; Chen et al., 2009; Margot et al., 1994; Rashid et al., 1995)
D,L-Endopeptidase I family (endopeptidase I of *B. sphaericus*, aa 101-396)					
YqgT					
D,L-Endopeptidase II family (endopeptidase II of *B. sphaericus*)					
CwlT (YddH)		Induction with mitomycin C	bifunctional γ-D-Glu-*m*-DAP endopeptidase and muramidase		(Fukushima et al., 2008)
LytF (CwlE,YhdD)	Cell wall	Vegetative (σ^D)	γ-D-Glu-*m*-DAP endopeptidase	Cell separation	(Chen et al., 2009; Margot et al., 1999; Ohnishi et al., 1999)
YojL	Cell wall				
YwtD					
LytE (CwlF)		Vegetative (σ^A) and late stationary phase (σ^H)		Cell separation, cell lysis	(Ishikawa et al., 1998a; Margot et al., 1998)
YkfC		Late vegetative			
YvcE					

Family/ Protein	Location	Expression	Activity	Function	Reference
Lysostaphin family (lysostaphin of *S. simulans*, aa 236-383)					
YomI*				SP β-mediated lysis?	
YunA					
SpoIIQ		Sporulation (σ^F)		Prespore engulfment	(Londono-Vallejo et al., 1997)
GSLE family (SleB of *B. cereus*)					
SleB		Sporulation (σ^G)	Lytic transglycosylase?	Germination	(Boland et al., 2000; Moriyama et al., 1996)
YkvT					
CwlJ		Sporulation (σ^E)		Germination	(Ishikawa et al., 1998b)
L,D-Endopeptidase family (endopeptidase AcpA of *L. monocytogenes* phage A500)					
CwlK (YcdD)	membrane	Vegetative	L-Ala-D-Glu-Endopeptidase		(Fukushima et al., 2007)
Slt 70 family (Slt70 of *E. coli*)					
YjbJ		Vegetative		None during sporulation	(Blackman et al., 1998)
YomI*				SP β-mediated lysis?	
Enterococcal muramidase (glucosaminidase) family (AlyS of *E. faecalis*)					
LytG (YubE)		Vegetative (σ^A)	Exo-Glucosaminidase	Peptidoglycan maturation	(Horsburgh et al., 2003)
YpbE					
LrgB family (LrgB of *S. aureus*)					
YsbB					
YwbG				Cell separation	
YxaC					
XlyA amidase family (XlyA of *B. subtilis* prophage PBSX)					
XlyA		PBSX induction	Amidase	PBSX-mediated lysis	(Longchamp et al., 1994)
XlyB				PBSX-mediated lysis?	
YqeE (CwlH)				Mother cell lysis	(Nugroho et al., 1999)
CwlA		Apparently silent	Amidase	*skin*-mediated lysis?	(Foster, 1991; Foster, 1993; Kuroda and Sekiguchi, 1990)
BlyA (YomC)		SP β induction	Amidase	SP β-mediated lysis	(Regamey and Karamata, 1998)
YdhD					
YocH					

* YomI is homologous to both lysostaphin and Slt70 which show no significant similarity to one another. The reference sequence used for calculation of percentage identities for each family is shown in parenthesis after the name of the family. The table is an adaptation from Smith *et al.*, 2000.

Recycling of the turnover products

Peptidoglycan recycling is a process that is defined as reutilization of turnover products derived from the endogenous murein (Höltje, 1998). Peptidoglycan turnover and recycling have been studied in great detail in the Gram-negative model organism *E. coli*. In *E. coli* the principal cell wall turnover products are anhydromuropeptides consisting of GlcNAc-1,6-anhydroMurNA(anhMurNAc)-L-Ala-γ-D-Glu-*m*-DAP-D-Ala. For *E. coli* it was shown that these products are efficiently reutilized (i.e. recycled) thereby forming new peptidoglycan precursors (Höltje, 1998). The anhydromuropeptides are transported into the cytoplasm by a specific transmembrane permease, AmpG (Cheng and Park, 2002; Jacobs et al., 1994). The anhydro-muropeptides are further degraded in the cytoplasm by the concerted action of anhydro-*N*-acetylmuramyl-L-alanine AmpD (Höltje et al., 1994; Jacobs et al., 1995), L,D-carboxypeptidase LdcA (Templin et al., 1999) and β-*N*-acetylglucosaminidase NagZ (Cheng et al., 2000; Vötsch and Templin, 2000) yielding GlcNAc, anhMurNAc and the tripeptide L-Ala-γ-D-Glu-*m*-DAP (see Fig. 11).

The peptide moiety of the anhydromuropeptides is released from MurNAc by amidase AmpD that is specific for anhMurNAc-containing muropeptides and therefore does not degrade the murein precursor molecules such as UDP-MurNAc-pentapeptide which are also present in the cytoplasm. The L,D-carboxypeptidase LdcA releases the last D-alanine from the tetrapeptide yielding the tripeptide L-Ala-γ-D-Glu-*m*-DAP which can be reutilized directly by muropeptide ligase Mpl linking it to UDP-MurNAc of the peptidoglycan synthesis pathway (Mengin-Lecreulx et al., 1996). Among the genes involved in murein recycling a mutation in the *ldcA* gene is the only mutation which causes a phenotype. Cells lacking *ldcA* appear as thick, oval cells and some of them lyse. An explanation for this phenotype is that in the absence of LdcA the tetrapeptide accumulates in the cytoplasm and the Mpl ligase generates UDP-MurNAc-tetrapeptide which is incorporated in the murein sacculus instead of MurNAc-pentapeptide (Templin et al., 1999). Consequently the absence of the pentapeptide, which is required for the cross-linking of murein, leads to a weakened cell wall eventually resulting in cell lysis. Besides anhydromuropeptides also tetra- and tripeptides occur in cell wall turnover which are products of the action of amidases (AmiA, B, C) during maturation of the peptidoglycan and cell septation (Heidrich et al., 2001; Priyadarshini et al., 2006). The tetra-/tripeptides are taken up to the cytoplasm by the ABC-transporter MppA/Opp (Park, 1993; Park et al., 1998). Again Mpl can link the peptides to UDP-MurNAc (besides tripeptides it also accepts tetra- and pentapeptides as substrates (Herve et al., 2007)). In the absence of Mpl the tripeptides can be further degraded to individual amino acids by MpaA, a γ-D-Glu-*m*-DAP amidase (Uehara and Park, 2003) which releases *m*-DAP. The released dipeptide L-Ala-γ-D-Glu can be converted to the L-amino-acids by epimerase YcjG (Schmidt et al., 2001) and the resulting L-Ala-γ-L-Glu can be then cleaved by dipeptidase PepD (Schroeder et al., 1994).

The fate of the amino sugar part of the turnover products was only investigated recently. The anhydro-disaccharide is cleaved in the cytoplasm by a cytoplasmic β-*N*-acetylglucosaminidase activity in *E. coli*, first observed by Yem and Wu (Yem and Wu, 1976a; Yem and Wu, 1976b). The β-*N*-acetylglucosaminidase named NagZ hydrolyzes the β-1,4-glycosidic bond between GlcNAc and (anh)MurNAc(peptides) in the peptidoglycan degradation products (Cheng et al., 2000; Vötsch and Templin, 2000) and both amino sugars reenter the metabolic pathway for the synthesis of murein, lipopolysaccharides or glycolysis by convertion to GlcNAc-6-P. The free amino sugar GlcNAc is directly converted to GlcNAc-6-P by *N*-acetylglucosamine kinase NagK (Uehara and Park, 2004), whereas anhMurNAc is first phosphorylated by anhydro-*N*-acetylmuramic acid kinase AnmK (Uehara et al., 2005). In addition to phosphorylation the reaction catalyzed by AnmK involves the concomitant cleavage of the 1,6-anhydro bond to yield MurNAc-6-P which can be converted to GlcNAc-6-P with the release of D-lactate by the MurNAc-6-P etherase MurQ (Jaeger et al., 2005; Jaeger and Mayer, 2008a; Uehara et al., 2006). The conversion of GlcNAc-6-P to UDP-GlcNAc requires deacetylation by NagA as well as isomerization to GlcN-1-P by phosphoglucomutase GlmM (Mengin-Lecreulx and van Heijenoort, 1996). The following reacetylation to GlcNAc-1-P and the reaction with UTP to form UDP-GlcNAc are catalyzed by the bifunctional uridyltransferase GlmU (Mengin-Lecreulx and van Heijenoort, 1993; Mengin-Lecreulx and van Heijenoort, 1994). Alternatively GlcNAc-6-P can enter the glycolysis pathway by convertion to fructose-6-P by NagB (White, 1968). Recently it was shown that GlcNAc is also formed in the periplasm and is taken up by the phosphotransferase system NagE (Plumbridge, 2009).

E. coli was also shown to be able to utilize the amino sugars GlcNAc and MurNAc as sole sources of carbon. Both can enter the cell by their specific phosphotransferase system (PTS), NagE and MurP, respectively, with concomitant phosphorylation (Dahl et al., 2004; Lengeler et al., 1994; Plumbridge, 1989).

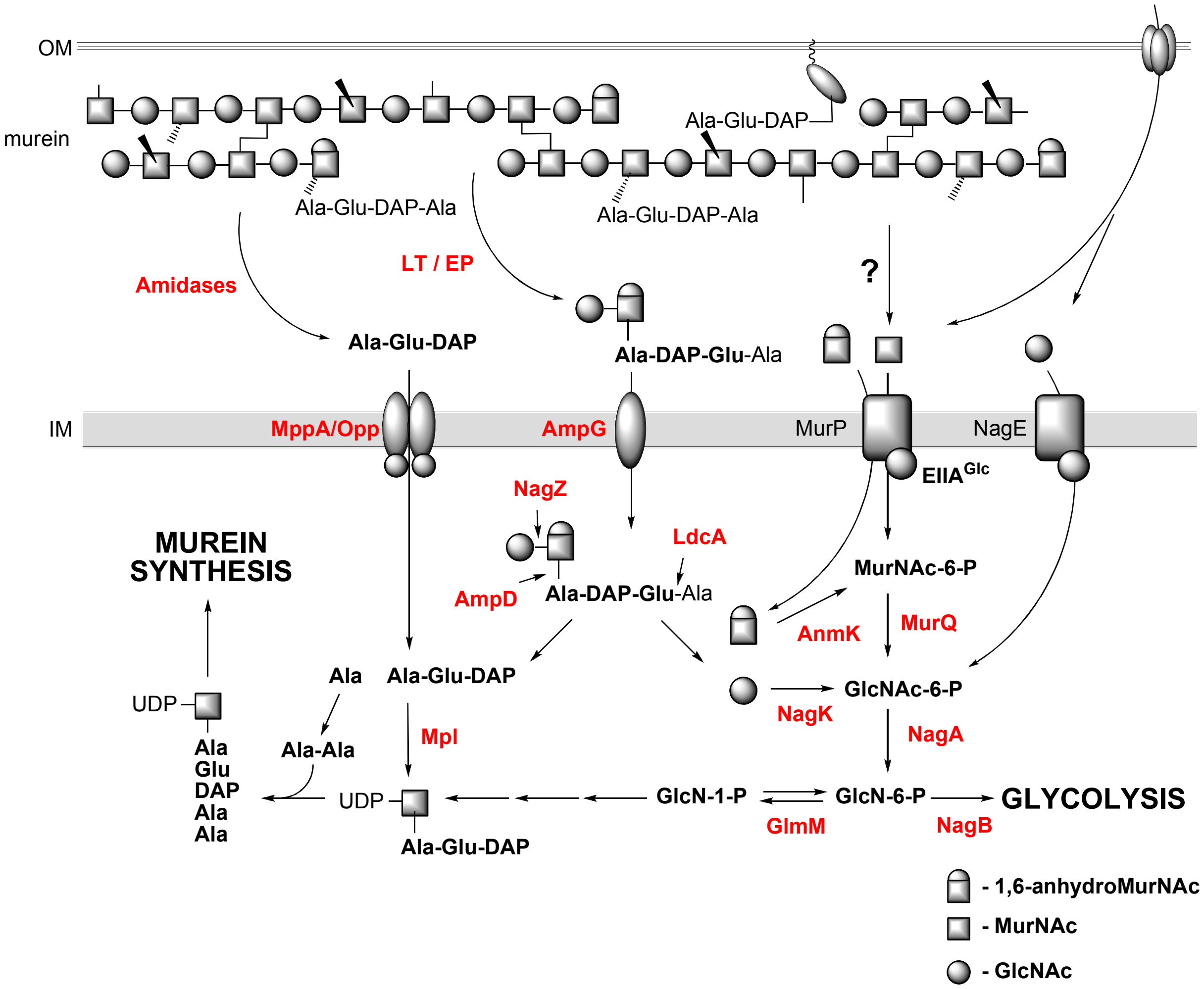

Figure 11: Recycling of the peptidoglycan turnover products in *E. coli*. The turnover products, generated by the action of lytic transglycosylases and endopeptidases, enter the cell via permease AmpG. In the cytoplasm the anhydromuropeptides are degraded by the combined action of AmpD, LdcA and NagZ yielding the tripeptide (L-Ala-γ-D-Glu-*m*-DAP; short: Ala-Glu-DAP) and the free amino sugars GlcNAc and 1,6-anhydroMurNAc. GlcNAc is converted to GlcNAc-6-P by NagK, whereas 1,6-anhydroMurNAc is first phosphorylated by AnmK with concomitant cleavage of the 1,6-anhydro bond yielding MurNAc-6-P. Afterwards MurNAc-6-P is converted to GlcNAc-6-P by etherase MurQ. GlcNAc-6-P is transferred to GlcN-6-P, which either enters glycolysis or the murein biosynthesis pathway. The tripeptide either directly reenters the biosynthetic pathway catalyzed by Mpl (muropeptide ligase) or is further degraded into its separate amino acids. During cell separation muropeptides are also generated in the periplasm and can enter the cell by the MppA/Opp transporter. Furthermore *E. coli* can grow on GlcNAc and MurNAc as sole carbon sources provided from the exterior. The amino sugars are taken up with concomitant phosphorylation by their specific phosphotransferase systems (PTS) into the cytoplasm. 1,6-anhydroMurNAc can also be taken up by the MurNAc-specific PTS, but it is not phosphorylated (Uehara et al., 2006). The picture was taken from Jaeger and Mayer, 2008a. The used symbols for GlcNAc, MurNAc and 1,6-anhydroMurNAc are shown as figure insert. The peptides L-Ala-γ-D-Glu-*m*-DAP-D-Ala-D-Ala are abbreviated with Ala-Glu-DAP-Ala-Ala.

Despite the fact of cell wall turnover (Mauck et al., 1971; Mauck and Glaser, 1970) and the identification of more than 30 candidates of peptidoglycan hydrolases (Smith et al., 2000), a pathway for peptidoglycan recycling in *B. subtilis* and other Gram-positive bacteria could not be identified.

Although *B. subtilis* lacks the transmembrane permease AmpG and therefore the uptake of the turnover products is unclear, it contains orthologs of recycling enzymes of *E. coli*: a β-*N*-acetylglucosaminidase NagZ (formerly YbbD), a MurNAc phosphotransferase system MurP (YbbF), a MurNAc-6-phosphate etherase MurQ (YbbI) and also orthologs of LdcA (YkfA), MpaA (YqgT) and YcjG (YkfB) (Park and Uehara, 2008).

Interestingly the gene encoding the β-*N*-acetylglucosaminidase of *B. subtilis*, *nagZ* (formerly *ybbD*), is organized in a cluster together with genes showing high sequence identity to genes involved in MurNAc dissimilation and murein recycling in *E. coli*: *ybbI*, an ortholog of the MurNAc-6-phosphate etherase (*murQ*), *ybbH*, an ortholog of the MurNAc-6-phosphate-specific transcriptional repressor (*murR*) and *ybbF*, an ortholog of the MurNAc-specific phosphotransferase system (*murP*). Furthermore two putative muropeptidases (*amiE*, formerly *ybbE*, and *ybbC*) are also localized in the cluster (Fig. 12). In contrast to the β-*N*-acetylglucosaminidase NagZ of *E. coli* (*Ec*NagZ), NagZ of *B. subtilis* (*Bs*NagZ) as well as AmiE (formerly YbbE) and YbbC of *B. subtilis* possess a signal sequence and hence are secretory proteins.

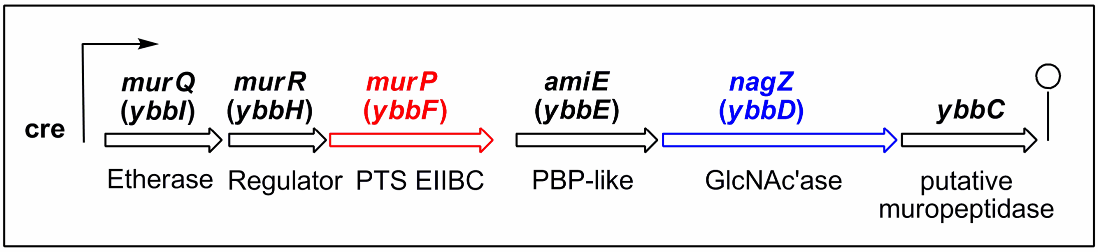

Figure 12: The gene cluster of *B. subtilis* presumably involved in peptidoglycan recycling. Peptidoglycan recycling has not yet been clarified in Gram-positive bacteria. On the chromosome of *B. subtilis* a cluster of six genes encoding orthologos to enzymes involved in MurNAc dissimilation and murein recycling in *E. coli* was identified. It contains genes encoding orthologs of the MurNAc-6-phosphate etherase, MurQ (YbbI), the MurNAc-6-phosphate-specific repressor, MurR (YbbH) and the MurNAc phosphotransferase system, MurP (YbbF). Furthermore NagZ (formerly YbbD), an ortholog of the recycling β-*N*-acetylglucosaminidase of *E. coli*, as well as two putative muropeptidases, AmiE (formerlyYbbE) and YbbC, are encoded by this cluster.

In *E. coli murP* and *murQ* are part of an operon (Jaeger et al., 2005) and are constitutive expressed at low level. The transcriptional regulatory protein, MurR, is divergently transcribed from the *murQP* operon and functions as a repressor of the operon by binding as tetramer to the operator (Jaeger and Mayer, 2008b). Both, *murR* and *murQ*, are expressed from unusual convergent promoters. MurNAc-6-P, the substrate of the etherase MurQ, is the inducer and interferes with MurR-DNA binding. Furthermore the expression of *murR* and *murQ* is subject to catabolite repression. The transcription of *murQ* depends on activation by cAMP-CAP (catabolite activator protein) in absence of glucose, whereas the transcription of *murR* is probably inhibited by cAMP-CAP. The constitutive expression of low-levels of MurQ is required for the recycling of peptidoglycan fragments that are continuously released from the murein sacculus during growth, whereas growth on external MurNAc as sole source of carbon depends on high-level expression of the operon (Jaeger and Mayer, 2008b).

The regulatory features of the *ybb*-cluster in *B. subtilis* have not been studied as yet. The expression of the cluster seems also to be regulated by carbon catabolite repression since the highly conserved catabolite response element (*cre*) of Gram-positive bacteria is located upstream of the cluster. Furthermore accumulation of MurNAc-6-P could also induce the transcription of the cluster as it is the case in *E. coli*.

Structure and mechanism of β-*N*-acetylglucosaminidases

Bacterial β-*N*-acetylglucosaminidases including NagZ of *E. coli* (*Ec*NagZ) and NagZ of *B. subtilis* (*Bs*NagZ) show high amino acid sequence identitity with enzymes of family 3 of glycoside hydrolases (classified in the CAZY database according to sequence identities: www.cazy.org) comprising primarily β-glucosidases, β-xylosidases and exo-β-1,3-1,4-glucanases. The β-*N*-acetylglucosaminidases build up a subgroup of family 3 glycosidases that are characterized by the conserved sequence pattern K-H-(FI)-P-G-(HL)-G-x(4)-D-(ST)-H which is presumably involved in *N*-acetyl group binding (Mayer et al., 2000a; Vocadlo et al., 2000). The mechanism of family 3 β-glucosidases and β-glucan exohydrolases was investigated in detail in the last years showing that enzymes in this family operate via a double displacement retaining mechanism. In general retaining enzymes catalyze the hydrolysis of their substrates via two steps, in which two carboxylic groups assist in the formation and the breakdown of a glycosyl-enzyme intermediate (Fig. 13) (Rye and Withers, 2000). The first carboxyl group functions as a nucleophile which attacks the sugar anomeric center and displaces the leaving group yielding a glycosyl-enzyme intermediate. The other carboxyl group acts as an acid/base catalyst. In the first step (glycosylation) it functions as an acid accelerating the departure of the leaving group by protonation of the glycosidic oxygen. In the second step (deglycosylation) it acts as a base catalyst to promote the attack of water at the anomeric center of the glycosyl-enzyme intermediate resulting in cleavage of the glycosidic bond with release of the product and the free enzyme (Mayer et al., 2000a).

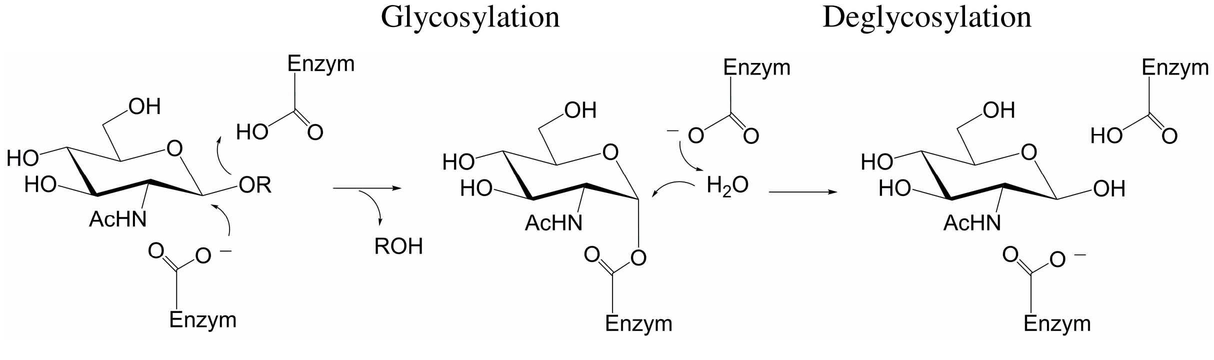

Figure 13: Mechanism of retaining family 3 glycosyl hydrolases. Family 3 of glycoside hydrolases catalyze the hydrolysis of β-glycosidic linkages using a two-step double displacement mechanism under retention of the anomeric configuration. Two carboxyl groups in the active site are involved in cleavage of the glycosidic bond. The first carboxyl group functions as nucleophile to yield a covalent glycosyl-enzyme intermediate, the other functions as acid/base catalyst.

The first crystal structure of a family 3 enzyme was that of the β-glucan exohydrolase of *Hordeum vulgare* (*Hv*ExoI) (Varghese et al., 1999). The structure reveals two distinct domains, a $(\alpha/\beta)_8$-TIM-barrel domain (*N*-terminal domain) and a six-stranded β-sandwich domain (*C*-terminal domain) (Fig. 14). The active site forms a cleft within the interface of the two domains and on the basis of the structure Asp285 was identified as the catalytic nucleophile residing on the TIM-barrel domain, whereas Glu491 on the sandwich domain was proposed to function as the general acid/base catalyst (Harvey et al., 2000; Hrmova et al., 2004; Varghese et al., 1999).

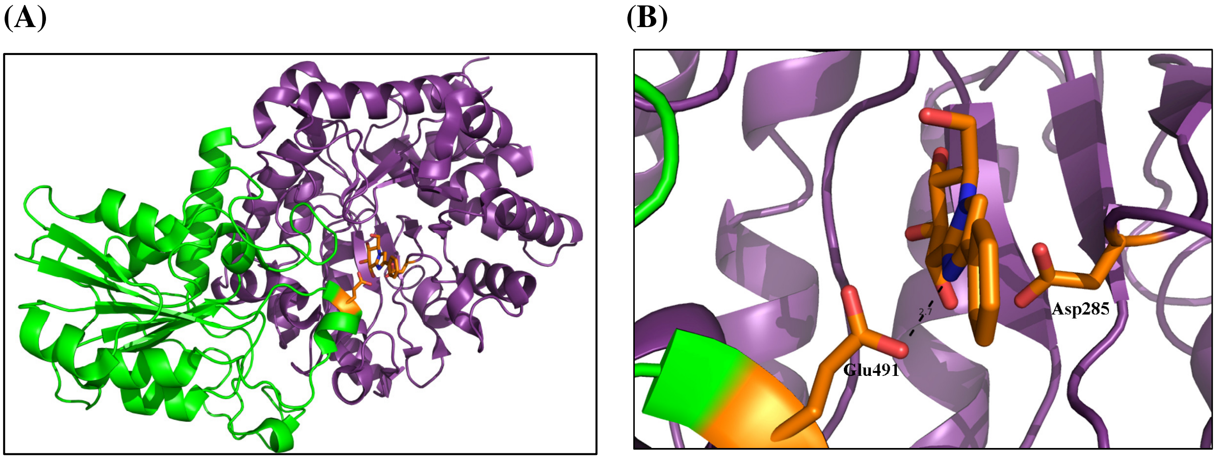

Figure 14: A. Structure of ExoI of *Hordeum vulgare* in complex with gluco-phenylimidazole. ExoI consists of two domains. The *N*-terminal domain (purple) forms a $(\alpha/\beta)_8$ TIM-barrel, whereas the *C*-terminal domain is a $(\alpha/\beta)_6$-sandwich (green). **B. Detailed view of the active site of ExoI.** The conserved aspartate residue (Asp285) on the *N*-terminal domain has been identified as the catalytic nucleophile, whereas Glu491 functions as acid/base catalyst.

Furthermore the catalytic nucleophile was identified for several family 3 glycosidases by trapping the glycosyl-enzyme intermediate using fluorinated substrate analogues (Chir et al., 2002; Dan et al., 2000; Hrmova et al., 2001; Mayer et al., 2000a; Vocadlo et al., 2000). The catalytic nucleophile of a family 3 β-*N*-acetylglucosaminidase, ExoII of *Vibrio furnisii*, was identified using the slow substrate *N*-acetyl-5-fluoro-α-L-idopyranosyminyl fluoride (Vocadlo et al., 2000). This residue, an aspartate, is conserved within all family 3 glycosidases. An amino acid functioning as the general acid/base catalyst in β-*N*-acetylglucosaminidases could not yet be identified and is apparently missing since ExoII of *Vibrio furnisii*, NagZ of *E. coli* and other β-*N*-acetylglucosaminidases of Gram-negative bacteria comprise only the $(\alpha/\beta)_8$-TIM-barrel domain. It had been speculated that in NagZ of *E. coli*, which hydrolyzes the glycosidic bond between GlcNAc and MurNAc, the acidic residue of the lactyl group of the *N*-acetylmuramic acid could function as acid/base catalyst.

In contrast the β-*N*-acetylglucosaminidase NagZ of *B. subtilis* comprises two modules and it is an extracellular protein, whereas *Ec*NagZ and other β-*N*-acetylglucosaminidases of Gram-negative bacteria are cytoplasmic and consist only of one domain.

Hence the detailed mechanism of family 3 β-*N*-acetylglucosaminidases remains enigmatic and raises the question whether these enzymes operate by general acid/base catalysis involving an as yet unidentified enzymatic glutamate as other glycosidases of family 3.

Aim of this thesis

The general aim of this thesis is the characterization of a gene cluster of *B. subtilis* putatively involved in peptidoglycan recycling in this organism. This cluster encodes orthologs of enzymes involved in MurNAc dissimilation and muropeptide recycling in *E. coli*, e.g the MurNAc-6-phosphate etherase MurQ, the MurNAc-6-phosphate-specific transcriptional repressor MurR and the MurNAc-specific phosphotransferase system MurP. Two further gene products of this cluster, NagZ (formerly YbbD), a putative β-*N*-acetylglucosaminidase as well as the putative muropeptidase AmiE (YbbE) and their role in peptidoglycan recycling in *B. subtilis* were investigated and are subject of Chapter 1.

The β-*N*-acetylglucosaminidase NagZ of *B. subtilis* as its *E. coli* ortholog *Ec*NagZ belongs to family 3 of glycosyl hydrolases. These enzymes catalyze the hydrolysis of their substrates by two carboxyl groups functioning as nucleophile and general acid/base catalyst. While the nucleophile is conserved within all family 3 glycosidases, the general acid/base catalyst was only identified in β-glucosidases of this family. It resides on the *C*-terminal domain that is missing in *Ec*NagZ. In contrast NagZ of *B. subtilis* possesses an additional *C*-terminal domain which may take part in the reaction mechanism. We were interested in identifying a possible general acid/base catalyst of NagZ of *B. subtilis*. Structural and kinetic analyses of NagZ gave insights into the mechanism of β-*N*-acetylglucosaminidases involved in cell wall metabolism and are presented in Chapter 2.

LIST OF PUBLICATIONS

This thesis is based on the following submitted paper and manuscript:

CHAPTER 1: **Silke Litzinger**, Katja Nitzsche, Christian Risinger, Valentin Wittmann and Christoph Mayer (2009)
Muropeptide recycling in *Bacillus subtilis* involves sequential hydrolysis by exo-β-*N*-acetylglucosaminidase and *N*-acetylmuramyl-L-alanine amidase
submitted to *J. Bact.*, 18.09.2009 (Manuscript number: JBO 1256-09)

CHAPTER 2: **Silke Litzinger**, Stefanie Fischer, Patrick Polzer, Kay Diederichs, Wolfram Welte and Christoph Mayer (2009)
A unique glycosidase mechanism: an Asp-His dyad is the general acid/base catalyst of family 3 β-*N*-acetylglucosaminidases
to be submitted to *PNAS*

Additional publications:

Silke Litzinger and Christoph Mayer (2009). The Murein Sacculus.
Chapter 2 *In* Prokaryotic cell wall compounds - Structure and biochemistry.
H. König, H. Claus and A. Varma, editors. Springer, Heidelberg, Berlin, New York, in press

Silke Litzinger and Christoph Mayer (2009). Bacterial cell wall recycling.
Encyclopedia of Life Sciences (http://www.els.net/),
in preparation

CHAPTER 1

Muropeptide recycling in *Bacillus subtilis* involves sequential hydrolysis by exo-β-*N*-acetylglucosaminidase and *N*-acetylmuramyl-L-alanine amidase

ABSTRACT

We identified a pathway in the Gram-positive bacterial model organism *Bacillus subtilis* that is destined for recovery of *N*-acetylglucosamine-*N*-acetylmuramic acid-peptides (muro-epides) derived from the peptidoglycan of the cell wall. The pathway is encoded by a cluster of six genes of which the first three are orthologs of *Escherichia coli* genes involved in *N*-acetylmuramic acid (MurNAc) dissimilation, encoding the MurNAc-6-phosphate etherase (MurQ), the MurNAc-6-phosphate-specific transcriptional regulator (MurR) and the MurNAc-specific phosphotransferase system (MurP). Here we characterized two further genes of this cluster. The first was shown to encode a cell wall associated exo-β-*N*-acetylglucosaminidase (NagZ, formerly YbbD) that cleaves the terminal non-reducing *N*-acetylglucosamine of muropeptides and also accepts chromogenic/fluorogenic β-*N*-acetylglucosaminides. The second was shown to encode an amidase (AmiE, formerly YbbE) that hydrolyzes the *N*-acetylmuramyl-L-Ala bond of MurNAc-peptides but not of muropeptides. Hence AmiE requires NagZ and in conjunction the enzymes liberate MurNAc by sequential hydrolysis of muropeptides. We recognized that NagZ is identical to an enzyme that was partially purified and characterized in the early 1970s. It is non-covalently associated with the cell wall and can be released from particulate wall material with salt. Protein production was induced at late exponential phase and reached some 6-fold higher level in the stationary/autolysis phase. The muropeptide catabolic pathway presented here is the first evidence for cell wall recycling in a Gram-positive organism that proceeds distinct from the cell wall recycling pathway of *E. coli* and other Gram-negative bacteria.

INTRODUCTION

Bacteria are covered by a firm cell wall that protects the fragile membrane-enclosed cell, the protoplast, and withstands the high internal pressure of the cell, the turgor (Höltje, 1998). Despite its stabilizing function the cell wall is not rigid and static but highly flexible and undergoes a permanent resynthesis, remodelling and degradation (turnover) by which an estimated 50% of the murein or peptidoglycan, the stabilizing component of the bacterial cell wall, is released in one generation during logarithmic growth (Boothby et al., 1973; Park and Uehara, 2008). In contrast to Gram-negative bacteria, which possess an outer membrane that keeps most of the cell wall turnover products within the periplasmic space, Gram-positive bacteria lack such a membrane barrier and therefore cannot retain their turnover products. The Gram-positive model organism *Bacillus subtilis* was shown to release extensive amounts of murein fragments into the growth medium during growth (Mauck et al., 1971; Mauck and Glaser, 1970). Since these early findings more than 30 peptidoglycan hydrolases of *B. subtilis* were characterized or identified as autolysin candidates on the basis of amino acid sequence identity (Smith et al., 2000). However a cell wall recycling/recovery pathway has not been identified in this organism or in any other Gram-positive bacteria, so far.

In contrast cell wall turnover and recycling in the Gram-negative model bacterium *Escherichia coli* is well studied (for a recent review see (Park and Uehara, 2008)). *E. coli* also degrades about 50% of the murein (peptidoglycan) of the cell wall in each generation during growth and the turnover products are efficiently reutilized (i.e. recycled) (Goodell, 1985). The principal degradation products are GlcNAc-1,6-anhydroMurNAc-peptides (anhydromuropeptides) which are released from the peptidoglycan during cell growth by the action of lytic transglycosylases, endopeptidases and carboxypeptidases, yielding primarily GlcNAc-1,6-anhydroMurNAc (anhMurNAc)-L-Ala-γ-D-Glu-*meso*-diaminopimelic acid (*m*-Dap)-D-Ala (reviewed in (Höltje, 1998)). Anhydromuropeptides are taken up by the secondary transport system AmpG (Cheng and Park, 2002) and are further degraded in the cytoplasm by NagZ, a β-*N*-acetylglucosaminidase (Cheng et al., 2000; Vötsch and Templin, 2000), AmpD, an anhMurNAc-L-Ala amidase (Höltje et al., 1994; Jacobs et al., 1995) and LdcA, an L,D-carboxypeptidase (Templin et al., 1999) together releasing GlcNAc, anhMurNAc, D-Ala and L-Ala-γ-D-Glu-*m*-Dap in the cytosol. The tripeptide is directly fed into the murein biosynthesis pathway by muropeptide ligase Mpl that transfers the tripeptide to UDP-MurNAc (Mengin-Lecreulx et al., 1996) but the tripeptide can also be degraded to its individual amino acids by γ-D-glutaminyl-*m*-Dap amidase (MpaA) and L-Ala-D/L-Glu epimerase (YcjG) (Schmidt et al., 2001; Uehara and Park, 2003). GlcNAc and anhMurNAc are also recycled (Park, 2001). GlcNAc is converted to GlcNAc-6-phosphate by GlcNAc kinase NagK (Uehara and Park, 2004), whereas anhMurNAc is first phosphorylated by kinase AnmK yielding MurNAc-6-phosphate which is then converted to GlcNAc-6-phosphate by etherase MurQ cleaving the lactyl ether substituent of MurNAc-6-phosphate (Hadi et al., 2008; Jaeger et al., 2005; Jaeger and Mayer, 2008a; Uehara et al., 2006; Uehara et al., 2005). Besides recycling anhydromuropeptides, *E. coli* was shown to utilize MurNAc as the sole source of carbon (Jaeger et al., 2005). MurNAc is imported and phosphorylated by the specific phosphotransferase system MurP yielding cytoplasmic MurNAc-6-phosphate (Dahl et al., 2004). MurQ, the same lactyl etherase that is required for recycling of anhMurNAc, is also essential for growth on MurNAc (Jaeger et al., 2005). Recently the transcriptional regulator MurR was characterized which together with the catabolite activator protein CAP regulates the MurNAc etherase operon in *E. coli* (Jaeger and Mayer, 2008b).

We have now identified a cluster of six genes displayed on the chromosome of *B. subtilis* which show high sequence similarity with genes involved in MurNAc dissimilation and cell wall recycling in *E. coli* (Fig. 15): *ybbI*, an ortholog of the MurNAc-6-phosphate etherase (*murQ)*, *ybbH*, an ortholog of the MurNAc-6-phosphate-specific transcriptional repressor (*murR)* and *ybbF*, an ortholog of the MurNAc-specific phosphotransferase system (*murP).* Amino acid sequence identities of the *Bacillus* proteins towards the *E. coli* orthologs are 47%, 26% and 38%, respectively. In this work we characterized two further proteins encoded by genes of the putative recycling cluster, *ybbD* (renamed *nagZ)* and *ybbE* (renamed *amiE). B. subtilis nagZ* (*BsnagZ*) is an ortholog of the recycling β-*N*-acetylglucosaminidase of *E. coli nagZ* (*EcnagZ*) but in contrast to the latter the protein is secreted and harbours an additional *C*-terminal domain of unknown function. Here we showed that *BsnagZ* encodes an enzyme which is identical to an entity that was characterized in the early 1970s and that was proposed to be involved in the recycling of the own cell wall during growth (Berkeley et al., 1973; Ortiz et al., 1972). The enzyme hydrolyzes cell wall derived muropeptides as well as chromogenic/fluorogenic β-*N*-acetyl-D-glucosaminides and occurred in the late exponential and stationary growth phase mainly in a particulate form in the supernatant, but to a small extent also in association with the cells (Ortiz et al., 1972). NagZ is required to generate the substrate of another protein that is encoded by a gene of this recycling cluster, an *N*-acetylmuramyl-L-alanine amidase AmiE (formerly YbbE). Both enzymes together are part of a muropeptide recycling/recovery pathway in *B. subtilis*.

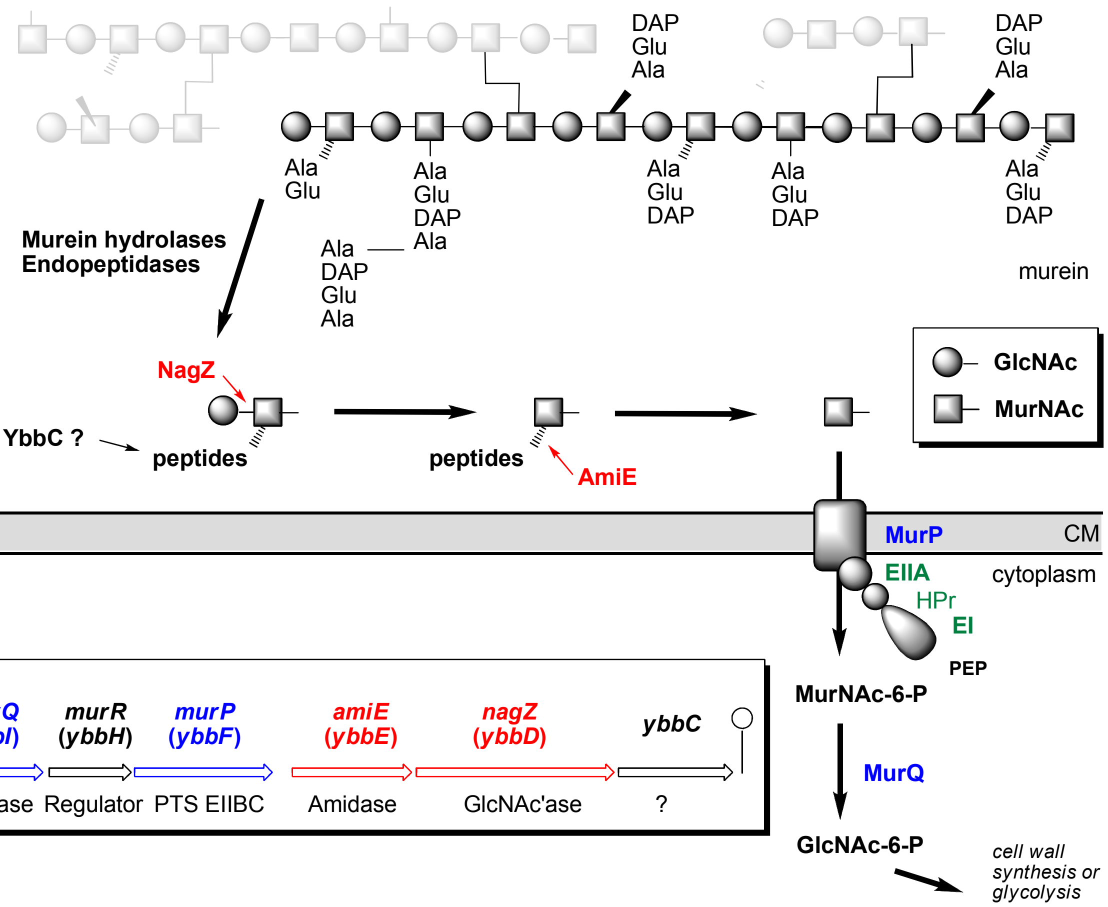

Figure 15. Scheme of the muropeptide recycling/recovery pathway of *B. subtilis* and organisation of the corresponding gene cluster. Muropeptides (GlcNAc-MurNAc-peptides, symbols as indicated; the peptides L-Ala-γ-D-Glu-*m*-DAP-D-Ala are abbreviated with Ala-Glu-DAP-Ala) released from the endogenous cell wall of *B. subtilis* or originating from the medium are further processed in the wall compartment by NagZ, cleaving the β-1,4-glycosidic bond, and subsequently by AmiE, cleaving the muramyl-L-Ala amide bond, thereby releasing GlcNAc, MurNAc and peptides. Recovery of MurNAc then proceeds similarly to MurNAc dissimilation in *E. coli*, involving a MurNAc-specific phosphotransferase system YbbF (MurP), by which MurNAc is taken up and simultaneously phosphorylated yielding MurNAc-6-phosphate. In the cytoplasm the etherase YbbI (MurQ) converts MurNAc-6-phosphate to GlcNAc-6-phosphate. YbbH (MurR) is a putative MurNAc-6-phosphate-specific transcriptional regulator and YbbC is so far of unknown function.

MATERIALS AND METHODS

Bacterial strains, plasmids, chemicals and growth conditions. All *E.coli* and *B. subtilis* strains and plasmids used in this work are listed in Table 2. Bacteria were grown aerobically at 37°C in LB. When appropriate, the chromosomal drug resistance marker in *B. subtilis* was selected with erythromycin (1 µg/ml). *E. coli* cells carrying plasmids were selected with ampicillin (100 µg/ml). 4-methylumbelliferyl-β-D-glucosaminide (4-Mu-β-GlcNH$_2$) was synthesized by Christian Risinger, AG Wittmann, Fachbereich Chemie, University of Konstanz. All reagents were from Sigma-Aldrich unless otherwise stated.

Table 2. Bacterial strains and plasmids used in this study.

Strains or plasmids	Relevant genotype[a] and features	Reference or source
	Strains	
E. coli		
MG1655	sequenced *E. coli* K-12 genome	(Blattner et al., 1997)
BL21(DE3)	F^- *ompT hsdS$_B$*($r_B^- m_B^-$) *gal dcm* (DE3)	(Studier and Moffatt, 1986)
B. subtilis		
B. subtilis 168	*trpC2*; sequenced *B. subtilis* genome	*Bacillus* Genetic Stock Center
ybbD::pMUTIN4	pMUTIN4 insertion into *nagZ*, Erm^r	*Bacillus* knockout collection (http://bacillus.genome.jp/) (Kobayashi et al., 2003)
	Plasmids	
pET16b	*E. coli* expression vector, P_{T7}, Amp^r, *ori*$_{pBR322}$, *lacI*, *N*-term. His$_{10}$-tag	Novagen
pASK-IBA32	*E. coli* expression vector, P_{tet}, Amp^r, *ori*$_{f1}$, *ompA*, *C*-term. His$_6$-tag	IBA
pET16b-*Bs*NagZ	IPTG-inducible cytoplasmic *Bs*NagZ-His$_{10}$ expression vector	This study
pASK-IBA32-*Bs*AmiE	anhydrotetracycline-inducible periplasmic *Bs*AmiE-His$_6$ expression vector	This study

[a] Amp^r, ampicillin resistant; Erm^r, erythromycin resistant

Cloning of *nagZ* and *amiE*. DNA preparation, restriction enzyme digest, ligation and transformation were performed according to standard techniques. *nagZ* was amplified by PCR without signal sequence using 30 ng of chromosomal DNA from *Bacillus subtilis* 168, 5 U PWO DNA-polymerase (Genaxxon Biosciences, Biberach, Germany) and the following primers: *Bs*NagZ/FP, 5'-AAA ACC ATG GGC CAT ATG TTT TTC GGG GCC AGA CAG AC-3' and *Bs*NagZ/RP, 5'-T TTT CTC GAG TTA AAG CGG TCT TCC CGT TTT G-3' (the recognition sites for the restriction endonucleases *Nde* I and *Xho* I are underlined, respectively). *amiE* was amplified without signal sequence using Phusion DNA-polymerase (Finnzymes Oy, Espoo, Finland) and primers with recognition sites for restriction endonuclease *Bsa* I (underlined): *Bs*AmiE/FP, 5'-ATC GTC GGT CTC AGG CCC AAA CAG CAG GCA ACT TGA TTG AG-3'; *Bs*AmiE/RP, 5'-ATC GTC GGT CTC AGC GCT CTC CAT CGC TTC ATA AAT CGC G-3'. Thirty cycles (15 s at 94°C, 30 s at 55°C and 120 s at 72°C) for *nagZ* and thirty five cycles (10 s at 98°C, 30 s at 50°C and 30 s at 72°C) for *amiE* were performed in a thermal cycler and revealed single 1.9-kb (*nagZ)* and 1.3-kb (*amiE*) fragments as analyzed by agarose gel electrophoresis. *nagZ* was cloned into vector pET16b under control of the T7 promoter (pET16b-*Bs*NagZ) and overexpressed in *E. coli* as a cytoplasmic *N*-terminal His$_{10}$-fusion protein. *amiE* was cloned into vector pASK-IBA32 (pASK-IBA32-*Bs*AmiE) under control of the tetracycline promoter and overexpressed in *E. coli* as periplasmic *C*-terminal His$_6$-fusion protein.

Overexpression and Purification of NagZ and AmiE. *E. coli* strains BL21(DE3) harbouring pET16b-*Bs*NagZ and pASK-IBA32-*Bs*AmiE were grown at 37°C in LB supplemented with ampicillin (100 µg/ml) under vigorous shaking. Expression of NagZ was induced at log-phase (OD$_{578}$ 0.5-0.6) by the addition of isopropyl-β-D-thiogalactopyranoside (IPTG) at a final concentration of 1 mM; expression of AmiE was induced at OD$_{578}$ 1.5 by addition of 200 µg L^{-1} anhydrotetracycline. Incubation was continued for further 3 h. Cells were harvested by centrifugation (4000 x *g* for 30 min at 4°C), resuspended in ice-cold sodium phosphate buffer (20 mM Na_2HPO_4 x $2H_2O$, 500 mM NaCl, pH 7.5) and disrupted by passing them three times through a French pressure cell. Debris and unbroken cells were removed by centrifugation at 100,000 x *g* for 1 h at 4°C. The His-tagged proteins in the supernatant were purified by Ni^{2+}-affinity chromatography on a 5 ml HiTrap HP column (Amersham-Pharmacia, Freiburg, Germany) pre-equilibrated with 20 mM sodium phosphate buffer, pH 7.5 and eluted from the column with elution buffer (sodium phosphate buffer supplemented with 500 mM imidazole, pH 7.5). The purity of the enzymes was assessed by sodium dodecyl sulfate polyacrylamide gel electrophoresis (SDS-PAGE). Peak fractions containing pure protein were concentrated and desalted by dialysis at 4°C against sodium phosphate buffer for enzymatic assays. The protein concentrations were determined by UV-absorption at 280 nm (calculated molar extinction coefficients are NagZ: $\varepsilon_{280\ \mathrm{nm}} = 36\ 330\ \mathrm{M}^{-1}\ \mathrm{cm}^{-1}$; AmiE: $\varepsilon_{280\ \mathrm{nm}} = 50\ 770\ \mathrm{M}^{-1}\ \mathrm{cm}^{-1}$) and by the Bradford method with bovine serum albumin as standard (Bradford, 1976).

Sedimentation of NagZ and extraction by salt. 8 ml overnight cultures of *B. subtilis* 168 grown in 50 ml LB medium in 300 ml Erlenmeyer flasks at 37°C under vigorous shaking were fractionated by centrifugation at 1200 x *g* for 10 min, 30,000 x *g* for 30 min or 100,000 x *g* for 30 min. The pellets were resuspended in 1 ml Clark and Lubs buffer (0.1 M KH_2PO_4/0.1 M NaOH, pH 5.8) and the supernatants were concentrated to 1 ml using Amicon Ultra-15 Centrifugal Filter Devices (Millipore). The amounts of the enzyme present in the supernatant and in the pellet after centrifugation were assayed as described below.

2 ml of the overnight cultures were mixed with 6 ml of aqueous solutions of NaCl at different concentrations made up in 0.05 M Tris-HCl buffer (pH 8.0). The cell suspensions were incubated at room temperature for 20 min and then centrifuged at 30,000 x *g* for 30 min according to a protocol by (Ortiz et al., 1972). The sedimented cells were resuspended in 1 ml Clark and Lubs buffer, pH 5.8 and the amount of NagZ remaining in the pellets was assayed as described below.

Expression of NagZ during growth. For expression studies strains *B. subtilis* 168 and *ybbD*::pMUTIN4 were cultivated in 5 L shaking flasks at 37°C in 1 L LB. Growth was monitored at 600 nm using an Ultrospec 3000 spectrophotometer (Pharmacia Biotech). After measuring the optical density (OD) a volume of the samples was taken that yields an OD 10.0 by centrifugation and slurrying the cell sediment in 1 ml of Clark and Lubs buffer, pH 5.8 (see above). The expression of NagZ was determined by an enzyme assay as described below.

Enzyme assays. NagZ activity was determined in 300 µl reactions at 37°C in 96-well plates (Greiner bio-one) over a period of 5 to 30 min by mixing equal volumes of enzyme solutions (cell suspension or supernatant), Clark and Lubs buffer, pH 5.8 (see above) and substrate, 3 mM 4-methylumbelliferyl-β-*N*-acetyl-D-glucosaminide (4-Mu-β-GlcNAc) or 4-nitrophenyl-β-*N*-acetyl-D-glucosaminide (pNP-β-GlcNAc). The reaction was initiated by addition of pretemperated substrate. The release of 4-methylumbelliferone was determined by fluorescence measurement on a Spectramax M2 Microplate Reader (Molecular Devices) with excitation wavelength of 362 nm and emission wavelength of 448 nm. The release of 4-nitrophenole was determined on the same device by measuring the absorption at 400 nm. One unit was defined as the amount of enzyme that hydrolyzes 1 µmol of substrate per min at pH 5.8 at 37°C. The extinction coefficient was determined by calibration using 4-methylumbelliferone and 4-nitrophenole standards. Kinetic parameters were determined using different concentrations of 4-Mu-β-GlcNAc in Clark and Lubs buffer, pH 5.8 and evaluated by nonlinear regression of the reaction curve using the program Prism 4 (GraphPad). The pH-activity profile of NagZ was determined in 0.1 M citric acid/0.2 M disodium phosphate buffer (McIlvaine) ranging from pH 4.0 to 8.0, in 0.2M sodium acetate acetic acid buffer ranging from pH 4.0 to 5.6 and in Clark and Lubs buffer in the range of pH 5.8 to 8.0. Enzyme reactions (300 µl; 1.5 mM 4-Mu-β-GlcNAc and NagZ concentrations of 1.5 x 10^{-3} mg ml^{-1}) were incubated over a period of 5 to 30 min at 37°C and were stopped by adding 9 volumes of 0.2 M Na_2CO_3 solution, pH 10.0.

Preparation of peptidoglycan from *E. coli* and *B. subtilis*. Peptidoglycan was isolated from *B. subtilis* 168 and *E. coli* MG1655 as described previously (Glauner, 1988; Harz et al., 1990; Young, 1996). In brief, bacteria were grown at 37° and harvested at OD_{578} 0.5 to 0.7. Cells were rapidly cooled to 4°C followed by centrifugation at 4000 x *g* for 30 min at 4°C. Cell pellets were resuspended in ice-cold distilled water (0.2 g/ml) and added dropwise under vigorous stirring to an equal volume of boiling 8% sodium dodecyl sulphate (SDS). When all cells were added, boiling was continued for 30 min to solubilize the membranes and degrade the DNA. The lysate was cooled to room temperature (RT) and the SDS-insoluble material was collected by centrifugation (100,000 x *g* for 60 min at RT). The pellet was resuspended in H_2O and dialyzed against H_2O until most of the SDS was removed. SDS content in the supernatant was controlled by the methylene blue assay as described earlier (Hayashi, 1975). Thereafter the peptidoglycan preparation was pelleted again by ultracentrifugation and resuspended in a minimal volume of H_2O. High molecular weight glycogen contamination trapped in the peptidoglycan preparation (Leutgeb and Weidel, 1963) was degraded by adding 100 µg/ml α-amylase (*Bacillus licheniformis*, Type XII-A, in 10 mM Tris-HCl, pH 7.0, 10 mM NaCl) for 2 h at 37°C. To inhibit lysozyme contaminations in the α-amylase preparation, 0.32 M imidazol (in 10 mM Tris-HCl, pH 7.0, 10 mM NaCl) was added. Afterwards degradation of lipoproteins covalently bound to *E. coli* peptidoglycan (Braun, 1975; Braun and Sieglin, 1970) was achieved by incubation for 1.5 h at 60°C with 200 µg/ml pronase (in

10 mM Tris-HCl, pH 7.0, plus 10 mM NaCl). Pronase (from *Streptomyces griseus,* Type XXV) was pre-treated by incubation for 2 h at 60°C. The sample was added again to an equal volume of boiling 8% SDS and kept boiling for 15 min. Afterwards the purified peptidoglycan was ultracentrifuged and was washed free from SDS by dialysis as described above.

Preparation of muropeptides. Muropeptides were prepared by digestion of peptidoglycan at 37°C overnight with 1 µg/40 µl mutanolysin (from *Streptomyces globisporus*; 1 mg/ml in 20 mM sodium phosphate buffer, pH 5.5). The enzyme reaction was stopped by boiling for 5 min, insoluble contaminations were removed by centrifugation and the released muropeptides in the supernatant were stored at -20°C. After digestion with mutanolysin the muropeptides released from the peptidoglycan have MurNAc as terminal reducing sugar (Young, 1996), which can be labelled with 8-aminonaphthalene-1,3,6-trisulfonic acid (ANTS) and separated by polyacryamide gel electrophoresis as described below.

Muropeptide degradation by NagZ and AmiE. Muropeptides as well as intact peptidoglycan from *E. coli* or *B. subtilis* were incubated with the purified proteins (NagZ and AmiE; 10 µg/40µl) at 37°C for 2 h and the reaction was monitored by reversed-phase HPLC (RP-HPLC) and fluorophore-assisted carbohydrate electrophoresis (FACE). A RP-C18 column (Gemini 5 µ C18 150 x 4.60 mm; Phenomenex) was used to separate the muropeptides and other cell wall components that were monitored at multiple wavelengths (205, 235 and 280 nm) using an UV-detector (UltiMate 3000 Photodiode Array Detector). 25 µl samples were applied to the HPLC-column and elution was performed for 5 min with buffer A (0.05% trifluoroacetic acid) and then for 50 min with a linear gradient from 0 to 100 % with buffer B (0.035% trifluoroacetic acid and 10% CH_3CN) at a flow rate of 0.5 ml/min (according to (Cheng et al., 2000)). The peaks obtained were collected and lyophilized. One part of the samples were tagged with ANTS and separated by FACE as described below and another part was analyzed by matrix-assisted laser desorption/ionisation-time-of-flight mass spectrometry (MALDI-TOF). For analysis by MALDI-TOF the samples were dissolved in acetonitrile. 0.7 µl of the sample solution were mixed with 0.7 µl of the matrix solution (saturated solution of CHCA (α-cyano-4-hydroxycinnamic acid in acetonitrile) directly on the MALDI target. MALDI-TOF mass spectra were recorded on a Bruker Biflex III spectrometer in positive, reflectron mode with a delayed extraction MALDI source and a pulsed nitrogen laser (337 nm).

Fluorescent labelling of carbohydrate standards and muropeptides. Reducing carbohydrates and muropeptides were tagged at their terminal semi-acetal with the charged, fluorescent molecule 8-aminonaphthalene-1,3,6-trisulfonic acid (ANTS) as published previously (Jackson, 1990; Stack and Sullivan, 1992). 10 mM carbohydrate stock solutions were prepared from D-glucose, maltose, maltotriose, maltotetraose, maltopentaose, maltohexaose, maltoheptaose, GlcNAc, MurNAc and GlcNAc-MurNAc in water (Goins and Cutler, 2000). 1 µmol aliquots of the carbohydrate solutions and 40 µl aliquots of the muropeptides/cell wall fragments were dried in a speed vac (Jackson, 1994). The dried carbohydrate/muropeptide samples were suspended in 5.0 µl of 0.2 M ANTS dissolved in acetic acid:water (3:17, vol/vol) and 5.0 µl 1.0 M sodium cyanoborohydride ($NaCNBH_3$) dissolved in dimethyl sulfoxide (DMSO). After incubation for 16 h (overnight) at 37°C the samples were dried again in a speed vac at 45°C for 4 h. The carbohydrate standards were suspended to 100 pmol/µl in loading buffer (62.5 mM Tris-HCL, pH 6.8 and 20% glycerol) and stored at -80°C. The cell wall samples were dissolved in 50 µl loading buffer and diluted subsequently in loading buffer as required and also stored at -80°C.

Electrophoresis and visualization of ANTS-labelled muropeptides. FACE was performed as reported by (Goins and Cutler, 2000). Gels 8.3 cm (width) x 7.2 cm (height) x approx. 0.75 mm (thickness) were prepared. The resolving gel was 32% acrylamide and 2.4% bisacrylamide (Goins and Cutler, 2000). For 10 ml of resolving gel (2 acrylamide gels), 5 µl of *N,N,N´,N´,*-tetramethylethylenediamine (TEMED) and 50 µl of 10% ammonium persulfate (APS) were added. The stacking gel consisted of 8% acrylamide and 0.6% bisacrylamide containing 5 µl TEMED and 50 µl APS for 5 ml of stacking gel. The gel buffer was 0.42 M Tris-HCL, pH 8.5 and the running buffer was 0.025 M Tris base and 0.192 M glycine, pH 8.4 (Goins and Cutler, 2000). 800 pmol of the carbohydrate standards and the muropeptides were loaded on the acrylamide gel. Trace amounts of bromphenol blue in loading buffer were loaded in a single well as a visual reference. Electrophoresis was run constant at 30 mA for 3 h in a cooled system. Fluorescent-labelled carbohydrates and muropeptides were visualized by exposing the gel to a 312 nm wavelength UV-light and pictures were taken with a gel imaging system.

RESULTS

***nagZ* encodes an exo-GlcNAc'ase that is identical to an enzyme characterized in the 1970s.** The enzyme NagZ was overexpressed as cytoplasmic construct in *E. coli* and purified by Ni^{2+}-affinity chromatography to apparent homogeneity. The protein has a molecular weight of about 70 to 75 kDa as analyzed by sodium dodecyl sulfate polyacrylamide gel electrophoresis (SDS-PAGE) and displayed *N*-acetylglucosaminidase activity. Kinetic parameters for NagZ were determined with the chromogenic and fluorogenic substrates pNP-β-GlcNAc and 4-Mu-β-GlcNAc, respectively (Table 3). Notably the enzyme did not show activity against 4-Mu-β-$GlcNH_2$.

Table 3. Kinetic parameters.

Substrate	K_M [µM]	v_{max} [µmol min^{-1} mg^{-1}]	k_{cat} [s^{-1}]	k_{cat}/K_M [s^{-1} mM^{-1}]
4-Mu-β-GlcNAc	109.6 ± 4.3	5.39 ± 0.07	6.4	58.4
pNP-β-GlcNAc	171.6 ± 7.7	8.33 ± 0.04	9.9	57.7

The purified protein was stable for several months at 4°C in the pH range 4.0 to 8.0. We also studied the pH activity dependency of purified NagZ using a discontinuous assay with 4-Mu-β-GlcNAc as substrate as described in Materials and Methods. Plotting k_{cat} against pH revealed a bell-shaped curve with an optimum pH in the range of 5.8 to 6.2 (Fig. 16).

NagZ is found associated with particulate material in the culture supernatant. We showed that by increasing the centrifugal force the amount of NagZ present in the culture supernatant decreased to one-third of the initial value, whereas the amount in the pellet increases, respectively (Table 4). NagZ was released from particulate material of overnight cultures through treatment by different NaCl concentrations as shown in Fig. 17. With 750 mM NaCl about 75% of the enzyme was released from sedimented material. Notably a significant amount of *N*-acetylglucosaminidase activity (about 20% of the total activity) remained cell wall associated (Table 4) and could not be removed by salt (Fig. 17)

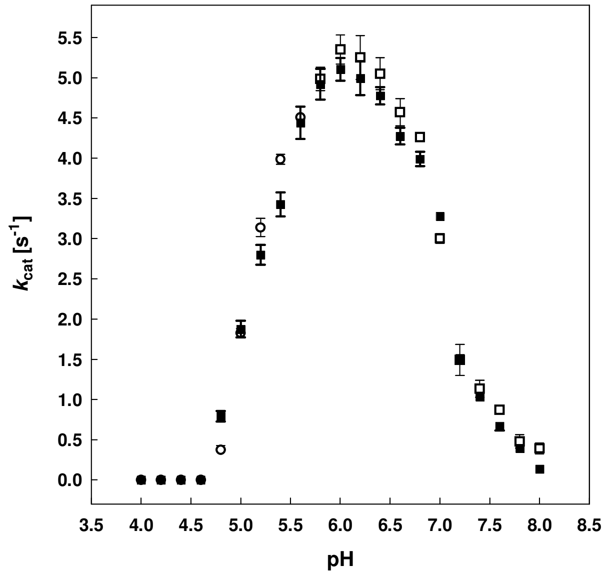

Figure 16. pH-activity profile of NagZ. The k_{cat} versus pH plot revealed a bell-shaped curve with a pH-optimum in the range of 5.8 to 6.2. The buffers were: 0.1 M citric acid/0.2 M disodium phosphate buffer (McIlvaine) ranging from pH 4.0 to 8.0 (■); 0.2M sodium acetate acetic acid buffer ranging from pH 4.0 to 5.6 (○) and Clark and Lubs solution (0.1 M KH_2PO_4/0.1 M NaOH) in the range of pH 5.8 to 8.0 (□).

Table 4. Sedimentation of β-*N*-acetylglucosaminidase activity from cultures of *B. subtilis*.

Treatment	% of enzyme remaining in the supernatant	
	This study	According to (Ortiz et al., 1972)
1200 x *g* for 10 min	81	87
30,000 x *g* for 30 min	37	31
100,000 x *g* for 30 min	25	26

Overnight cultures (8 ml) of *B. subtilis* wild-type 168 were harvested by centrifugation at centrifugal forces as indicated. The amounts of enzyme present in the pellet and the supernatant remaining after centrifugation were assayed as described in Materials and Methods. Values were compared with published data of a partially purified *N*-acetylglucosaminidase (Ortiz et al., 1972).

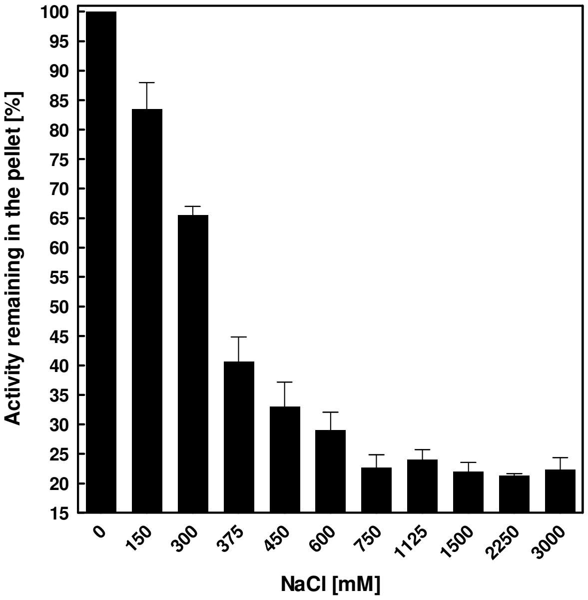

Figure 17. Release of NagZ from particulate material by salt. Overnight cultures of *B. subtilis* 168 were incubated for 20 min at RT with NaCl at different concentrations and then centrifuged at 30,000 x *g* for 30 min. The amount of enzyme remaining in the pellet was determined and indicated as percentage of the amount found in the pellet without NaCl treatment.

We further studied the expression of NagZ during growth of *B. subtilis* by measuring the activity with 4-Mu-β-GlcNAc in wild-type cells and deletion strain (*ybbD*::pMUTIN4). GlcNAc'ase activity appeared during the late exponential/early stationary phase of vegetative growing *B. subtilis* wild-type cells (Fig. 18). However the expression level was 6-fold higher after 25 h when the cells entered the autolysis phase. In this growth phase GlcNAc'ase activity in the deletion strain was marginal (less than 5% of wild-type activity).

All the results described above indicate that NagZ is identical to the β-*N*-acetylglucosaminidase first reported by Ortiz and Berkeley (Berkeley et al., 1973; Ortiz et al., 1972). In 1972 Ortiz and colleagues reported on an exo-β-*N*-acetylglucosaminidase that is produced towards the end of growth and mainly found in a sedimentable form in the growth medium (Ortiz et al., 1972) which was further characterized by Berkeley and colleagues one year later (Berkeley et al., 1973). A comparison of the characteristics of the protein described by Oritz and Berkeley and NagZ is given in Table 5, on which basis it was concluded that both enzymes are identical.

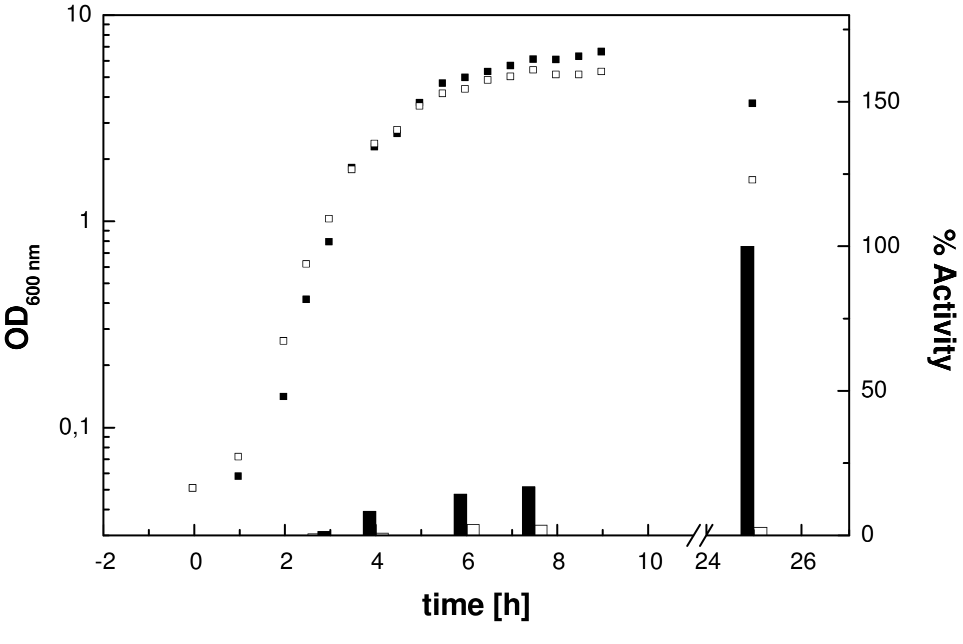

Figure 18. Occurrence of NagZ during growth of wild-type *B. subtilis* 168 and mutant *ybbD*::pMUTIN4. *N*-acetylglucosaminidase activity appeared in *B. subtilis* 168 cells during growth at 37°C in LB in the exponential phase, increased in stationary phase (black squares) but reached highest levels in the late stationary/decay phase (25h). The activity was measured using a discontinuous assay with the fluorescent substrate 4-Mu-β-GlcNAc. 100% activity equals 7.4 x 10^{-5} U/(OD_{600} = 1). Note that *N*-acetylglucosaminidase activity throughout the time course of a culture of the *nagZ* mutant (*ybbD*::pMUTIN4) was less than 30% of that of wild-type *B. subtilis* during early stationary phase and less than 5% in the late stationary/decay phase.

Table 5. Comparison of the biochemical characteristics of NagZ and partially purified GlcNAc'ase of *B. subtilis*.

	NagZ (this study)	Partially purified GlcNAc'ase of *B. subtilis* (Berkeley et al., 1973; Ortiz et al., 1972)
Occurence	produced towards the end of growth (i.e. late log phase, stationary phase)	
Compartmentalisation	released into medium mainly found in a sedimentable form (about 70 % in the 30,000 x *g* sediment) with increasing culture age more particulate material (after 15h: about 90 % in the 30,000 x *g* sediment)	
NaCl extraction	> 90 % released from cells and from sedimented material with 3 to 4 M NaCl at 30,000 x *g*	
pH optimum	5.8-6.2	5.9-6.0
most stable at	4.0- 8.0	8.5
pI	9.37 (calculated)	“seems to be 3.8”
MW	[a]71.3 kDa	75 kDa
K_M; specific activity pNP-β-GlcNAc	171.6 µM; 8.33 µmol min^{-1} mg^{-1}	150 µM 14.50 µmol min^{-1} mg^{-1}
K_M; specific activity 4-Mu-β-GlcNAc	109.6 ± 4.3 µM; 5.39 ± 0.07 µmol min^{-1} mg^{-1}	110 µM; 5.26 µmol min^{-1} mg^{-1}
K_M; Specific activity GlcNAc-MurNAc	n.d.	18 µM; 32.6 µmol min^{-1} mg^{-1}
4-Mu-β-GlcNH$_2$	no substrate	n.d.
4-Mu-β-GalNAc	no substrate	no substrate

[a] molecular weight of the cloned protein; n.d.: not determined

NagZ cleaves muropeptides. To determine the activity of NagZ with natural substrates, muropeptides were released from peptidoglycan of *E. coli* and *B. subtilis* by mutanolysin treatment. The degradation products were subjected to isolated NagZ and differences in the muropeptide composition before and after digestion were analyzed by two independent methods, fluorophore-assisted carbohydrate electrophoresis (FACE) and reversed-phase high-performance liquid chromatography (RP-HPLC) (see Materials and Methods). For FACE the products were labelled with the fluorescent dye 8-aminonaphthalene-1,3,6-trisulfonic acid

(ANTS) at their reducing ends, then separated by polyacrylamide electrophoresis and visualized by UV-light. Fig. 19 shows the results of the NagZ action on muropeptides generated from *E. coli* (A) and *B. subtilis* (B) cell walls by the FACE method. The muropeptides were identified by comparison with published data of muropeptide FACE-analyses (Young, 1996) and by mass spectrometry (the composition on identity of the muropeptides is summarized in Table 6). The major muropeptides obtained from *E. coli* cell walls by mutanolysin treatment were identified as multimeric muropeptides like Tetra-Tetra (identifier 1 and 2, Fig 19A and Table 6A) as well as monomeric muropeptides like Tetra (identifier 3) and Tri (identifier 4). In *B. subtilis* 2 prominent bands could be visualized upon mutanolysin treatment of isolated peptidoglycan (Fig. 19B). These muropeptides were identified by comparison with the vegetative cell wall peptidoglycan composition of *B. subtilis* described by Atrih *et al*., 1999 (Atrih et al., 1999a) and by mass spectrometry (Table 6B): Tri-Tetra with two amidations (identifier 9), which accounts for 27.7% of muropeptides and Tri with one amidation (identifier 10), which amounts to 20.5% of the total cell wall fragments (Atrih et al., 1999a). A gel with lower polyacrylamide concentration revealed that the band of Tri-Tetra (identifier 9) consisted of at least 2 fragments, likely Tri-Tetra and another multimeric muropeptide (data not shown). NagZ was able to hydrolyze muropeptides generated from both, *E. coli* and *B. subtilis* peptidoglycan, releasing GlcNAc (Fig. 19). Multimeric muropeptides of *E. coli* containing Tetra-Tetra (identifier 1 and 2; Fig. 19A) as well as monomeric muropeptides Tetra (identifier 3) and Tri (identifier 4) were converted to the respective products lacking the terminal GlcNAc residues: dimer of two MurNAc-tetrapeptide monomers (identifier 5 and 6), MurNAc-tetrapeptide (identifier 7) and MurNAc-tripeptide (identifier 8). MALDI-TOF analysis of Tetra (identifier 3, Fig. 19A) and MurNAc-tetrapeptide (identifier 7, Fig. 19A) revealed additional masses that are matching that of Tri-Arg-Lys and MurNAc-tripeptide-Arg-Lys (Table 6). These peptidoglycan fragments orginate from peptidoglycan that had been covalently bound to Braun’s lipoprotein (Braun and Sieglin, 1970). In *B. subtilis* multimeric muropeptides containing Tri-Tetra (identifier 9) and amidated Tri (identifier 10) were converted to multimeric MurNAc-peptides, e.g. MurNAc-tripeptide-MurNAc-tetrapeptide (identifier 11, 12) and MurNAc-tripeptide (identifier 13). As shown by MALDI-TOF some muropeptides of *B. subtilis* are amidated (identifier 10, Table 6B) most likely at the *m*-DAP residue, which is a modification that was recognized before (Vollmer, 2008). NagZ also released GlcNAc from muropeptides prepared from *Micrococcus luteus* peptidoglycan (data not shown) and cleaves the disaccharide GlcNAc-MurNAc (Fig. 19C). This indicates that NagZ is neither restricted by the peptide composition of the muropeptide substrate nor depends on the peptides for activity. However no GlcNAc was released from unsoluble peptidoglycan (of any sources) by NagZ indicating that it solely functions as an exo-β-*N*-acetylglucosaminidase.

In a second approach muropeptide specificity of NagZ was analyzed by RP-HPLC. Under the applied conditions muropeptides and cell wall sugars/sugar peptides were detected in two peaks relating to their α- and β-anomeric forms. Fig. 20 illustrates the RP-HPLC elution patterns of muropeptides derived from mutanolysin digested peptidoglycan of *E. coli* (Fig. 20A, black line) and *B. subtilis* (Fig. 20B, black line). NagZ catalyzed hydrolysis of muropeptides (*E. coli* and *B. subtilis*, Fig. 20, red lines) are shown by the reduction of peak heights or complete loss of several peaks as well as the appearance of new compounds including GlcNAc. The main peaks before and after hydrolysis by NagZ were collected and analyzed by FACE, thereby the release of GlcNAc and the conversion of muropeptides into MurNAc-peptides as shown in Table 6 were confirmed (identifiers are indicated). Although not all peaks in the RP-HPLC analysis could be identified, the specificity of NagZ, cleavage of the β-1,4-glycosidic bond between GlcNAc and MurNAc as well as the broad specificity regarding peptide substitutions at MurNAc was shown by two autonomous methods.

AmiE functions as *N*-acetylmuramyl-L -alanine amidase. Muropeptide mixtures were not affected by treatment with incubated AmiE as shown by FACE analysis (Fig. 19A and 19B lane G). Consistently, the RP-HPLC elution pattern of muropeptides of *B. subtilis* upon treatment with AmiE showed only minor differences compared to muropeptide pattern derived by mutanolysin treatment alone (Fig. 20B, blue line). This indicates that AmiE was not able to hydrolyze muropeptides containing GlcNAc at their non-reducing end. In contrast the enzyme was active after previous digestion of the muropeptides with NagZ (Fig. 19A and 19B, lane H; Fig. 20B, green line). Release of MurNAc from muropeptides by digests with both, NagZ and AmiE, shows that AmiE functions as an *N*-acetylmuramyl-L-alanine amidase that hydrolyzes the amide bond between MurNAc and the L-alanine residue of the stem peptide. In contrast to NagZ, AmiE did not degrade muropeptides of *M. luteus*, although they were substrates for NagZ (data not shown).

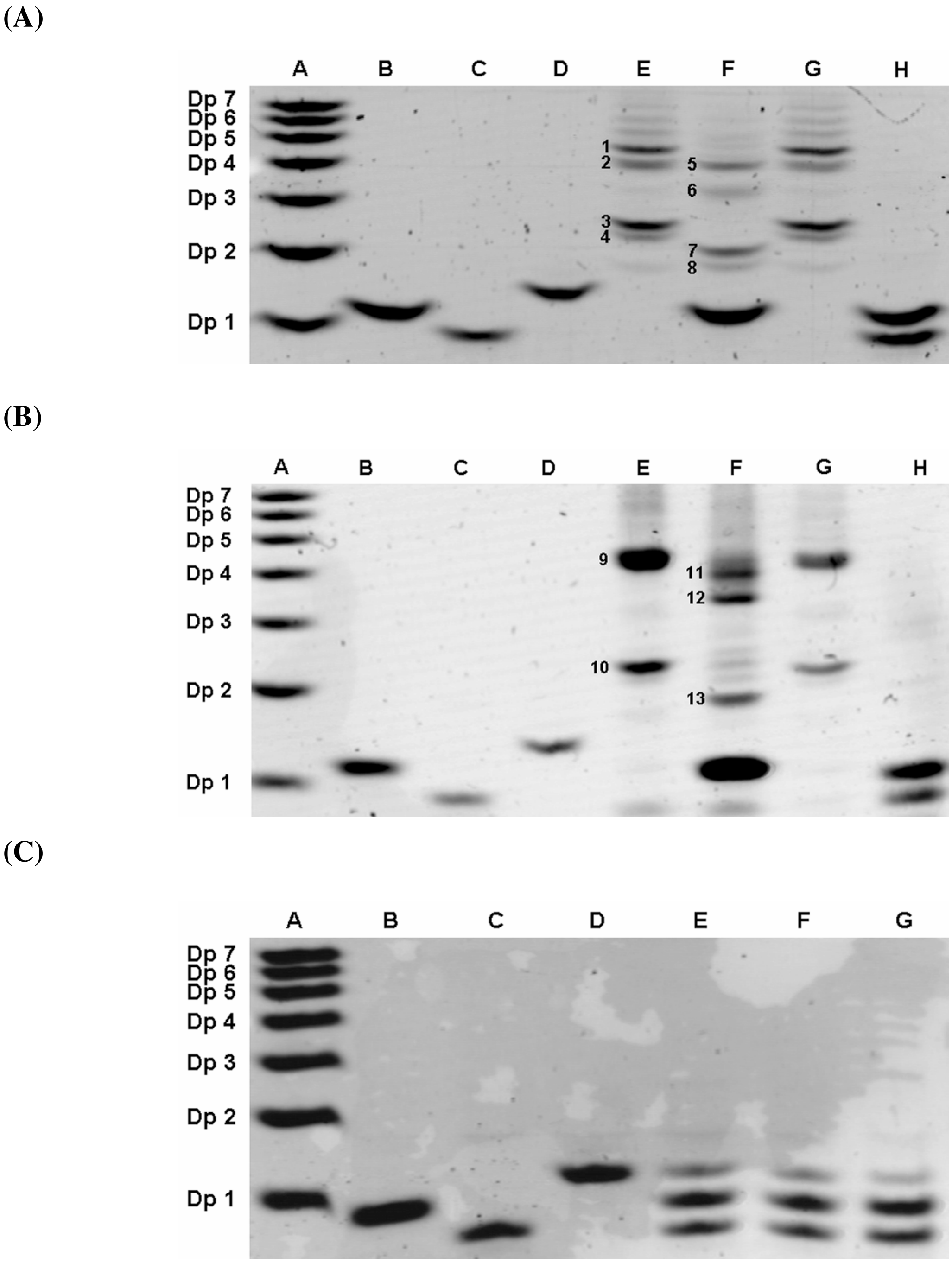

Figure 19. Fluorophore-assisted carbohydrate electrophoresis (FACE) of muropeptides and GlcNAc-MurNAc degraded with NagZ and/or AmiE. Muropeptides and amino sugars derived by mutanolysin digestion from peptidoglycan of *E. coli* (A) and *B. subtilis* (B) were treated with NagZ and/or AmiE, labelled with the fluorophore ANTS and separated by electrophoresis in a 32% polyacrylamide gel. The numbers on the left side indicate the degree of polymerization (DP) of a carbohydrate mix (DP 1-7: glucose, maltose, maltotriose, maltotetraose, maltopentaose, maltohexaose and maltoheptaose). Lane A: carbohydrate mix; lane B: GlcNAc; lane C: MurNAc; lane D: GlcNAc-MurNAc; lane E: mutanolysin treated cell walls from *E. coli* (A) and *B. subtilis* (B), respectively; lane F: samples as in lane E digested with NagZ; lane G: sample as in lane E digested with AmiE; lane H: sample as in lane E, digested with NagZ and AmiE. (C) lane E, F, G: GlcNAc-MurNAc digested with NagZ for 30, 60, and 120 min. Muropeptides were identified by mass spectrometry (Table 6), HPLC (see Fig. 20) and comparison with published data (Atrih et al., 1999a; Young, 1996). Numbers beside the bands are identifiers for muropeptides as used in Table 6 (see also Fig. 20).

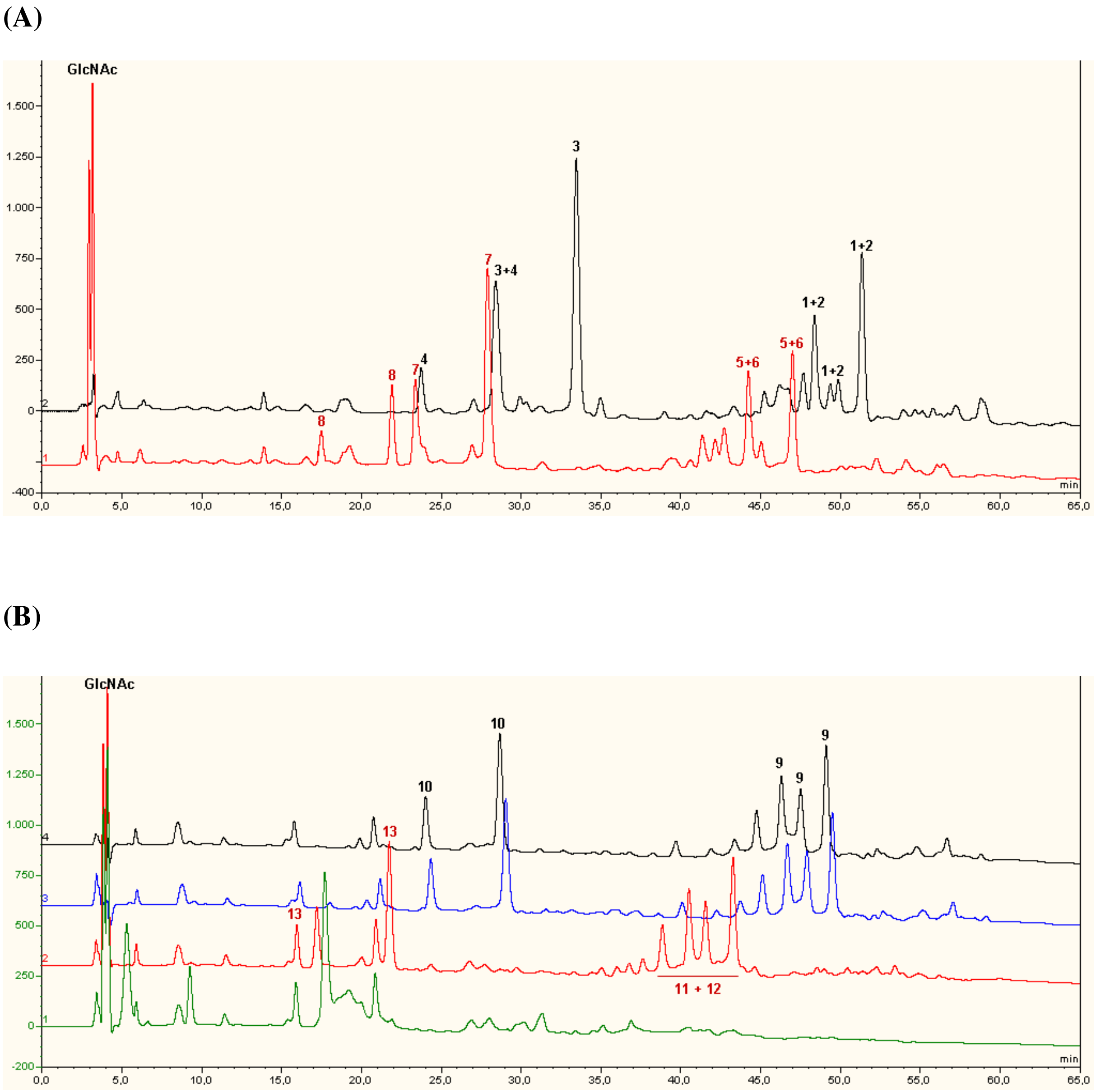

Figure 20. RP-HPLC profiles of muropeptides of peptidoglycan from *E. coli* (A) and *B. subtilis* (B). Peptidoglycan of *E. coli* and *B. subtilis* was hydrolyzed with: mutanolysin (black line); mutanolysin and NagZ (red line). *B. subtilis* muropeptides were additionally hydrolyzed with: mutanolysin and AmiE (blue line); mutanolysine, NagZ and AmiE (green line). Peaks are related and numbered corresponding to their α- and β-isomers. Peaks of *E. coli* corresponding to: 1, 2: multimeric muropeptides, e.g. Tetra-Tetra; 3, Tetra; 4, Tri; 5, 6: multimeric MurNAc-peptides, e.g a dimer of two MurNAc-tetrapeptide monomers; 7, MurNAc-tetrapeptide; 8, MurNAc-tripeptide. Peaks of *B. subtilis* corresponding to: 9: multimeric muropeptides, e.g. Tri-Tetra with 2 amidations; 10, Tri with 1 amidation; 11, 12, multimeric MurNAc-peptides, e.g. MurNAc-tripeptide-MurNAc-tetrapeptide and 13, MurNAc-tripeptide.

Table 6. Identification of muropeptides and MurNAc-peptides of digests of *E. coli* (A) and *B. subtilis* (B).

(A)

Identifier[a]	Fragment[b]	Identification [m/z]	Structure
1, 2	Multimeric muropeptides: e.g. Tetra-Tetra	§	(GlcNAc-MurNAc-L-Ala-D-Glu-*m*-DAP-D-Ala)$_2$
3	Tetra	Calc.: 962.4 [M+Na]$^+$, 978.4 [M+K]$^+$ Found: 962.3 [M+Na]$^+$, 978.3 [M+K]$^+$	GlcNAc-MurNAc-L-Ala-D-Glu-*m*-DAP-D-Ala
	Tri-(Arg-Lys)	Calc.: 1154.6 [M+H]$^+$ Found: 1153.5 [M+H]$^+$	GlcNAc-MurNAc-L-Ala-D-Glu-*m*-DAP-(D-Lys-D-Arg)
4	Tri	§	GlcNAc-MurNAc-L-Ala-D-Glu-*m*-DAP
5, 6	Multimeric MurNAc-peptides: e.g. MurNAc-tetrapeptide dimer	§	(MurNAc-L-Ala-D-Glu-*m*-DAP-D-Ala)$_2$
7	MurNAc-tetrapeptide	Calc.: 759.3 [M+H]$^+$, 775.3 [M+K]$^+$ Found: 759.2 [M+Na]$^+$, 775.1 [M+K]$^+$	MurNAc-L-Ala-D-Glu-*m*-DAP-D-Ala
	MurNAc-tripeptide with Arg-Lys	Calc.: 951.5 [M+H]$^+$ Found: 950.3 [M+H]+	MurNAc-L-Ala-D-Glu-*m*-DAP-(D-Lys-D-Arg)
8	MurNAc-tripeptide	§	MurNAc-L-Ala-D-Glu-*m*-DAP

[a] numbers indicate bands visualized by FACE analysis (cf. Fig. 19) as well as peaks detected by HPLC (cf. Fig. 20). [b]Tri, disaccharide-tripeptide monomer; Tetra, disaccharide-tetrapeptide monomer; Tetra-Tetra, dimer of two Tetra monomers. Tri-(Arg-Lys) and MurNAc-tripeptide-(Arg-Lys) stem from cell wall fragments that were covalently linked to lipoprotein via the *C*-terminal Lys residue and cleaved by pronase before Arg. [§] identified by retention in FACE analyses according to (Li et al., 2004; Young, 1996).

(B)

Identifier[a]	Fragment[b]	Identification [m/z]	Structure
9	Multimeric muropeptides: e.g. Tri-Tetra with 2 amidations	§	(GlcNAc-MurNAc-L-Ala-D-Glu-*m*-DAP)-(D-Ala-*m*-DAP-D-Glu-L-Ala-MurNAc-GlcNAc)
10	Tri with 1 amidation	Calc.: 890.4 [M+Na]$^+$, 906.4 [M+K]$^+$ Found: 890.5 [M+Na]$^+$, 906.5 [M+K]$^+$	GlcNAc-MurNAc-L-Ala-D-Glu-*m*-DAP
11, 12	Multimeric MurNAc-peptides: e.g. MurNAc-tripeptide-MurNAc-tetrapeptide	§	(MurNAc-L-Ala-D-Glu-*m*-DAP)-(D-Ala-*m*-DAP-D-Glu-L-Ala-MurNAc)
13	MurNAc-tripeptide	Calc.: 666.3 [M+H]$^+$, 688.3 [M+K]$^+$; Found: 666.1 [M+H]$^+$, 688.1 [M+K]$^+$	MurNAc-L-Ala-D-Glu-*m*-DAP

[a] numbers indicate bands visualized by FACE analysis (cf. Fig. 19) as well as peaks detected by HPLC (cf. Fig. 20). [b]Tri, disaccharide-tripeptide monomer; Tetra, disaccharide-tetrapeptide monomer; Tetra-Tetra, dimer of two Tetra monomers. [§] identified by retention in FACE analyses according to (Li et al., 2004; Young, 1996).

DISCUSSION

Murein recycling in Gram-positive bacteria remains enigmatic. Curiously the current view is that Gram-positive bacteria do not recycle their endogenous wall. This was assumed from early studies showing that cell wall turnover products accumulate in the culture medium (e.g. (Mauck et al., 1971; Mauck and Glaser, 1970)). However, if the cell wall turnover products were not recovered this would lead to a tremendous loss of resources since peptidoglycan usually accounts for more than 20% of the total cell mass of Gram-positive bacteria. In some Gram-positive bacteria the turnover rates are reaching values, similar to *E. coli*, of up to 50% of the cell wall material per generation (e.g. in *B. subtilis* W-23 (Mauck and Glaser, 1970) and other Gram-positive bacteria like *B. megaterium*, *B. cereus* and *Lactobacillus acidophilus* (Boothby et al., 1973; Chaloupka and Kreckova, 1971; Daneo-Moore et al., 1975)). It is obvious that cell wall turnover products would serve as fortuitous carbon and energy source, in particular for cells entering starvation (e.g. stationary phase entry).

In *E. coli*, anhydromuropeptides are the primary turnover products that are continuously generated during growth and that are transported in the cytoplasm by the permease AmpG, where the further processing involves the recycling enzymes AmpD, the anhydroMurNAc-amidase and AnmK, the anhydroMurNAc-kinase amongst others (Cheng and Park, 2002; Höltje et al., 1994; Jacobs et al., 1994; Jacobs et al., 1995; Uehara et al., 2005). *B. subtilis* apparently lacks AmpG, AmpD and AnmK orthologs. Therefore peptidoglycan recycling in *B. subtilis* needs to proceed different from *E. coli*. Although anhMurNAc has been recognized in *Bacillus*, anhydromuropeptides and the lytic transglycosylases, which generate them, play only a minor role in peptidoglycan metabolism in this organism (Atrih et al., 1999a). In *B. subtilis* a large range of cell wall lytic enzymes (autolysins) exist but their precise specificity and function, in particular that of muramidases and lytic transglycosylases, is mostly unknown (Smith et al., 2000). Three putative G-type lysozymes/lytic transglycosylases (family 23 of glycosidases) exist: YocA (BSU19130), YjbJ (BSU11570) and YomI (BSU21350). Furthermore two additional enzymes were annotated which belong to the SLT-family: YqbO (BSU26030; P45931) and XKDO (P54334). Recently the putative lytic transglycosylase CwlT (YddH; BSU 04970) was shown to act as a lysozyme-like muramidase rather than a lytic transglycosylase (Fukushima et al., 2008). CwlT is a bifunctional two-domain enzyme; the *N*-terminal domain functions as an *N*-acetylmuramidase and the *C*-terminal domain of CwlT harbours D,L-endopeptidase activity, capable of hydrolyzing D-γ-glutamyl-*m*-DAP-linkages. This protein releases mostly peptidyltetra-, hexa- and octasaccharides from the peptidoglycan and only very low amounts of disaccharides (Fukushima et al., 2008).

In our group a pathway for the recovery of MurNAc was identified consisting of the MurNAc-specific PTS (MurP), the MurNAc-6-phosphate etherase (MurQ) and the MurNAc-6-phosphate-sensitive transcriptional repressor MurR (Dahl et al., 2004; Jaeger et al., 2005; Jaeger and Mayer, 2008a; Jaeger and Mayer, 2008b). Moreover very recently, Plumbridge showed that NagE, the phosphotransferase system for GlcNAc, is involved in murein recycling in *E. coli* (Plumbridge, 2009) which implies that – in addition to *Ec*NagZ, the cytoplasmic *N*-acetylglucosaminidase of *E. coli* that is required for anhMurNAc hydrolysis – a secreted, cell wall-associated *N*-acetylglucosaminidase that acts on muropeptides should exist. *B. subtilis* possesses a NagE ortholog and orthologs of the MurNAc-6-phosphate etherase (*murQ*/*murI*), the MurNAc-6-phosphate-specific transcriptional repressor (*murR*/*ybbH*) and the MurNAc-specific phosphotransferase system (*ybbF/murP*) capable of recovering GlcNAc and MurNAc. Interestingly the *mur* genes are encoded in a putative operon together with an ortholog of the β-*N*-acetylglucosaminidase NagZ of *E. coli*, *Bs*NagZ (formerly YbbD) which is a secreted and cell wall associated protein. The protein was annotated to be a lipoprotein, however a signal sequence for signal peptidase I was identified that potentially cleaves of the *N*-terminal cystein that would be required for covalent binding to phospholipids. Our results showed that *Bs*NagZ mainly occurs in the culture supernatant and can be extracted from cell walls with salt, therefore it is not a lipoprotein.

In this study we characterized NagZ and AmiE (formerly YbbE) which together are destined for MurNAc release from muropeptides. Notably both proteins are acting outside of the cell. NagZ releases GlcNAc residues from the non-reducing end. NagZ acts on muropeptides generated from *B. subtilis*, *E. coli* or *M. luteus* peptidoglycan. It could possibly also release GlcNAc from larger muropeptide fragments such as that produced by CwlT, however it was not able to degrade polymeric peptidoglycan, hence it is neither a processive hydrolase nor an autolysin. NagZ is associated with the cell wall and cell wall derived particular material, likely via ionic interactions of the positively charged protein (the calculated pI is 9.37) with the negatively charged *Bacillus* cell wall and can be released from the wall by high concentrations of salt. AmiE can cleave off peptides from MurNAc-peptides of *E. coli* and *B. subtilis* but not of MurNAc-peptides of *M. luteus*, likely due to differences in the peptide composition. In *M. luteus* the peptide subunits have the sequence *N*-[L-alanyl-γ-(α-D-glutamylglycine)-L-lysyl-D-alanine], whereas in *E. coli* and *B. subtilis* the peptides consist of *N*-[L-alanyl-γ-D-glutamyl-*m*-DAP-D-alanine]. Furthermore in *M. luteus* the peptidoglycan is cross-linked by peptide bridges of repeating tetrapeptide sequences.

NagZ is the major exo-β-*N*-acetylglucosaminidase of *B. subtilis* since a mutant shows severely decreased activity with the substrate analogue 4-Mu-β-GlcNAc. At least during the mid-exponential growth phase a second exo-acting enzyme might be present since the null mutant has also activity compared to the wild-type during this time of growth. This activity could be associated with the exo-acting *N*-acetylglucosaminidase LytG which is mainly expressed during this growth phase under control of the σ^A-dependent promoter (Horsburgh et al., 2003). Lack of LytG resulted in the appearance of GlcNAc at the non-reducing terminus and hence it could be possible that LytG has a role in modifying glycan strand length, because in *B. subtilis* the glycan strands of mature peptidoglycan have a MurNAc at the non-reducing end.

The regulation of the gene cluster of *B. subtilis* involved in MurNAc dissimilation was not object of this study. However, we recognized a σ^A-dependent promoter in the region upstream from *ybbI* (*murQ*). In addition the expression of the cluster likely is regulated by carbon catabolite repression since the highly conserved catabolite response element (*cre*) is located upstream of the σ^A-dependent promoter. Glucose starvation will result in the switch to utilization of alternative carbon sources mediated mainly by the catabolite control protein CcpA. Furthermore the accumulation of MurNAc-6-phosphate might induce the transcription of the operon as it is the case in *E. coli* (Jaeger and Mayer, 2008b).

Eichenberg *et al.* have shown that *ybbFEDC* is also part of the σ^E regulon, which influences the transcription of more than 250 genes during sporulation in *B. subtilis* (Eichenberger et al., 2003). NagZ is expressed during transition to stationary growth but highest activity was reached in the late stationary or rather decay phase which can be attributed to σ^E in the onset of sporulation. The *nagZ* mutant has a normal cell morphology and no change in growth rate was observed during exponential growth in rich medium. A severe decrease in OD was observed for the *nagZ* mutant compared to wild-type in stationary phase. It is known that *B. subtilis* responds to nutritional limitation by entering sporulation (Driks, 1999; Itaya and Tanaka, 1997). The formation of an endospore is an energy and time intensive process; therefore under nutrient limitation *B. subtilis* cells exhibit cannibalistic tendency by killing their sister cells and feeding on the released nutrients to delay sporulation (Engelberg-Kulka and Hazan, 2003; Gonzalez-Pastor et al., 2003). Additionally the released peptidoglycan fragments of the lysed cells can serve as energy sources. Recently Bernhardt *et al.* showed that already after few hours of glucose starvation few sporulation-specific proteins appear

(Bernhardt et al., 2003). This indicates that at least a portion of the cell population already initiate sporulation. That the cells of the null mutant of NagZ showed increased lysis compared to the wild-type during the late decay phase leads to the assumption that these cells are not able to metabolize the released cell wall fragments and enter sporulation faster then wild-type.

Besides the regulation of the muropeptide cluster of *B. subtilis* the origin of the substrate of NagZ (GlcNAc-MurNAc-peptides) must be investigated. In addition to CwlT a further muramidase is missing in *B. subtilis* that in conjunction with NagZ would lead to complete degradation of peptidoglycan fragments. One candidate, an exo-muramidase, was discovered in crude enzyme preparations that was able to hydrolyze the disaccharide MurNAc-GlcNAc (Del Rio et al., 1973) but till now neither the responsible enzyme nor the corresponding gene were identified.

CHAPTER 2

A unique glycosidase mechanism: an Asp-His dyad is the general acid/base catalyst of family 3 β-*N*-acetylglucosaminidases

ABSTRACT

Three-dimensional structures of NagZ of *Bacillus subtilis*, the first structures of a two-domain β-*N*-acetylglucosaminidase of family 3 of glycosidases, were determined with and without the transition state inhibitor PUGNAc bound to the active site at 1.7 and 1.4 Å resolution, respectively. The structures along with kinetic analyses of NagZ mutants provide compelling support for an Asp-His dyad involved in catalysis: His234 of NagZ acts as general acid/base catalyst and is hydrogen bonded by Asp232 for proper function. Replacement of both, His234 and Asp232, with glycine reduced the rate of hydrolysis of the fluorogenic substrate 4-methylumbelliferyl-β-*N*-acetyl-D-glucosaminide 1900- and 4600-fold, respectively and rendered activity pH-independent in the alkaline range consistent with a role of these residues in acid/base catalysis. *N*-acetylglucosaminyl-enzyme intermediate accumulated in the His234Gly mutant as identified by mass spectrometry and the β-*N*-acetylglucosaminyl-azide was formed in the presence of sodium azide. The Asp-His dyad is strictly conserved within β-*N*-acetylglucosaminidases but absent in β-glucosidases of family 3 which carry instead a "classical" glutamate acid/base catalyst. This glutamate residue superimposes with the Asp-His dyad but, in contrast to NagZ, protrudes from the second domain of the enzyme into the active site. This is the first report of an Asp-His catalytic dyad involved in hydrolysis of glycosidases resembling in function the Asp-His-Ser triad of serine proteases. Our findings will facilitate the development of mechanism-based inhibitors that selectively target family 3 β-*N*-acetylglucosaminidases which are involved in cell wall recycling/recovery and β-lactamase-induction in bacteria.

INTRODUCTION

Glycosidases that catalyze the hydrolysis of glycosidic linkages under retention of anomeric configuration (retaining glycosidases) proceed via a two-step double displacement mechanism (Rye and Withers, 2000; Zechel and Withers, 2000). In almost all cases the catalytic machinery of these enzymes involves two carboxylic acids which function as catalytic nucleophile and general acid/base catalyst, respectively, that are located approximately 5.5 Å apart in the active site (Fig. 22A). In the first step (glycosylation) a carboxylic acid that hydrogen bonds to the glycosidic oxygen acts as general acid facilitating leaving group departure simultaneously with a nucleophilic attack by the second carboxylate that forms a covalent glycosyl-enzyme intermediate. In the second step (deglycosylation) the first residue then functions as a general base to activate an incoming water molecule for nucleophilic attack that hydrolyzes the glycosyl-enzyme to form a sugar hemiacetal product with overall retention of stereochemistry (Rye and Withers, 2000; Zechel and Withers, 2000).

This mechanism is performed by many glycosidases including the well-studied lysozyme that hydrolyzes the β-glycosidic linkage between *N*-acetylmuramic acid (MurNAc) and *N*-acetylglucosamine (GlcNAc) of the backbone polysaccharide of the bacterial cell wall compound peptidoglycan (murein). Vocadlo *et al.* showed that lysozyme proceeds through a covalent glycosyl-enzyme intermediate (Vocadlo et al., 2001) and not a long-lived oxocarbenium-ion intermediate as proposed earlier (Phillips, 1967). We are studying the group of β-*N*-acetylglucosaminidases which hydrolyze the other glycosidic linkage in peptidoglycan, that one between GlcNAc and MurNAc in peptidoglycan (Horsch et al., 1997; Mayer et al., 2006; Mayer et al., 2000a; Vocadlo et al., 2000). An aspartate nucleophile and a glycosyl-enzyme intermediate were identified in the β-*N*-acetylglucosaminidase of *Vibrio furnisii* (*Vf* ExoII) as well as in related β-glucosidases. The catalytic nucleophile was identified by trapping the glycosyl-enzyme intermediate using slow substrates, proteolytic digest and subsequent mass spectrometry of the labelled peptide (Dan et al., 2000; Mayer et al., 2000a; Vocadlo et al., 2000).

Some retaining β-*N*-acetylglucosaminidases (or β-*N*-acetylhexosaminidases) operate by a mechanism that deviates from the general scheme of the double displacement mechanism of glycosidases. In these glycosidases the catalytic nucleophile is not provided by the enzyme but comes from the acetamido group of the substrate itself and an oxazoline/oxazolidinium-ion intermediate instead of a covalent glycosyl-enzyme is generated (Vocadlo and Withers, 2005). This so-called anchimeric assistance mechanism is not only performed by some exo- (Mark et al., 2001; Tews et al., 1996) and endo-*N*-acetylhexosaminidases (Abbott et al., 2009; Fujita et al., 2007) but also by certain chitinases (van Aalten et al., 2001), hyaluronidases (Markovic-Housley et al., 2000) as well as *O*-GlcNAc'ases (Cetinbas et al., 2006). Another group of enzymes that require anchimeric assistance from the acetamido group of the substrate are lytic transglycosylases which cleave the same bond as lysozyme in peptidoglycan but are not hydrolases. Instead they cleave the glycosidic bond by catalyzing an intramolecular transglycosylation (Scheurwater et al., 2008).

Glycosidases can be classified on basis of the catalyzed reaction and substrate specificity (i.e. enzyme commission, E.C. classification) which does not reflect the evolutionary relationship between enzymes which may be closely related despite having rather distinct substrate specificities. In this respect a very useful classification of glycosidases that bases on amino acid sequence and secondary structure cluster analyses is the carbohydrate active enzymes (CAZY) database (at URL: www.cazy.org). It provides a convenient tool to derive mechanistic information for members of one family (at present 115 glycosidase families are known). Family 3 of glycosidases of the database comprises a heterogenous group of retaining β-glycosidases that besides β-*N*-acetylglucosaminidases (EC 3.2.1.52) include β-glucosidases (EC 3.2.1.21), xylan 1,4-β-xylosidases (EC 3.2.1.37), glucan 1,3- and 1,4-β-glucosidases (EC 3.2.1.58, 3.2.1.74), α-L-arabinofuranosidases (EC 3.2.1.55), exo-1,3-1,4-glucanases (EC 3.2.1.-). Phylogenetic analysis revealed that family 3 glycosidases, which are characterized by their conserved *N*-terminal or A domain, diverge in the less conserved *C*-terminal or B domain of these enzymes thereby forming three subfamilies AB, AB', and AB". The AB" subfamily solely contains bacterial β-*N*-acetylglucosaminidases (Cournoyer and Faure, 2003).

In all β-glycosidases in which the general acid/base catalyst has been reliably identified to date, it was a glutamic or aspartic acid residue (cf. www.cazy.org), accept for myrosinases, in which an ascorbate cofactor substitutes for the function of the general base (Burmeister et al., 2000). Also for some β-glucosidases of family 3 a good evidence is provided by kinetic analyses for a glutamate presumably acting as the acid/base catalyst, e.g. the exo-β-glucanase of *Hordeum vulgare* (Harvey et al., 2000; Hrmova et al., 2004; Hrmova et al., 2001; Varghese et al., 1999), β-glucosidase of *Flavobacterium meningosepticum* (Chir et al., 2002; Li et al., 2002) and the β-glucosylceramidase of *Paenibacillus sp.* TS12 (Paal et al., 2004). Intriguingly the structure of the exo-β-glucanase of *Hordeum vulgare* (*Hv*ExoI) reveals a glutamate that resides on a short helix on the less conserved B-domain coming into close contact to the active site region of domain A (Fig. 22B and 22C). A conserved glutamate which could act as the acid/base catalyst was never identified in β-*N*-acetylglucosaminidases of family 3 (Fig. 21). Moreover some β-*N*-acetylglucosaminidases of this family even completely lack a *C*-terminal B-domain and therefore need to provide a different residue for acid/base catalysis.

We report here the structure of NagZ of *Bacillus subtilis*, a two-domain family 3 β-*N*-acetylglucosaminidase. Our findings provide evidence for participation during catalysis of the side chains of the conserved Asp and His residues that reside on the *N*-terminal A-domain. We propose that the histidine instead of a glutamate acts as acid/base catalyst which undergoes hydrogen bonding with the aspartate residue thereby forming a catalytic dyad that protonates the glycosidic oxygen in the first (glycosylation) step and deprotonates and activates water for nucleophilic attack of the glycosyl-enzyme in the second (deglycosylation) step of the reaction. We showed earlier that family 3 β-*N*-acetylglucosaminidases are characterized by the highly conserved sequence pattern K-H-(F/I)-P-G-(H/L)-G-x(4)-**D**-(S/T)-**H** on their A-domain (Fig. 21) and proposed an involvement in acetamido group binding of the substrate (Mayer et al., 2000a; Mayer et al., 2000b; Vocadlo et al., 2000). Here we show that the **D**-(S/T)-**H** motive within this pattern is directly involved in the mechanism of the β-*N*-acetylglucosaminidase subfamily of family 3 of glycosidases. The function of the Asp-His dyad in glycoside hydrolysis resembles in function the Asp-His-Ser triad of serine proteases (Hedstrom, 2002).

1 domain β-*N*-acetylglucosaminidases

P75949	NAGZ_ECOLI	161	TGKHFPGHGAVTADSHKE
Q8ZQ06	NAGZ_SALTY	161	TGKHFPGHGAVTADSHKE
P96157	NAGZ_VIBFU	158	TGKHFPGHGAVIADSHLE
Q9KU37	NAGZ_VIBCH	158	TGKHFPGHGAVIADSHLE
P44955	NAGZ_HAEIN	163	TGKHFPGHGHVLADSHLE
Q9HZK0	NAGZ_PSEAE	159	TGKHFPGHGWAEADSHVA
Secondary structure			=β5==

2 domain β-*N*-acetylglucosaminidases

P40406	**NAGZ_BACSU**	219	ALKHFPGHGDTDVDSHYG	509	YIITGSYVVKNDPVVNDGVI
P48823	**HEXA_PSEO7**	206	ALKHFPGHGDTHVDSHTG	481	MIIAAHASPPQSAVEIGGM
O82840	**NAGA_STRTL**	261	TAKHFPGHGDTAVDSHTG	530	AVVATYNVTAGSAQQTLVE
Q9RDG9	**NAGA_STRCO**	245	CAKHFPGHGDTATDSHTG	514	AVVATYNVTAGSAQRTLVT
Q93RU1	**HEXA_STRCO**	241	CAKHFPGHGDTGQDSHTG	510	AVVATDNVNATSAQRTLVS
Q8XNR6	**HEXA_CLOPE**	224	TAKHFPGHGDTSTDSHYG	509	YIIVASLSSNANGLKPGAW
Q97ML4	**NAG3_CLOAB**	178	VAKHFPGHGDTDVDSHLS	440	SIVIGIYNAYNHEGQRKLV
Secondary structure			=β5==		=β4=> => =>

β-glucosidases

Q9XEI3	**EXO1_HORVD**	229	CAKHFVGDGGTVDGINEN	480	AIVAVGEHPYTETKGDNLNL
Q42835	**EXO2_HORVU**	225	CAKHYVGDGGTFMGINEN	490	AIVVVGEPPYAETFGDNLN
P33363	**BGLX_ECOLI**	206	SVKHFAAYGAVEGGKEYN	505	VVAVVGEAQGMAHEASSRT
Q56078	**BGLX_SALTY**	206	SVKHFAAYGAVEGGKEYN	505	VVAVVGESQGMAHEASSRT
O30713	**BGLA_FLAME**	166	CVKHFALYGAPEGGRDYN	460	VVLAIGETAELSGESSSRA
Q8GAT9	**GLUC_PAESP**	141	SLKHFAVN-NQEHRRMTT	398	AVLFVGLPDRYESEGYDRT
P27034	**BGLU_AGRTU**	141	TIKHFVAN-ESEIERQTM	546	VLLLVGREGEWDTEGLDLP
Secondary structure			=β5=> //// ///		=β4=> ////

Figure 21. Partial multiple sequence alignment of selected glycosidases of family 3, including one domain and two domain β-*N*-acetylglucosaminidases as well as two domain β-glucosidases. The subfamilies can be distinguished by differences in the sequence pattern next to the conserved K-H-(F/Y)-motive on the *N*-terminal domain that extends from β-strand 5 of the *N*-terminal $(\beta/\alpha)_8$-barrel domain into a loop region. The D-(S/T)-H-motive of β-*N*-acetylglucosaminidases which contains the catalytic dyad is missing in β-glucosidases of family 3. The *C*-terminal domain region (extending from β-strand 4 of the *C*-terminal $(a/\beta)_6$-sandwich domain) that carries the general acid/base in β-glucosidases is not conserved in β-*N*-acetylglucosaminidases or even missing. The structural elements were from the β-*N*-acetylglucosaminidase of *Vibrio cholerae* (Stubbs et al., 2007), the β-*N*-acetylglucosaminidase of *Bacillus subtilis* (this work) and the β-exo-glucanase of *Hordeum vulgare* (Varghese et al., 1999). The SwissProt database identifier and protein names of the genes are indicated.

MATERIALS AND METHODS

Bacterial strains and plasmids. *Bacillus subtilis* 168 was obtained from the *Bacillus* Genetic Stock Center. *E. coli* BL21(DE3) and the *E. coli* expression vectors pET16b (P_{T7}, Amp^{r}, ori_{pBR322}, *lacI*, *N*-term. 10x His-tag) and pET29b (P_{T7}, Kan^{r}, ori_{pBR322}, *lacI*, *C*-terminal 6x His-tag) were from Novagen. The reagents 4-methylumbelliferyl-β-*N*-acetyl-D-glucosaminide (4-Mu-β-GlcNAc) and 4-nitrophenyl-β-*N*-acetyl-D-glucosaminide (pNP-β-GlcNAc) were obtained from Glycosynth. All other reagents were from Sigma-Aldrich unless otherwise stated.

Cloning and site-directed mutagenesis of *nagZ* and *nagZ'*. DNA preparation, restriction enzyme digest, ligation and transformation were performed according to standard techniques using 5 U PWO DNA-polymerase (Genaxxon Biosciences, Biberach, Germany) and 30 ng of chromosomal DNA. *nagZ* from *B. subtilis* 168 was cloned into pET16b without signal sequence (pET16b-*Bs*NagZ) using the following primer: *Bs*NagZ/FP, 5'-AAA ACC ATG GGC CAT ATG TTT TTC GGG GCC AGA CAG AC-3' and *Bs*NagZ/RP, 5'-T TTT CTC GAG TTA AAG CGG TCT TCC CGT TTT G-3' (the recognition sites for the endonucleases *Nde* I and *Xho* I are underlined, respectively). Thirty cycles (15 s at 94°C, 30 s at 55°C and 120 s at 72°C) were performed in a thermal cycler and revealed a single 1.9-kb fragment (*nagZ). nagZ*' missing the *N*-terminal signal sequence and the *C*-terminal domain was amplified using primers with recognition sites for restriction endonucleases *Nde* I and *Xho* I, respectively (underlined): *Bs*NagZ'/FP, 5'-AAA ACC ATG GGC CAT ATG TTT TTC GGG GCC AGA CAG-3' and *Bs*NagZ'/RP 5'-GGG CTC GAG TGC TTT TTC AGC TAA TTT TTT CTC TGC-3' (Thermo Fisher). Thirty cycles (30 s at 94°C, 30 s at 50°C and 60 s at 72°C) were performed and the 1.3 kb fragment was cloned into vector pET29b (pET29b-*Bs*NagZ'). The vector pET16b-*Bs*NagZ was used as template for site-directed mutagenesis of His234Gly and Asp232Gly. The following degenerated primers (Thermo Fisher) were used: His234Gly/FP as well as Asp232Gly/FP, 5'-GG AGA TAT ACC ATG GGC CAT C-3'; His234Gly/RP, 5'-C TTG GCC ATG GGA AAC GAG CGG CAG TCC ATA **AYM** GCT GTC AAC GTC CGT GTC TCC-3'; and Asp232Gly/RP, 5'-C TTG GCC ATG GGA AAC GAG CGG CAG TCC ATA ATG GCT **CBC** AAC GTC CGT GTC TCC ATG TC-3' (the mutated codon is shown in bold with Y = C or T, M = A or C and B = C, G, or T; the restriction site for *Nco* I is underlined). Thirty cycles (30 s at 94°C, 30 s at 50°C and 60 s at

72°C) were performed. The amplified 758 bp fragments carrying the mutation were cleaved with *Nco* I and exchanged with the wild-type fragments of pET16b-*Bs*NagZ.

Overexpression and Purification of Proteins. *E. coli* strains BL21(DE3) (F^- *ompT* $hsdS_B(r_B^- m_B^-)$ *gal dcm*) harbouring pET16b-*Bs*NagZ, pET16b-His234Gly, pET16b-Asp232Gly or pET29b-*Bs*NagZ' were grown at 37°C in Luria-Bertani (LB) medium supplemented with ampicillin (100 µg/ml) or kanamycin (50 µg/ml) under vigorous shaking to log-phase (OD_{600} 0.5-0.6). Expression of the enzyme was induced by the addition of isopropyl-β-D-thiogalactopyranoside (IPTG) to a final concentration of 1 mM. Incubation was continued for further 3 h and the cells were harvested by centrifugation (4000 x *g* for 30 min at 4°C), resuspended in ice-cold phosphate buffer (20 mM Na_2HPO_4 x $2H_2O$, 500 mM NaCl, pH 7.5) and lysed by passing them three times through a French pressure cell. The lysates were clarified by centrifugation at 100,000 x *g* for 1 h at 4°C. The His-tagged proteins in the supernatant were purified by Ni^{2+}-affinity chromatography on a 5 ml HisTrap column (Amersham-Pharmacia, Freiburg, Germany) pre-equilibrated with phosphate buffer and eluted from the column with imidazole (phosphate buffer supplemented with 500 mM imidazole, pH 7.5). To avoid cross contamination of the proteins new columns were used for each protein. The purity of the enzymes was assessed by sodium dodecyl sulfate polyacrylamide gel electrophoresis (SDS-PAGE). Fractions containing homogeneous protein were pooled, concentrated and desalted by dialysis against 10 mM sodium acetate, pH 4.5 for crystallisation or against 20 mM phosphate buffer, pH 7.5 for enzymatic assay studies at 4°C. The protein concentrations were measured according to the method of Bradford with bovine serum albumin as a standard. 3 to 5 mg of pure protein were obtained from a 1 L culture.

Crystallization and Data Collection. Purified NagZ was concentrated to 14 mg/ml using an Amicon Ultra centricon (Millipore) with a 10 kDa cutt off. Complexes of NagZ with the inhibitor for co-crystallization were prepared by mixing PUGNAc with NagZ solution at a 10:1 molar ratio and incubating for 30 minutes at room temperature. Crystals of unliganded NagZ and its co-crystals with inhibitor were grown in 0.1 M sodium acetate, pH 4.9, using 24-well hanging drop plates. Presaturated protein drops were prepared by mixing protein and reservoir solution at ratios 1:1, 1:2, and 2:1 yielding final drop volumes of 2 to 3 µl. The reservoir contained 0.1 M sodium acetate, pH 4.9, and varying concentrations of polyethylene glycol 1000. Crystals were shock-frozen in liquid nitrogen. Data sets were collected at the

Swiss Light Source beamline X06SA of the Paul Scherer Institut, Villigen, Switzerland. Data processing was done using XDS (Kabsch, 1993), (see Table S1 of supporting information).

Structure determination. The structure of NagZ without ligand was solved first. An ensemble of pdb files (1EX1, 1IEX, 1J8V, 1LQ2, 1X38 (Hrmova et al., 2002; Hrmova et al., 2004; Hrmova et al., 2005; Hrmova et al., 2001; Varghese et al., 1999)) was defined in PHASER (Read, 2001; Storoni et al., 2004) as starting point for molecular replacement. Several refinement cycles in Refmac5 (Murshudov et al., 1997) improved the figure of merit (FOM) to 0.338. Then Buccaneer (Cowtan, 2006) was used to build parts of two molecules of NagZ (996 out of 1284 residues as poly-Ala model). ARP/wARP (Morris et al., 2002) and Resolve (Terwilliger, 2000; Terwilliger, 2002) were used for completing the model. By using Resolve, 2-fold non-crystallographic symmetry (NCS) could be determined and used for phase improvement, leading finally to an almost complete model with 1139 amino acids of the NagZ sequence. The resulting electron density map was used for further manual model building in COOT (Emsley and Cowtan, 2004) and refinement with Refmac5 and Phenix (Adams et al., 2002). After modelling water molecules and adding hydrogen atoms the last anisotropic refinement resulted in a final R-factor of 12.7% (Rfree, 16.6%). The structure of NagZ in complex with its inhibitor PUGNAc was determined by using the first structure of NagZ as search model in Molrep (Vagin and Teplyakov, 1997). The pseudo-merohedral twinning law was identified with the help of the CCP4 (N, 1994) program SFCHECK (Vaguine et al., 1999). Model refinement was done in Refmac5 and in Phenix which allows refinement of the twinned structures. Manual modifications were done in COOT. After adding waters and modelling the inhibitor PUGNAc the last isotropic refinement resulted in a final R-factor of 21.5% (Rfree, 25.8%). Refinement statistics are presented in Table S1. Atomic coordinates have been deposited in the Protein Data Bank with the accession code 3BMX and 3CQM for NagZ and its inhibitor complex, respectively.

Kinetic studies. All Michaelis-Menten kinetics were carried out at least in triplicates using a discontinous assay measuring the release of 4-methylumbelliferone from 4-Mu-β-GlcNAc. The fluorescence of the released 4-methylumbelliferone was measured using a 96-well plate (Greiner bio-one) in a Spectramax M2 Microplate Reader (Molecular Devices) (excitation, 362 nm; emission, 448 nm) at 37°C. Enzyme activity was measured using various concentrations of 4-Mu-β-GlcNAc in Clark and Lubs solution (0.1 M KH_2PO_4/0.1 M NaOH) at pH 5.8. Reactions (300 µl) were initiated by addition of enzyme (0.0158 mg His, 0.01465 mg Asp and 1.5 x 10^{-5} mg NagZ) and incubated over a period of 5 to 30 minutes at 37°C.

The pH-activity profiles of wild-type NagZ and the mutants were determined in 0.1 M citric acid/0.2 M disodium phosphate buffer (McIlvaine) ranging from pH 4.0 to 8.0, in 0.2M sodium acetate-acetic acid buffer ranging from pH 4.0 to 5.6 and in Clark and Lubs solution (0.1 M KH_2PO_4/0.1 M NaOH) in the range of pH 5.8 to 8.0. Reactions (300 µl) were initiated by addition of 1.5 mM 4-Mu-β-GlcNAc and incubated over a period of 5 to 30 min at 37°C. Used protein concentrations were 4.5 x 10^{-5} mg, 0.0114 mg and 0.01465 mg for NagZ, His234Gly and Asp232Gly, respectively.

All reactions were stopped by adding 9 volumes of 0.2 M Na_2CO_3 solution, pH 10.0. Kinetic parameters were evaluated by nonlinear regression of the reaction curve using regression analysis of the data by Prism 4 (GraphPad). The extinction coefficient was determined with a straight calibration line using methylumbelliferone as substrate. One unit is defined as the amount of enzyme that hydrolyzes 1 µmol of substrate per min at pH 5.8 at 37°C.

Mass spectrometry and HPLC analysis. His234Gly (100 µl; 15.8 mg/ml) was incubated with pNP-β-GlcNAc (100 µl; 15 mM) over a period of 10 min until the enzyme-substrate solution exhibited a light yellow color indicating the release of 4-nitrophenol (pNP). The mass spectrometry analysis of the trapped intermediate (glycosyl-enzyme) was performed by electrospray ionisation-time-of-flight mass spectrometry (ESI-TOF-MS) (ZMBH, University of Heidelberg). High performance liquid chromatography (HPLC) was used for analysis of the β-GlcNAc-N_3 in the reaction of His234Gly with 4-Mu-β-GlcNAc in 20 mM sodium phosphate, pH 7.5 and 500 mM sodium azide. In brief a RP-C18 column (Gemini, 150 by 4.6 mm, 5 µM particle size, Phenomenex) was used at a flow rate of 0.5 ml/min, isocratic elution with 0.05% trifluoacetic acid for 5 min, followed by a gradient from 0.05% trifluoracetic acid to 10% acetonitrile containing 0.035% trifluoracetic over a periode of 50 minutes according to (Cheng et al., 2000).

RESULTS

Purification, crystallization and structure determination. NagZ was overexpressed in *E. coli* cytoplasm and purified by Ni^{2+}-affinity chromatography to apparent homogeneity. The protein retained activity for several months at 4°C and in the pH range between pH 4.0 and 8.0. NagZ tends to precipitate at a pH above 6.0 and low ionic strength but can be kept soluble at 12-13 mg/ml and high ionic strength (e.g. 20 mM sodium phosphate, pH 7.5, 500 mM sodium chloride). At acid pH the protein shows weak enzymatic activity but the solubility behaviour is reversed. It is soluble at low ionic strength (e.g. 20 mM sodium acetate, pH 4.5) but precipitates upon addition of 100 mM sodium chloride. Crystals of unliganded NagZ and its complex with the transition state-like inhibitor PUGNAc (*O*-(2-Acetamido-2-deoxy-D-glucopyranosylidene) amino-*N*-phenylcarbamate; chemical structures of PUGNAc and substrates of NagZ are shown in Fig. S1) were grown at pH 4.9 and 18°C by vapour phase equilibration as described under Methods. The best results were obtained at polyethylene glycol 1000 reservoir concentrations between 27% w/v and 33% w/v. Within 2 to 3 weeks crystals reached a size of approx. $(50\ \mu m)^3$ and exhibited triangular, rhombic or cuboid habits. Data were collected at the Swiss Light source synchrotron to resolutions of 1.4 Å and 1.7 Å for the unliganded and inhibitor complex crystals, respectively. All crystals belonged to space group P1 and possessed very similar unit cells with two NagZ molecules per cell (see Table S1). The inhibitor complex crystals displayed pseudo-merohedral twinning with a twinning fraction of 17.7 %. The structures of unliganded NagZ and of its inhibitor complex were solved by molecular replacement as described in the Methods section.

NagZ has a unique two-domain structure. The final atomic model comprises residues 26 to 642 from both monomers at the asymmetric unit (structural parameters and refinement statistics, see Table S1). NagZ structure reveals two separate domains (Fig. 23B). The *N*-terminal domain (residues 26-420) adopts a $(\beta/\alpha)_8$-barrel fold (TIM-barrel) typical for catalytic domains of glycosidases and which contains the conserved aspartate, the catalytic nucleophile of family 3 glycosidases. The *C*-terminal domain (residues 421-642) displays a αβα-sandwich fold. The surface buried between the domains of 1407.5 $Å^2$ indicates that both domains are intimately associated (Bahadur et al., 2004); no part of the *C*-terminal domain comes into close contact with the substrate/inhibitor binding site on top of the $(\beta/\alpha)_8$-

TIM-barrel domain (Fig. 23B and 23C). This contrasts NagZ with *Hv*ExoI which displays weak (22%) overall amino acid sequence identity with the *Bacillus* enzyme (Varghese et al., 1999). As mentioned above, in *Hv*ExoI a short helix of the *C*-terminal domain which carries the general acid/base catalyst (Glu491), protrudes into the active site (Fig. 22B and 22C). This helix is missing in NagZ (Fig. 23B and 23C).

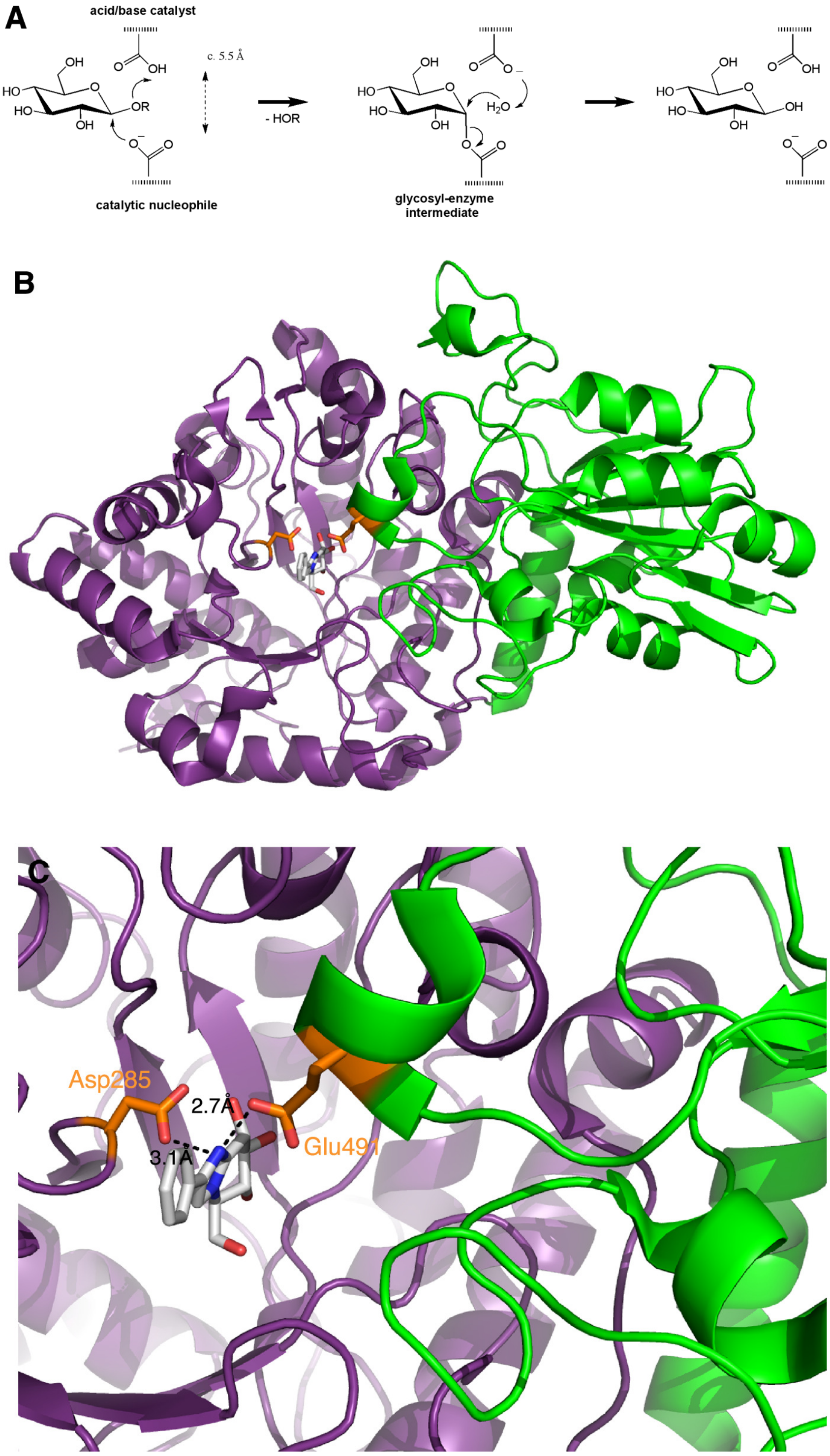

Figure 22. *Hv*ExoI mechanism and structure. (A) Schematic of the general two-step double displacement mechanism of retaining β-glycosidases as proposed also for the family 3 β-exo-glucanase ExoI of *Hordeum vulgare* (*Hv*ExoI). Two catalytic carboxyl groups which are located approximately 5.5 Å apart in the active site act as general nucleophile and general acid/base catalyst, respectively. **(B)** Ribbon model of *Hv*ExoI (PDB identifier 1X38). View of the top of the catalytic *N*-terminal $(\beta/\alpha)_8$ (-TIM)-barrel domain (magenta) to which the inhibitor gluco-phenylimidazole is bound (grey sticks; for chemical structure see Fig. S2) in the acvtive site that carries the catalytic nucleophile (orange stick, left). The *C*-terminal domain, shown in green, is in close contact with the TIM-barrel domain and also contributes to the active site (Varghese et al., 1999). **(C)** A short helix of the *C*-terminal domain approaches the bound inhibitor and carries a glutamate residue (Glu491) that acts as the catalytic acid/base residue (orange stick, right). The amino acid sequence of ExoI shows 22% identity with NagZ (cf. Figs. 21 and 23).

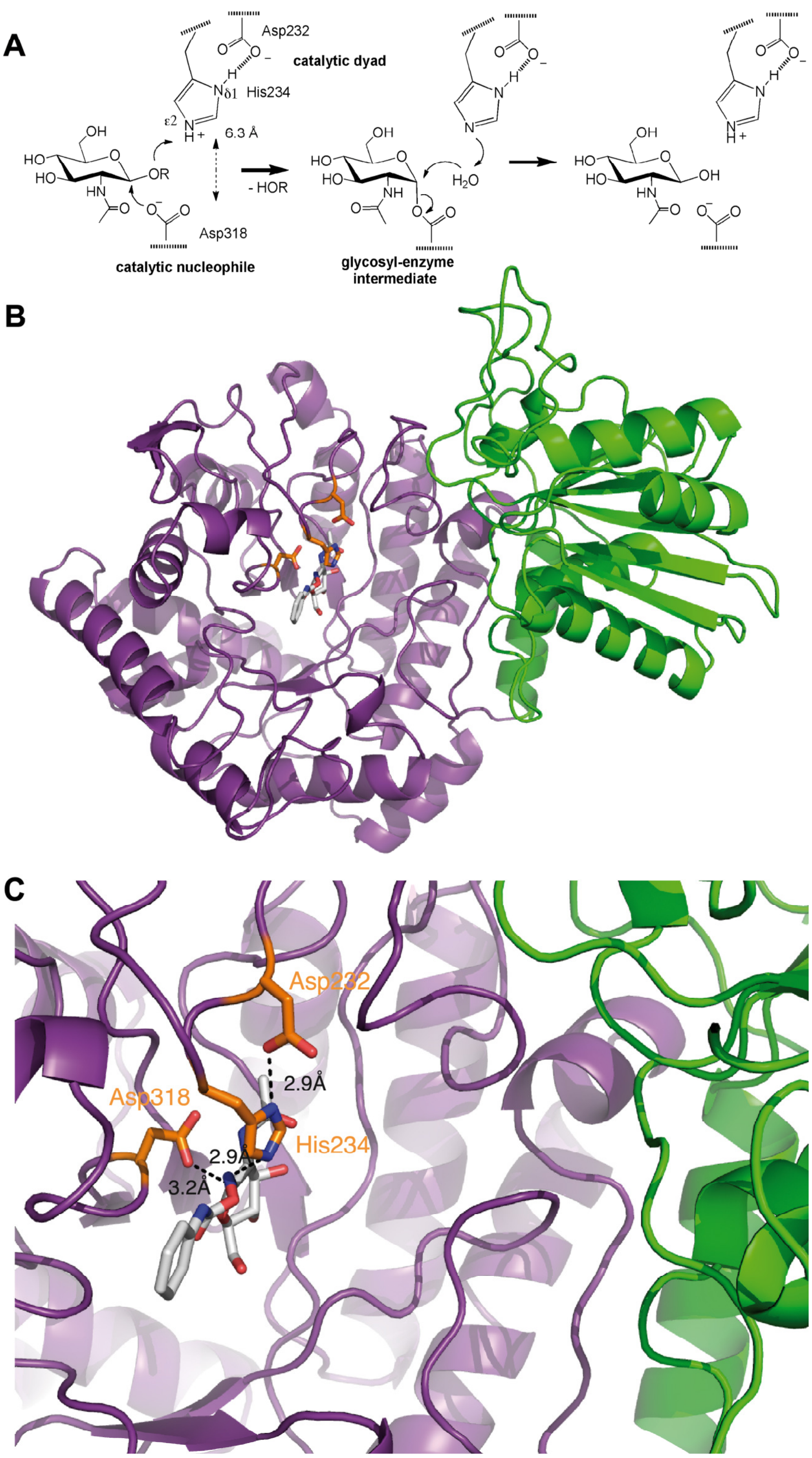

Figure 23. NagZ mechanism and structure. (A) Schematic of the modified double displacement mechanism as proposed for the retaining β-*N*-acetylglucosaminidase of *B. subtilis* NagZ. Besides the aspartate nucleophile (Asp318) the acid/base catalyst was now identified as an Asp-His catalytic dyad in β-*N*-acetylglucosaminidases of family 3. The catalytic groups are located approximately 6.3 Å apart in the active site. **(B)** Ribbon model of NagZ (PDB identifier 3CQM). View of the top of the catalytic *N*-terminal $(\beta/\alpha)_8$ (-TIM)-barrel domain (magenta) to which the inhibitor PUGNAc is bound (grey sticks; for chemical structure see Fig. S2) in the active site that carries the catalytic nucleophile (orange stick, left). In contrast to *Hv*ExoI the *C*-terminal domain of NagZ, shown in green, is further apart from the TIM-barrel domain and does not contribute to the active site (cf. Fig. 22). **(C)** The glutamate mediating the acid/base function in *Hv*ExoI (cf. Fig. 22A) is replaced in NagZ by an Asp-His dyad. Residues Asp232 and His234 (shown in orange) are in H-bond distancy to each other and His234, the acid/base catalyst, as well as Asp318, the catalytic nucleophile (shown in orange), are H-bonding the PUGNAc inhibitor.

An Asp-His dyad in the inhibitor binding site. The overall structures of NagZ with and without the inhibitor are basically identical including the inhibitor site arrangement. An acetate molecule in the unliganded NagZ structure (Fig. 24B) superimposes with the *N*-acetamido group of PUGNAc in the inhibitor bound structure (Fig. 24A). In the latter structure the inhibitor lies on top of the *N*-terminal $(\beta/\alpha)_8$-barrel domain and the GlcNAc residue of PUGNAc makes H-bond contacts with a set of amino acid site chains constituting the active site of NagZ. Intriguingly Nε2 of His234 comes in close, hydrogen bonding distance (2.7 Å) to C1 of PUGNAc (see Fig. 24). The histidine superimposes with the glutamate residue of *Hv*ExoI and is a likely candidate for the acid/base catalyst. Nδ1 of His234 furthermore forms an H-bond to Asp232 (distance of 2.7Å) (Fig. 24).

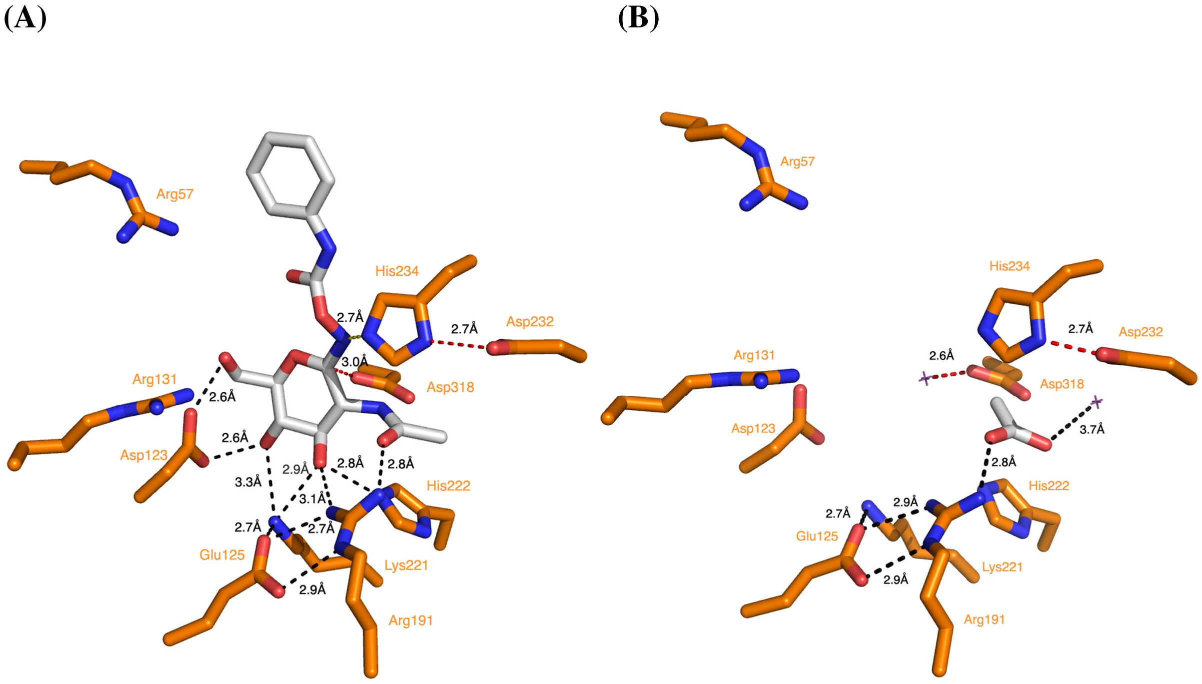

Figure 24. Comparison of the inhibitor binding site of NagZ in the structures with and without PUGNAc (PDB entries 3CQM and 3BMX, respectively). (A) The transition state inhibitor PUGNAc (grey sticks) is coordinated through hydrogen bonds by a set of amino acid side chains of the binding site. Residues that contribute to PUGNAc binding are indicated as well as H-bond distances. Lys221 and His222, as well as Arg131, Arg191 and Arg57 are highly conserved among members of the glucosidase family 3 (Cournoyer and Faure, 2003). Arg57 could be involved in the binding of the natural substrate GlcNAc-MurNAc-(peptide). The catalytic nucleophile (Oδ1 of Asp318) is in 3.0 Å distance to C1 of the GlcNAc part of the inhibitor. Nε2 of His234 is in hydrogen bond distance (2.7Å) to the nitrogen atom between GlcNAc and the aglycon ring of the inhibitor and Nδ1 of His234 is H-bonded to Oδ1 of Asp232. **(B)** The overall inhibitor binding site is almost identical in the structure without inhibitor bound. Instead an acetate molecule is in the binding site at the position that superimposes with the acetamido group of the PUGNAc in (A). In this structure the orientation of His234 by Asp232 is almost identical and the histidine forms a hydrogen bond to a water molecule that is situated in proximity of the acetate.

Kinetic activities. NagZ readily hydrolyzes the chromogenic substrate pNP-β-GlcNAc and the fluorogenic substrate 4-Mu-β-GlcNAc which are convenient substrates for continuous assays and kinetic studies. To investigate the role of His234 and Asp232 in family 3 β-*N*-acetylglucosaminidases, the residues were exchanged by a glycine in NagZ. Both mutants showed severely reduced activity and due to that fact we performed the kinetics with the substrate 4-Mu-β-GlcNAc which generates a fluorogenic product that can be measured with much higher sensitivity than chromogenic products. Hydrolysis of 4-Mu-β-GlcNAc by wild-type NagZ and mutants obeys Michaelis-Menten kinetics and the kinetic constants are given in Table 7. As shown in previous studies with β-glycosidases, the first step (glycosylation, reflected through $k_{\mathrm{cat}}/K_{\mathrm{M}}$) requires major assistance in protonation of the glycosidic oxygen by the general acid/base catalyst for cleavage of the substrates that have poor leaving groups. By contrast the second step (deglycosylation, reflected through k_{cat}) depends on the general acid/base catalyst functioning as base at this stage independent of the leaving group of the substrate.

Table 7. **Kinetic parameters for substrate hydrolysis by NagZ and its mutants.**

Enzyme	Substrate	K_{M} [μM]	k_{cat} [s^{-1}]	$k_{\mathrm{cat}}/K_{\mathrm{M}}$ [s^{-1} mM^{-1}]	$\frac{K_{\mathrm{M}}\ (\mathrm{wt})}{K_{\mathrm{M}}}$	$\frac{k_{\mathrm{cat}}\ (\mathrm{wt})}{k_{\mathrm{cat}}}$	$\frac{k_{\mathrm{cat}}/K_{\mathrm{M}}\ (\mathrm{wt})]}{(k_{\mathrm{cat}}/K_{\mathrm{M}})}$
NagZ (wt)	4-Mu-β-GlcNAc	109.6 ± 4.3	6.42 ± 0.07	58.58	1	1	1
His234Gly	4-Mu-β-GlcNAc	4.57 ± 0.39	3.37 x 10^{-3} ± 4.8 x 10^{-5}	0.74	24	1905	79.2
Asp232Gly	4-Mu-β-GlcNAc	56.24 ± 3.56	1.40 x 10^{-3} ± 2.6 x 10^{-5}	0.025	1.95	4586	2343

Exchanging His234 with glycine resulted in a 1900-fold reduction in k_{cat} but only a 80-fold reduction in $k_{\mathrm{cat}}/K_{\mathrm{M}}$ compared to wild-type NagZ and using 4-Mu-β-GlcNAc as substrate (a fairly good substrate; pK_{a} of methylumbelliferone = 7.79 compared to the natural substrate GlcNAc-MurNAc-peptide with an estimated pK_{a} of about 14). The apparent second-order-rate constant ($k_{\mathrm{cat}}/K_{\mathrm{M}}$) for substrate hydrolysis of 4-Mu-β-GlcNAc by His234Gly thus was much less affected than the apparent first-order rate constant (k_{cat}) indicating less impairment of the glycosylation step (reflected in $k_{\mathrm{cat}}/K_{\mathrm{M}}$) than the deglycosylation step (reflected in k_{cat}), indicating a particularly important role of His234 in base catalysis. This leads to a significant accumulation of the covalent glycosyl-enzyme intermediate being reflected in a 24-fold reduced Michaelis-Menten constant (K_{M}) for His234Gly compared to the wild-type enzyme.

The rate of 4-Mu-β-GlcNAc hydrolysis by the Asp232Gly mutant was 4600-fold reduced compared to wild-type which is an even larger reduction compared to the effect of the His234Gly mutation (Table 7). In contrast, the K_M was only little affected by the Asp232Gly mutation (Table 7). This indicates a shift in the rate-determining step in the Asp232Gly mutant compared to His234Gly from deglycosylation in the latter to glycosylation of the former. This might be explained by a larger impairement of the protonation of the leaving group of the substrate (glycosylation step) in Asp232Gly compared to His234Gly, presumably because Asp232 is required for His234 to function as a proton donor whereas protonation of the glycosidic oxygen by the His234Gly mutant might be substituted by small organic acids (phosphate, acetate) which cannot substitute the general base catalysis (deglycosylation step).

pH dependence of catalysis. The pH activity profile of wild-type NagZ was compared with that of the mutants His234Gly and Asp232Gly. The plots of k_{cat} as a function of pH are shown in Fig. 25 and 26. The pH activity profile for NagZ catalyzed hydrolysis of 4-Mu-β-GlcNAc resembles a bell-shaped curve as expected due to involvement of two ionizable groups in catalysis. The maximal catalytic activity ranges from pH 5.8 to 6.2 in Clark and Lubs solution (0.1 M KH_2PO_4/0.1 M NaOH) (Fig. 25) as well as in McIlvaine buffer (0.1 M citric acid/0.1 M disodium phosphate) (Fig. 26). The pH-activity profiles of NagZ (Fig. 25, 26) indicate acid ionization constants of the nucleophile and the general acid/base catalytic residue (pK_a1 and pK_a2) around 5.0 and 7.0, respectively. Hydrolysis of 4-Mu-β-GlcNAc by His234Gly and Asp232Gly mutants was extremely slow and the pH profiles for both mutants restained activity at alkaline pH, suggesting the elimination of a catalytic acid/base residue with a pK_a value of approximately 7.0 in the mutants.

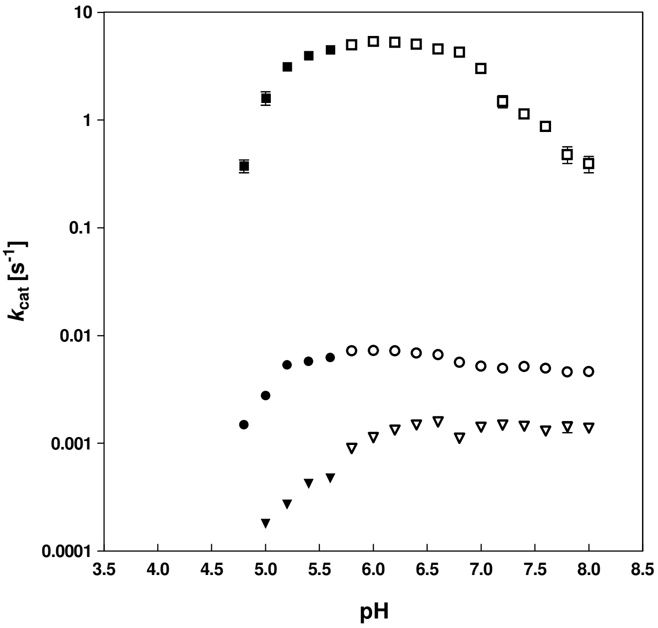

Figure 25. pH activity profiles of NagZ and the mutants. k_{cat} values at different pH were determined for wild-type NagZ (■, □) and the mutants His234Gly (●, ○) and Asp232Gly (▼, ▽). The buffers were: 0.1 M NaAc, pH 4.0 to 5.6, black symboles and 0.1 M $KHPO_4$/0.1 M NaOH, pH 5.8 at 8.0, open symboles. Shown are the means of triplicate experiments.

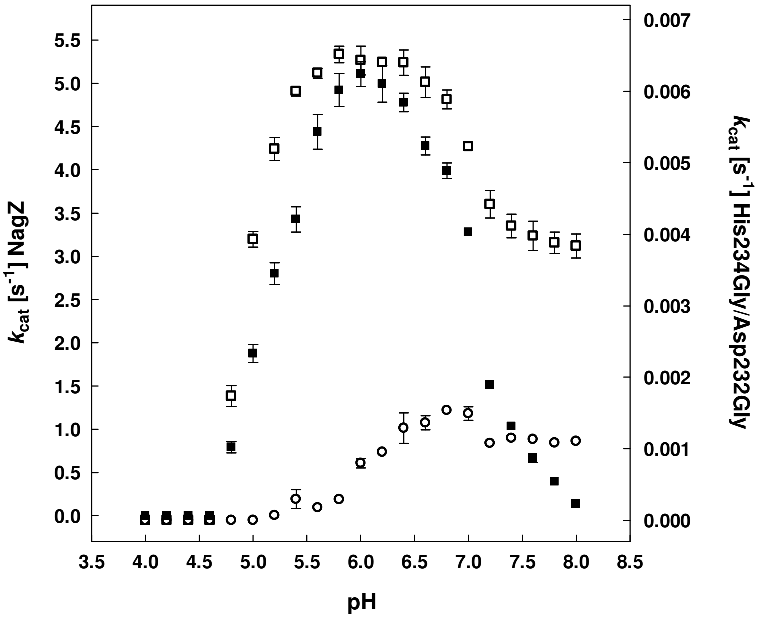

Figure 26. pH activity profiles of NagZ and mutants. The pH activity profiles of GlcNAc'ase NagZ (■) and the two mutants His234Gly (□) and Asp232Gly (○) using McIlvaine buffer ranging from pH 4.0 to 8.0. k_{cat} versus pH plot of GlcNAc'ase NagZ corresponds to the left axis and the k_{cat} versus pH of the mutants to the right axis. Shown are the means of triplicate experiments.

Azide effect and external nucleophile rescue. As shown above for His234Gly deglycosylation is the rate-limiting step in hydrolysis of 4-Mu-β-GlcNAc which leads to accumulation of the glycosyl-enzyme intermediate. It was shown for many glycosidases that the addition of external small nucleophiles like azide can compensate for the loss of the base residue, resulting in rescue of activity (Li et al., 2002; Paal et al., 2004). The activity of the His234Gly mutant of NagZ could not be restored by the addition of azide, although the His234 was replaced by the small glycine which should allow accommodation of small nucleophiles in the active site (Table 8). However, the β-azide product was formed upon 4-Mu-β-GlcNAc cleavage by His234Gly in the presence of azide (Fig 27). Possibly, binding of the small anionic azide to the active site is disfavoured by the negatively charged Asp232. With the Asp232Gly a two fold rate enhancement was observed in the presence of azide, possibly due to accelerating the rate determining glycosylation step.

Table 8. Kinetic parameters for substrate hydrolysis by NagZ and its mutants in the absence and presence of 500 mM sodium azide.

Enzyme	Substrate	K_M [μM]	k_{cat} [s^{-1}]	k_{cat}/K_M [s^{-1} mM^{-1}]
NagZ	4-Mu-β-GlcNAc	109.6 ± 4.3	6.42 ± 0.07	58.58
NagZ + azide	4-Mu-β-GlcNAc	93.48 ± 5.53	1.20 ± 0.019	12.84
His234Gly	4-Mu-β-GlcNAc	4.57 ± 0.39	$3.37 \times 10^{-3} \pm 4.84 \times 10^{-5}$	0.74
His234Gly+ azide	4-Mu-β-GlcNAc	7.84 ± 0.86	$3.03 \times 10^{-3} \pm 6.31 \times 10^{-5}$	0.39
Asp232Gly	4-Mu-β-GlcNAc	56.24 ± 3.56	$1.40 \times 10^{-3} \pm 2.56 \times 10^{-5}$	0.025
Asp232Gly + azide	4-Mu-β-GlcNAc	55.91 ± 4.07	$2.9 \times 10^{-3} \pm 6.01 \times 10^{-5}$	0.052

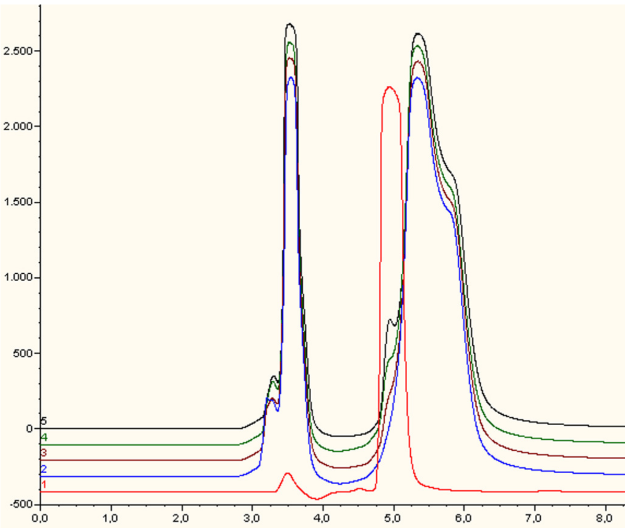

Figure 27. Formation of the β-GlcNAc-azide accumulation product by the His234Gly mutant. pNP-β-GlcNAc was incubated with the His234Gly mutant in the presence of sodium azide. HPLC analysis revealed the formation of an additional product besides 4-nitrophenol (pNP), which was identified by HPLC with a chemical synthesized standard as β-GlcNAc-N_3. This azide product was neither observed when the wild-type enzyme NagZ was used nor was it seen in the absence of the enzyme.

Accumulation of the glycosyl-enzyme intermediate in the His234Gly mutant. Removing the general acid/base catalyst in family 3 glycosidases leads to accumulation of the glycosyl-enzyme intermediate. This was also the case in the His234Gly mutant reflected by a small K_M value. Furthermore the direct evidence that His234 functions as acid/base catalyst was performed by ESI-MS measurement (Fig. 28). After reaction of the His234Gly mutant with the substrate pNP-β-GlcNAc two protein species were observed (Fig. 28). The mass of 71.133 kDa corresponds to the unmodified protein, whereas the mass of 71.336 kDa corresponds to the glycosyl-enzyme intermediate. The mass difference of 203 Da is in accordance with the mass of bound GlcNAc.

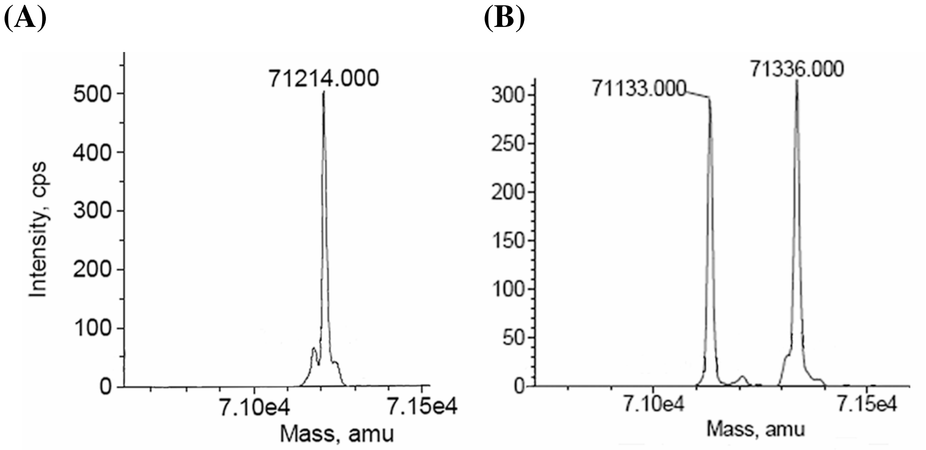

Figure 28. Transform of the electrospray mass spectrum of NagZ (A) and His234Gly (B) after incubation with pNP-β-GlcNAc for 10 min, respectively. The peak with a molecular mass of 71214 amu corresponds to NagZ (the calculated value for $[\text{NagZ}]^+$ lacking methionine is 71214 amu). The peak with a molecular mass of 71133 amu is the His234Gly mutant (the calculated value for $[\text{His234Gly}]^+$ with His_{10} tag and lacking methionine is 71133.6 amu), the peak with a molecular weight of 71336 amu is the His234Gly with covalently bound GlcNAc (the calculated value for $[\text{His234Gly}]^+$ with GlcNAc and lacking-methionine is 71336 amu). The mass shift of 202 Da corresponds to the GlcNAc residue covalently bound to His234Gly.

DISCUSSION

A detailed understanding of the mechanism of glycosidases is a prerequisite for the design of potent selective inhibitors that may serve as therapeutic agents. The classification of glycosidases into families based on amino acid sequence leading to the identification of evolutionary, structural and mechanistic relationships within these enzymes (www.cazy.org) has greatly facilitated the efforts towards the rational design of such inhibitors. Given that structure is more conserved than sequence, it is assumed that the mechanism of glycoside hydrolysis is identical for all members of a family which makes this classification particularly valuable. Indeed catalytic residues identified in one member of a family generally allowed the prediction of these residues in others. This does not hold for all cases. One example is the family 1 of glycosidases whose members operate by a two-step double displacement retention mechanism. Myrosinases of this family cleave the highly reactive S-glycoside sinigrin without requiring protonic assistance for the glycosylation step in catalysis, hence lacking a general acid residue. The subsequent deglycosylation step depends on the unusual coenzyme ascorbic acid that acts as a base catalyst in hydrolysis of the glycosyl-enzyme intermediate (Burmeister et al., 2000).

This study now shows that the β-*N*-acetylglucosaminidases of family 3 operate by catalytic mechanisms different from other members (β-glucosidases and β-xylosidases) of this family. In this paper we present the first crystal structure of a two-domain β-*N*-acetylglucosaminidase of family 3 of glycosidases. The NagZ structure along with kinetic data revealed that an Asp-His dyad is the acid/base residue in β-*N*-acetylglucosaminidases of this family, whereas a glutamate residue had been shown to be the general acid/base catalyst in other members of this family of glycosidases. Hence it may be justifiable to subdivide family 3 of glycosidases in two families.

Involvement of a histidine residue, respectively an Asp-His dyad, in glycoside hydrolysis is unique. It is commonly found in ribonucleases (Mignon et al., 2002; Quirk et al., 1998; Quirk and Raines, 1999; Schultz et al., 1998) and the Asp-His-Ser catalytic triad is prominent of serine proteases (Ekici et al., 2008; Hedstrom, 2002; Markley and Westler, 1996) and lipases (Brady et al., 1990; Chahinian et al., 2006; Schrag et al., 1991). In the well-studied serine proteases the Asp-His hydrogen bond in the catalytic triad is known to contribute greatly to catalysis, potentially via forming a low-barrier hydrogen bond (Ash et al., 1997) which might also hold for β-*N*-acetylglucosaminidases of family 3. There is no evidence for the formation of a low-barrier hydrogen bond between His234 and Asp232. Possibly the major role of Asp232 is its influence on proton dissociation of Nε2 of His 234 for catalysis. Ludwig suggested a cooperative behaviour that may sharpen the acid/base behaviour of the His (Ludwig, 2001). The catalytic triad His57-Asp102-Ser195 of chymotrypsinogen (bovine chymotrypsin numbering) functions in this way; Ser 195 functions as nucleophilic catalyst, assisted by Nε2 of His57 that serves as acid/base catalyst and residue Asp102 assists in acid/base catalysis by hydrogen bonding to Nδ1 of His57 increasing the pK_a of His57. In the NagZ structure lacking PUGNAc (Fig. 24B) electron density can be attributed to a water molecule in H-bond distance to Nε2 of His234. Although at 1.4 Å resolution this has to be taken with caution, the situation clearly resembles that of chymotrypsinogen in which the serine of the triad is H-bonded by the His (Hedstrom, 2002). According to the suggested mechanism (Fig. 23A) in NagZ the catalytic His234 builds an ion pair with Asp232 thereby allowing the protonation of the extracyclic oxygen of the glycosidic bond and facilitating the removal of the leaving group upon nucleophilic attack of Asp318. In a second step the His removes a proton of an incoming water molecule thereby hydrolyzing the glycosyl-enzyme intermediate. Both catalytic residues, the nucleophile and the acid/base catalyst, reside on the *N*-terminal domain. They are located approximately 6.3 Å apart which is in the range of catalytic residues involved in bond-cleavage via a two-step double displacement mechanism in glycosidases (Rye and Withers, 2000).

The two catalytic residues of NagZ are positioned at the carboxy-terminal ends of β-strands 5 and 7. The Asp-His dyad lays on an extended loop that occupies a position that is provided in the NagZ molecule due to the shortened loop after strand 4, thereby resembling the situation of the 4/7-superfamily of glycoside hydrolases (clan GH-A glycoside hydrolases) in which the acid/base catalyst lays in a loop extending β-strand 4 (Henrissat and Davies, 1997; Jenkins et al., 1995) and the nucleophiles are positioned at the *C*-terminus of β-strand 7. Further evidence on the residue His234 functioning as acid/base catalyst in family 3 β-*N*-acetylglucosaminidases was obtained from mutational enzyme kinetic studies. In general glycosidases reveal a bell-shaped pH profile due to participation of two ionizable carboxyl groups in substrate hydrolysis. Deletion of one of the carboxyl groups results in disappearance of such a curve. Indeed deletion of the acid/base catalyst His234 as well as Asp232 by site-directed mutagenesis did not show pH-dependence at higher pH ranges and therefore suggest that the group which is responsible for pH-dependence was removed.

Other evidence for the identity of His234 as the acid/base catalyst was obtained by determining the catalytic efficiency of the wild-type and the mutant enzyme. The second-order rate constant k_{cat}/K_M of NagZ is proportional to the association rate constant of an enzyme and the rate-limiting transition state during catalysis (Wolfenden, 1976). Accordingly exchange of His234 with glycine decreased the affinity of the enzyme for the transition state towards the glycosyl-enzyme by 10^4-fold for 4-Mu-β-GlcNAc. Together all these results, structural as well as kinetic data, provide evidence that His234 of the Asp-His dyad of family 3 β-*N*-acetylglucosaminidases acts as the general acid/base assisted by Asp232. This contrasts with a study on *Clostridium paraputrificum* M-21 β-*N*-acetylglucosaminidase (Nag3A). A conserved aspartate residue (Asp175) on the *N*-terminal domain was proposed as the acid/base catalyst (Li et al., 2006) and replacement of Asp175 with Ala abolished the activity of NagZ. However, clear kinetic evidence for a role as acid/base catalyst of the above mentioned residue is still lacking.

Recently the crystal structure of a single domain β-*N*-acetylglucosaminidases from *Vibrio cholerae*, *Vc*NagZ, in the presence of the competitive transition state like inhibitor PUGNAc has been reported (Stubbs et al., 2007). This structure provided no information regarding the identity of a putative acid/base catalyst since the Asp-His dyad is flipped outward together with a flexible loop. Moreover the aspartate nucleophile within this structure is distorted indicating an unphysiological conformation of the active site in the crystal or an unproductive binding of the inhibitor (Fig. 24B). It can be speculated that the proper orientation of the Asp-His dyad in this enzyme can be induced upon substrate binding providing the protein with a high degree of substrate specificity which is needed since the enzyme is destined for GlcNAc-1,6-anhydroMurNAc cleavage in the cytoplasm; affecting other GlcNAc-residues of the cell is not permissible. The classification of glycosidases in families based on sequence and secondary structure should imply that the members of a family are structurally similar and act by an identical mechanism despite a possible heterogeneity of substrate specificity. Indeed the residues His234 and Asp232 are completely conserved in the sequence pattern K-H-(F/I)-P-G-(H/L)-G-x(4)-D-(S/T)-H only in the subfamily of β-*N*-acetylglucosaminidases of family 3 glycosidases.

The obvious question is why family 3 of β-*N*-acetylglucosaminidases apparently are the only glycosidases that act by a histidine catalysis mechanism. One rational for the replacement of an acid/base glutamate for an Asp-His dyad might be the negative charge of the natural substrates of these enzymes - MurNAc or 1,6-anhydroMurNAc containing cell wall fragments as mentinoned above. The negative charge of the carboxylic acid of these molecules might inflict the use of a negative charged acid/base catalyst in the active site. A similar situation holds for sialidases which were shown to utilize tyrosine as a catalytic nucleophile rather than a carboxylate nucleophile (Watts et al., 2003; Watts et al., 2006). Here it was argued that the anomeric center of the sialic acid sugars bears an anionic carboxylate residue and the nucleophile attack by an anionic nucleophile is therefore disfavoured. It can be speculated that other families of glycosidases that use an Asp-His dyad, in particular such that act on negatively charged substrates, remain to be discovered.

SUPPORTING INFORMATION

Table S1. Comparison of structural quality between the experimental model and the homology model.

Parameters	**NagZ**	**NagZ-PUGNAc**
Crystal Information		
Space group	P1	P1
Solvent content (%)	48.1	47.2
Data Collection[a]		
Unit cell dimensions (Å)	$a = 58.4$, $b = 73.1$, $c = 83.6$	$a = 58.5$, $b = 73.2$, $c = 83.8$
Unit cell dimensions (deg)	$\alpha = 79.8$, $\beta = 69.6$, $\gamma = 88.3$	α = 79.8, β = 69. 5, γ =
Wavelength (Å)	0.9999	88.2
Resolution range (Å)	49.18-1.40 (1.50-1.40)	0.9792
Total observations	1601297 (66995)	48.55-1.70 (1.80-1.70)
Unique reflections	228046 (25215)	246547 (31269)
I/σ	13.3 (2.7)	127623 (18341)
Completeness (%)	90.8 (53.7)	7.5 (1.5)
R_{meas} (%)	9.0 (57.2)	89.9 (79.9)
$R_{mrgd\text{-}F}$ (%)	8.0 (60.5)	12.1 (63.6)
		19.3 (72.2)
Refinement		
Resolution range (Å)	42.84-1.40 (1.42-1.40)	48.55-1.70 (1.73-1.70)
R_{work}[b]	12.7 (31.5)	21.5 (30.3)
R_{free}[b]	16. 6 (38.5)	25.8 (36.3)
Model composition		
Protein residues	1234	1234
Ligand atoms	-	98
Water molecules	1388	1254
Average B (Å^2)	20.9	24.7
RMSD[c]		
Bond length (Å)	0.007	0.003
Bond angles (deg)	0.967	0.757
Ramachandran plot[d]		
Favored regions (%)	97.8	97.3
Allowed regions (%)	99.8	99.8
Twin law	-[e]	h, -k, h-l
Twin fraction (%)	-[e]	17.7

[a] Values in parentheses refer to the high resolution shell

[b] R_{work} and R_{free} = $\sum_h||F(h)_{obs}|-|F(h)_c||/|F(h)_o|$ for reflections in the working and test sets (5 % of all data), respectively.

[c] RMSD = root mean square deviation

[d] Regions defined by Molprobity (Lovell et al., 2003)

[e]..The twinning fraction was insignificant and therefore not taken into account during refinement.

Figure S1. Chemical structures of substrates of NagZ.

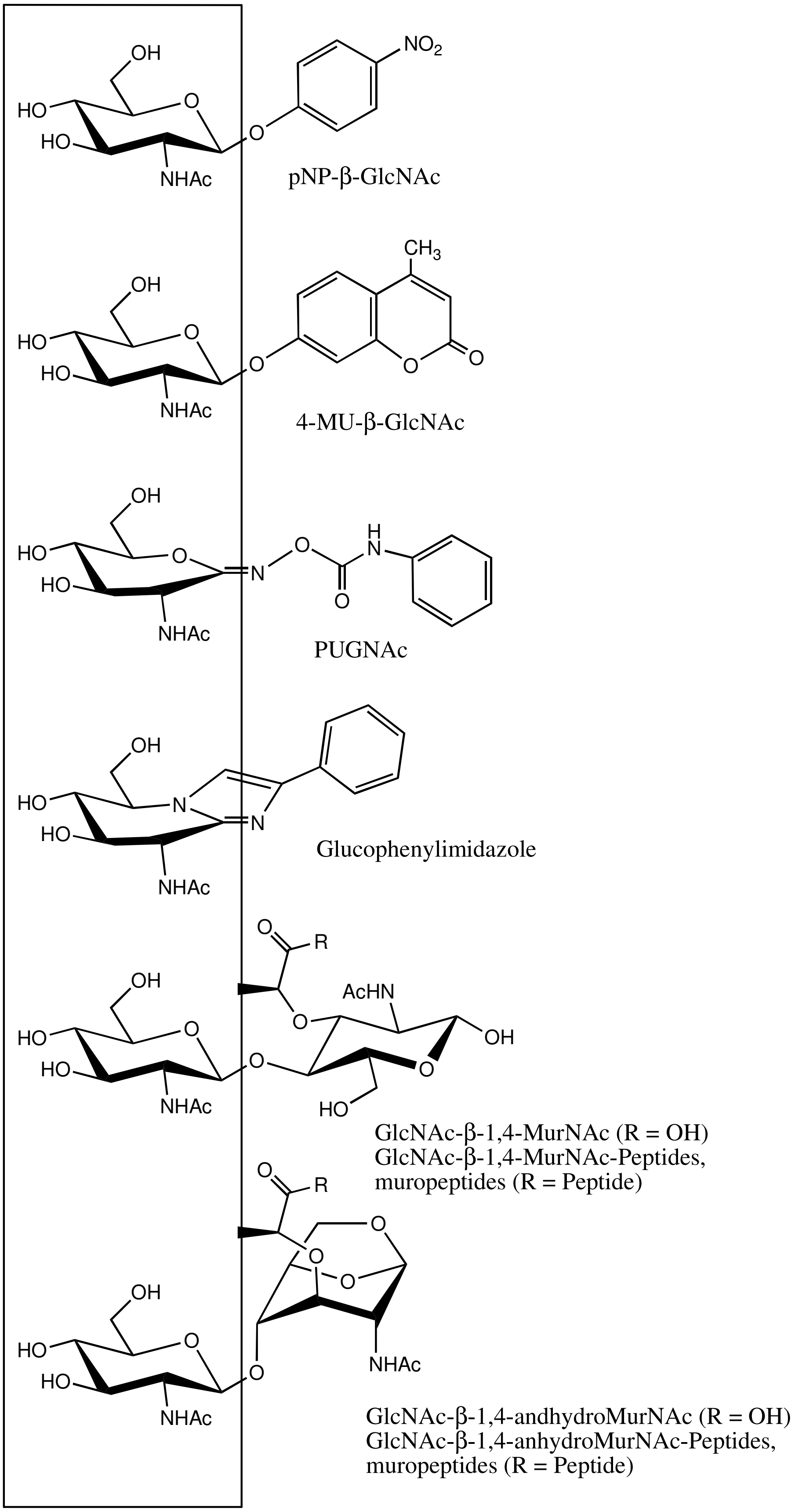

pNP-β-GlcNAc

4-MU-β-GlcNAc

PUGNAc

Glucophenylimidazole

GlcNAc-β-1,4-MurNAc (R = OH)
GlcNAc-β-1,4-MurNAc-Peptides,
muropeptides (R = Peptide)

GlcNAc-β-1,4-andhydroMurNAc (R = OH)
GlcNAc-β-1,4-anhydroMurNAc-Peptides,
muropeptides (R = Peptide)

Figure S2. Transition state to the glycosylated *Hv*ExoI and *Bs*NagZ.

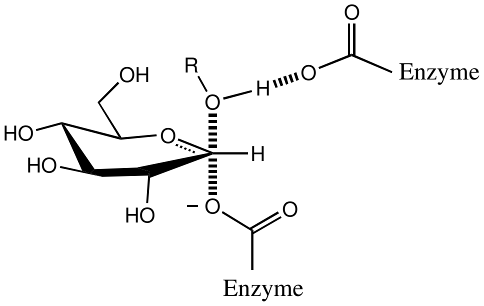

Transition state to the glycosylated *Hv*ExoI

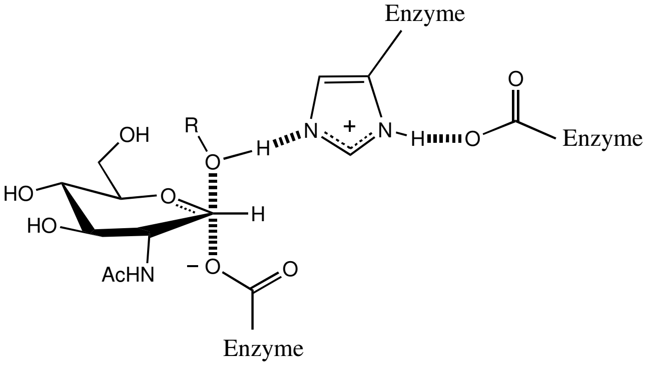

Transition state to the glycosylated *Bs*NagZ

GENERAL REFERENCES

Abbott, D.W., M.S. Macauley, D.J. Vocadlo, and A.B. Boraston. 2009. *Streptococcus pneumoniae* endohexosaminidase D, structural and mechanistic insight into substrate-assisted catalysis in family 85 glycoside hydrolases. *J Biol Chem*. 284:11676-11689.

Adams, P.D., R.W. Grosse-Kunstleve, L.W. Hung, T.R. Ioerger, A.J. McCoy, N.W. Moriarty, R.J. Read, J.C. Sacchettini, N.K. Sauter, and T.C. Terwilliger. 2002. PHENIX: building new software for automated crystallographic structure determination. *Acta Crystallogr D Biol Crystallogr*. 58:1948-1954.

Anderson, J.S., M. Matsuhashi, M.A. Haskin, and J.L. Strominger. 1965. Lipid-Phosphoacetylmuramyl-Pentapeptide and Lipid-Phosphodisaccharide-Pentapeptide: Presumed Membrane Transport Intermediates in Cell Wall Synthesis. *Proc Natl Acad Sci U S A*. 53:881-889.

Araki, Y., and E. Ito. 1989. Linkage units in cell walls of Gram-positive bacteria. *Crit Rev Microbiol*. 17:121-135.

Archibald, A.R., I.C. Hancock, and C.R. Harwood. 1993. Cell wall structure, synthesis, and turnover. *In: Sonnenshein, A.L., Hoch, J.A., Losick, R. (eds). Bacillus subtilis and other Gram-positve bacteria: Biochemistry, physiology, and molecular genetics. ASM press, Washington, D.C.*:381-410.

Ash, E.L., J.L. Sudmeier, E.C. De Fabo, and W.W. Bachovchin. 1997. A low-barrier hydrogen bond in the catalytic triad of serine proteases? Theory versus experiment. *Science*. 278:1128-1132.

Atrih, A., G. Bacher, G. Allmaier, M.P. Williamson, and S.J. Foster. 1999a. Analysis of peptidoglycan structure from vegetative cells of *Bacillus subtilis* 168 and role of PBP 5 in peptidoglycan maturation. *J Bacteriol*. 181:3956-3966.

Atrih, A., G. Bacher, R. Korner, G. Allmaier, and S.J. Foster. 1999b. Structural analysis of *Bacillus megaterium* KM spore peptidoglycan and its dynamics during germination. *Microbiology*. 145:1033-1041.

Atrih, A., P. Zollner, G. Allmaier, and S.J. Foster. 1996. Structural analysis of *Bacillus subtilis* 168 endospore peptidoglycan and its role during differentiation. *J Bacteriol*. 178:6173-6183.

Badet, B., P. Vermoote, and F. Le Goffic. 1988. Glucosamine synthetase from *Escherichia coli*: kinetic mechanism and inhibition by *N*3-fumaroyl-L-2,3-diaminopropionic derivatives. *Biochemistry*. 27:2282-2287.

Bahadur, R.P., P. Chakrabarti, F. Rodier, and J. Janin. 2004. A dissection of specific and non-specific protein-protein interfaces. *J Mol Biol*. 336:943-955.

Barnickel, G., H. Labischinski, H. Bradaczek, and P. Giesbrecht. 1979. Conformational energy calculation on the peptide part of murein. *Eur J Biochem*. 95:157-165.

Barreteau, H., A. Kovac, A. Boniface, M. Sova, S. Gobec, and D. Blanot. 2008. Cytoplasmic steps of peptidoglycan biosynthesis. *FEMS Microbiol Rev*. 32:168-207.

Berkeley, R.C., S.J. Brewer, J.M. Ortiz, and J.B. Gillespie. 1973. An exo-β-*N*-acetylglucosaminidase from *Bacillus subtilis* B; characterization. *Biochim Biophys Acta*. 309:157-168.

Bernhardt, J., J. Weibezahn, C. Scharf, and M. Hecker. 2003. *Bacillus subtilis* during feast and famine: visualization of the overall regulation of protein synthesis during glucose starvation by proteome analysis. *Genome Res*. 13:224-237.

Bertsche, U., E. Breukink, T. Kast, and W. Vollmer. 2005. In vitro murein peptidoglycan synthesis by dimers of the bifunctional transglycosylase-transpeptidase PBP1B from *Escherichia coli*. *J Biol Chem*. 280:38096-38101.

Beveridge, T.J. 2006. Visualizing bacterial cell walls and biofilms. Cryo-transmission electron microscopy is enabling investigators to examine native, hydrated structures in bacteria and biofilms. *Microbe*. 1:279-284.

Bhavsar, A.P., L.K. Erdman, J.W. Schertzer, and E.D. Brown. 2004. Teichoic acid is an essential polymer in *Bacillus subtilis* that is functionally distinct from teichuronic acid. *J Bacteriol*. 186:7865-7873.

Bi, E.F., and J. Lutkenhaus. 1991. FtsZ ring structure associated with division in *Escherichia coli*. *Nature*. 354:161-164.

Blackman, S.A., T.J. Smith, and S.J. Foster. 1998. The role of autolysins during vegetative growth of *Bacillus subtilis* 168. *Microbiology*. 144:73-82.

Blattner, F.R., G. Plunkett, 3rd, C.A. Bloch, N.T. Perna, V. Burland, M. Riley, J. Collado-Vides, J.D. Glasner, C.K. Rode, G.F. Mayhew, J. Gregor, N.W. Davis, H.A. Kirkpatrick, M.A. Goeden, D.J. Rose, B. Mau, and Y. Shao. 1997. The complete genome sequence of *Escherichia coli* K-12. *Science*. 277:1453-1462.

Boland, F.M., A. Atrih, H. Chirakkal, S.J. Foster, and A. Moir. 2000. Complete spore-cortex hydrolysis during germination of *Bacillus subtilis* 168 requires SleB and YpeB. *Microbiology*. 146:57-64.

Boothby, D., L. Daneo-Moore, M.L. Higgins, J. Coyette, and G.D. Shockman. 1973. Turnover of bacterial cell wall peptidoglycans. *J Biol Chem*. 248:2161-2169.

Born, P., E. Breukink, and W. Vollmer. 2006. In vitro synthesis of cross-linked murein and its attachment to sacculi by PBP1A from *Escherichia coli*. *J Biol Chem*. 281:26985-26993.

Bouhss, A., A.E. Trunkfield, T.D. Bugg, and D. Mengin-Lecreulx. 2008. The biosynthesis of peptidoglycan lipid-linked intermediates. *FEMS Microbiol Rev*. 32:208-233.

Bradford, M.M. 1976. A rapid and sensitive method for the quantitation of microgram quantities of protein utilizing the principle of protein-dye binding. *Anal Biochem*. 72:248-254.

Brady, L., A.M. Brzozowski, Z.S. Derewenda, E. Dodson, G. Dodson, S. Tolley, J.P. Turkenburg, L. Christiansen, B. Huge-Jensen, L. Norskov, and et al. 1990. A serine protease triad forms the catalytic centre of a triacylglycerol lipase. *Nature*. 343:767-770.

Braun, V. 1975. Covalent lipoprotein from the outer membrane of *Escherichia coli*. *Biochim Biophys Acta*. 415:335-377.

Braun, V., and U. Sieglin. 1970. The covalent murein-lipoprotein structure of the *Escherichia coli* cell wall. The attachment site of the lipoprotein on the murein. *Eur J Biochem*. 13:336-346.

Brown, K., F. Pompeo, S. Dixon, D. Mengin-Lecreulx, C. Cambillau, and Y. Bourne. 1999. Crystal structure of the bifunctional *N*-acetylglucosamine-1-phosphate uridyltransferase from *Escherichia coli*: a paradigm for the related pyrophosphorylase superfamily. *EMBO J*. 18:4096-4107.

Burmeister, W.P., S. Cottaz, P. Rollin, A. Vasella, and B. Henrissat. 2000. High resolution X-ray crystallography shows that ascorbate is a cofactor for myrosinase and substitutes for the function of the catalytic base. *J Biol Chem*. 275:39385-39393.

Cabeen, M.T., and C. Jacobs-Wagner. 2005. Bacterial cell shape. *Nat Rev Microbiol*. 3:601-610.

Cabeen, M.T., and C. Jacobs-Wagner. 2007. Skin and bones: the bacterial cytoskeleton, cell wall, and cell morphogenesis. *J Cell Biol*. 179:381-387.

Cetinbas, N., M.S. Macauley, K.A. Stubbs, R. Drapala, and D.J. Vocadlo. 2006. Identification of Asp174 and Asp175 as the key catalytic residues of human *O*-GlcNAcase by functional analysis of site-directed mutants. *Biochemistry*. 45:3835-3844.

Chahinian, H., T. Snabe, C. Attias, P. Fojan, S.B. Petersen, and F. Carriere. 2006. How gastric lipase, an interfacial enzyme with a Ser-His-Asp catalytic triad, acts optimally at acidic pH. *Biochemistry*. 45:993-1001.

Chaloupka, J., and P. Kreckova. 1971. Turnover of mucopeptide during the life cycle of *Bacillus megaterium*. *Folia Microbiol (Praha)*. 16:372-382.

Chen, R., S.B. Guttenplan, K.M. Blair, and D.B. Kearns. 2009. Role of the σ^D-dependent autolysins in *Bacillus subtilis* population heterogeneity. *J Bacteriol*. 191:5775-5784.

Cheng, Q., H. Li, K. Merdek, and J.T. Park. 2000. Molecular characterization of the β-*N*-acetylglucosaminidase of *Escherichia coli* and its role in cell wall recycling. *J Bacteriol*. 182:4836-4840.

Cheng, Q., and J.T. Park. 2002. Substrate specificity of the AmpG permease for recycling of cell wall anhydro-muropeptides. *J Bacteriol*. 184:6434-6436.

Chir, J., S. Withers, C.F. Wan, and Y.K. Li. 2002. Identification of the two essential groups in the family 3 β-glucosidase from *Flavobacterium meningosepticum* by labelling and tandem mass spectrometric analysis. *Biochem J*. 365:857-863.

Cournoyer, B., and D. Faure. 2003. Radiation and functional specialization of the family-3 glycoside hydrolases. *J Mol Microbiol Biotechnol*. 5:190-198.

Cowtan, K. 2006. The Buccaneer software for automated model building. 1. Tracing protein chains. *Acta Crystallogr D Biol Crystallogr*. 62:1002-1011.

Dahl, U., T. Jaeger, B.T. Nguyen, J.M. Sattler, and C. Mayer. 2004. Identification of a phosphotransferase system of *Escherichia coli* required for growth on *N*-acetylmuramic acid. *J Bacteriol*. 186:2385-2392.

Dan, S., I. Marton, M. Dekel, B.A. Bravdo, S. He, S.G. Withers, and O. Shoseyov. 2000. Cloning, expression, characterization, and nucleophile identification of family 3, *Aspergillus niger* β-glucosidase. *J Biol Chem*. 275:4973-4980.

Daneo-Moore, L., J. Coyette, M. Sayare, D. Boothby, and G.D. Shockman. 1975. Turnover of the cell wall peptidoglycan of *Lactobacillus acidophilus*. The presence of a fraction immune to turnover. *J Biol Chem*. 250:1348-1353.

Daniel, R.A., and J. Errington. 2003. Control of cell morphogenesis in bacteria: two distinct ways to make a rod-shaped cell. *Cell*. 113:767-776.

De Boer, W.R., F.J. Kruyssen, and J.T. Wouters. 1981. Cell wall turnover in batch and chemostat cultures of *Bacillus subtilis*. *J Bacteriol*. 145:50-60.

Del Rio, L.A., R.C. Berkeley, S.J. Brewer, and S.E. Roberts. 1973. An enzyme from *Bacillus subtilis* B with exo-β-*N*-acetylmuramidase activity. *FEBS Lett*. 37:7-9.

Demchick, P., and A.L. Koch. 1996. The permeability of the wall fabric of *Escherichia coli* and *Bacillus subtilis*. *J Bacteriol*. 178:768-773.

den Blaauwen, T., M.A. de Pedro, M. Nguyen-Disteche, and J.A. Ayala. 2008. Morphogenesis of rod-shaped sacculi. *FEMS Microbiol Rev*. 32:321-344.

Di Berardino, M., A. Dijkstra, D. Stuber, W. Keck, and M. Gubler. 1996. The monofunctional glycosyltransferase of *Escherichia coli* is a member of a new class of peptidoglycan-synthesising enzymes. *FEBS Lett*. 392:184-188.

Dijkstra, A.J., and W. Keck. 1996. Peptidoglycan as a barrier to transenvelope transport. *J Bacteriol*. 178:5555-5562.

Dmitriev, B.A., S. Ehlers, and E.T. Rietschel. 1999. Layered murein revisited: a fundamentally new concept of bacterial cell wall structure, biogenesis and function. *Med Microbiol Immunol*. 187:173-181.

Dmitriev, B.A., S. Ehlers, E.T. Rietschel, and P.J. Brennan. 2000. Molecular mechanics of the mycobacterial cell wall: from horizontal layers to vertical scaffolds. *Int J Med Microbiol*. 290:251-258.

Dmitriev, B.A., F.V. Toukach, O. Holst, E.T. Rietschel, and S. Ehlers. 2004. Tertiary structure of *Staphylococcus aureus* cell wall murein. *J Bacteriol.* 186:7141-7148.

Dmitriev, B.A., F.V. Toukach, K.J. Schaper, O. Holst, E.T. Rietschel, and S. Ehlers. 2003. Tertiary structure of bacterial murein: the scaffold model. *J Bacteriol.* 185:3458-3468.

Driks, A. 1999. *Bacillus subtilis* spore coat. *Microbiol Mol Biol Rev.* 63:1-20.

Ehlert, K., J.V. Höltje, and M.F. Templin. 1995. Cloning and expression of a murein hydrolase lipoprotein from *Escherichia coli*. *Mol Microbiol.* 16:761-768.

Eichenberger, P., S.T. Jensen, E.M. Conlon, C. van Ooij, J. Silvaggi, J.E. Gonzalez-Pastor, M. Fujita, S. Ben-Yehuda, P. Stragier, J.S. Liu, and R. Losick. 2003. The σ^E regulon and the identification of additional sporulation genes in *Bacillus subtilis*. *J Mol Biol.* 327:945-972.

Ekici, O.D., M. Paetzel, and R.E. Dalbey. 2008. Unconventional serine proteases: variations on the catalytic Ser/His/Asp triad configuration. *Protein Sci.* 17:2023-2037.

El Ghachi, M., A. Derbise, A. Bouhss, and D. Mengin-Lecreulx. 2005. Identification of multiple genes encoding membrane proteins with undecaprenyl pyrophosphate phosphatase (UppP) activity in *Escherichia coli*. *J Biol Chem.* 280:18689-18695.

Emsley, P., and K. Cowtan. 2004. Coot: model-building tools for molecular graphics. *Acta Crystallogr D Biol Crystallogr.* 60:2126-2132.

Engelberg-Kulka, H., and R. Hazan. 2003. Cannibals defy starvation and avoid sporulation. *Science.* 301:467-468.

Errington, J., R.A. Daniel, and D.J. Scheffers. 2003. Cytokinesis in bacteria. *Microbiol Mol Biol Rev.* 67:52-65.

Fan, D.P., and M.M. Beckman. 1971. Mutants of *Bacillus subtilis* demonstrating the requirement of lysis for growth. *J Bacteriol.* 105:629-636.

Foster, S.J. 1991. Cloning, expression, sequence analysis and biochemical characterization of an autolytic amidase of *Bacillus subtilis* 168 trpC2. *J Gen Microbiol.* 137:1987-1998.

Foster, S.J. 1993. Analysis of *Bacillus subtilis* 168 prophage-associated lytic enzymes; identification and characterization of CWLA-related prophage proteins. *J Gen Microbiol.* 139:3177-3184.

Foster, S.J., and D.L. Popham. 2002. Structure and synthesis of cell wall, spore cortex, teichoic acids, S-layers, and capsules. *In: Sonenshein AL, Hoch JA, Losick R (eds) Bacillus subtilis and its closest relatives: From genes to cells. ASM Press, Washington, D.C.*:21-41.

Fujita, K., R. Sato, K. Toma, K. Kitahara, T. Suganuma, K. Yamamoto, and K. Takegawa. 2007. Identification of the catalytic acid base residue of arthrobacter endo-β-*N*-acetylglucosaminidase by chemical rescue of an inactive mutant. *J Biochem.* 142:301-306.

Fukushima, T., T. Kitajima, H. Yamaguchi, Q. Ouyang, K. Furuhata, H. Yamamoto, T. Shida, and J. Sekiguchi. 2008. Identification and characterization of novel cell wall hydrolase CwlT: a two-domain autolysin exhibiting *N*-acetylmuramidase and DL-endopeptidase activities. *J Biol Chem*. 283:11117-11125.

Fukushima, T., Y. Yao, T. Kitajima, H. Yamamoto, and J. Sekiguchi. 2007. Characterization of new L,D-endopeptidase gene product CwlK (previous YcdD) that hydrolyzes peptidoglycan in *Bacillus subtilis*. *Mol Genet Genomics*. 278:371-383.

Ghuysen, J.M. 1968. Use of bacteriolytic enzymes in determination of wall structure and their role in cell metabolism. *Bacteriol Rev*. 32:425-464.

Ghuysen, J.M. 1991. Serine β-lactamases and penicillin-binding proteins. *Annu Rev Microbiol*. 45:37-67.

Glauner, B. 1988. Separation and quantification of muropeptides with high-performance liquid chromatography. *Anal Biochem*. 172:451-464.

Glauner, B., J.V. Höltje, and U. Schwarz. 1988. The composition of the murein of *Escherichia coli*. *J Biol Chem*. 263:10088-10095.

Goehring, N.W., and J. Beckwith. 2005. Diverse paths to midcell: assembly of the bacterial cell division machinery. *Curr Biol*. 15:514-526.

Goffin, C., and J.M. Ghuysen. 1998. Multimodular penicillin-binding proteins: an enigmatic family of orthologs and paralogs. *Microbiol Mol Biol Rev*. 62:1079-1093.

Goins, T.L., and J.E. Cutler. 2000. Relative abundance of oligosaccharides in *Candida* species as determined by fluorophore-assisted carbohydrate electrophoresis. *J Clin Microbiol*. 38:2862-2869.

Gonzalez-Pastor, J.E., E.C. Hobbs, and R. Losick. 2003. Cannibalism by sporulating bacteria. *Science*. 301:510-513.

Goodell, E.W. 1985. Recycling of murein by *Escherichia coli*. *J Bacteriol*. 163:305-310.

Goodell, E.W., and U. Schwarz. 1983. Cleavage and resynthesis of peptide cross bridges in *Escherichia coli* murein. *J Bacteriol*. 156:136-140.

Goodell, E.W., and U. Schwarz. 1985. Release of cell wall peptides into culture medium by exponentially growing *Escherichia coli*. *J Bacteriol*. 162:391-397.

Hadi, T., U. Dahl, C. Mayer, and M.E. Tanner. 2008. Mechanistic studies on *N*-acetylmuramic acid 6-phosphate hydrolase (MurQ): an etherase involved in peptidoglycan recycling. *Biochemistry*. 47:11547-11558.

Harvey, A.J., M. Hrmova, R. De Gori, J.N. Varghese, and G.B. Fincher. 2000. Comparative modeling of the three-dimensional structures of family 3 glycoside hydrolases. *Proteins*. 41:257-269.

Harz, H., K. Burgdorf, and J.V. Höltje. 1990. Isolation and separation of the glycan strands from murein of *Escherichia coli* by reversed-phase high-performance liquid chromatography. *Anal Biochem*. 190:120-128.

Hayashi, K. 1975. A rapid determination of sodium dodecyl sulfate with methylene blue. *Anal Biochem*. 67:503-506.

Hayhurst, E.J., L. Kailas, J.K. Hobbs, and S.J. Foster. 2008. Cell wall peptidoglycan architecture in *Bacillus subtilis*. *Proc Natl Acad Sci U S A*. 105:14603-14608.

Healy, V.L., I.A. Lessard, D.I. Roper, J.R. Knox, and C.T. Walsh. 2000. Vancomycin resistance in enterococci: reprogramming of the D-ala-D-Ala ligases in bacterial peptidoglycan biosynthesis. *Chem Biol*. 7:109-119.

Hedstrom, L. 2002. Serine protease mechanism and specificity. *Chem Rev*. 102:4501-4524.

Heidrich, C., M.F. Templin, A. Ursinus, M. Merdanovic, J. Berger, H. Schwarz, M.A. de Pedro, and J.V. Höltje. 2001. Involvement of *N*-acetylmuramyl-L-alanine amidases in cell separation and antibiotic-induced autolysis of *Escherichia coli*. *Mol Microbiol*. 41:167-178.

Heidrich, C., A. Ursinus, J. Berger, H. Schwarz, and J.V. Höltje. 2002. Effects of multiple deletions of murein hydrolases on viability, septum cleavage, and sensitivity to large toxic molecules in *Escherichia coli*. *J Bacteriol*. 184:6093-6099.

Henrissat, B., and G. Davies. 1997. Structural and sequence-based classification of glycoside hydrolases. *Curr Opin Struct Biol*. 7:637-644.

Herbold, D.R., and L. Glaser. 1975. *Bacillus subtilis N*-acetylmuramic acid L-alanine amidase. *J Biol Chem*. 250:1676-1682.

Herve, M., A. Boniface, S. Gobec, D. Blanot, and D. Mengin-Lecreulx. 2007. Biochemical characterization and physiological properties of *Escherichia coli* UDP-*N*-acetylmuramate:L-alanyl-γ-D-glutamyl-*meso*-diaminopimelate ligase. *J Bacteriol*. 189:3987-3995.

Höltje, J.V. 1996a. A hypothetical holoenzyme involved in the replication of the murein sacculus of *Escherichia coli*. *Microbiology*. 142:1911-1918.

Höltje, J.V. 1996b. Molecular interplay of murein synthases and murein hydrolases in *Escherichia coli*. *Microb Drug Resist*. 2:99-103.

Höltje, J.V. 1998. Growth of the stress-bearing and shape-maintaining murein sacculus of *Escherichia coli*. *Microbiol Mol Biol Rev*. 62:181-203.

Höltje, J.V., and C. Heidrich. 2001. Enzymology of elongation and constriction of the murein sacculus of *Escherichia coli*. *Biochimie*. 83:103-108.

Höltje, J.V., U. Kopp, A. Ursinus, and B. Wiedemann. 1994. The negative regulator of β-lactamase induction AmpD is a *N*-acetyl-anhydromuramyl-L-alanine amidase. *FEMS Microbiol Lett*. 122:159-164.

Höltje, J.V., D. Mirelman, N. Sharon, and U. Schwarz. 1975. Novel type of murein transglycosylase in *Escherichia coli*. *J Bacteriol*. 124:1067-1076.

Horsburgh, G.J., A. Atrih, M.P. Williamson, and S.J. Foster. 2003. LytG of *Bacillus subtilis* is a novel peptidoglycan hydrolase: the major active glucosaminidase. *Biochemistry*. 42:257-264.

Horsch, M., C. Mayer, U. Sennhauser, and D.M. Rast. 1997. β-*N*-acetylhexosaminidase: a target for the design of antifungal agents. *Pharmacol Ther*. 76:187-218.

Hove-Jensen, B. 1992. Identification of *tms-26* as an allele of the *gcaD* gene, which encodes *N*-acetylglucosamine 1-phosphate uridyltransferase in *Bacillus subtilis*. *J Bacteriol*. 174:6852-6856.

Hrmova, M., R. De Gori, B.J. Smith, J.K. Fairweather, H. Driguez, J.N. Varghese, and G.B. Fincher. 2002. Structural basis for broad substrate specificity in higher plant β-D-glucan glucohydrolases. *Plant Cell*. 14:1033-1052.

Hrmova, M., R. De Gori, B.J. Smith, A. Vasella, J.N. Varghese, and G.B. Fincher. 2004. Three-dimensional structure of the barley β-D-glucan glucohydrolase in complex with a transition state mimic. *J Biol Chem*. 279:4970-4980.

Hrmova, M., V.A. Streltsov, B.J. Smith, A. Vasella, J.N. Varghese, and G.B. Fincher. 2005. Structural rationale for low-nanomolar binding of transition state mimics to a family GH3 β-D-glucan glucohydrolase from barley. *Biochemistry*. 44:16529-16539.

Hrmova, M., J.N. Varghese, R. De Gori, B.J. Smith, H. Driguez, and G.B. Fincher. 2001. Catalytic mechanisms and reaction intermediates along the hydrolytic pathway of a plant β-D-glucan glucohydrolase. *Structure*. 9:1005-1016.

Ishikawa, S., Y. Hara, R. Ohnishi, and J. Sekiguchi. 1998a. Regulation of a new cell wall hydrolase gene, *cwlF*, which affects cell separation in *Bacillus subtilis*. *J Bacteriol*. 180:2549-2555.

Ishikawa, S., K. Yamane, and J. Sekiguchi. 1998b. Regulation and characterization of a newly deduced cell wall hydrolase gene (*cwlJ*) which affects germination of *Bacillus subtilis* spores. *J Bacteriol*. 180:1375-1380.

Itaya, M., and T. Tanaka. 1997. Experimental surgery to create subgenomes of *Bacillus subtilis* 168. *Proc Natl Acad Sci U S A*. 94:5378-5382.

Jackson, P. 1990. The use of polyacrylamide-gel electrophoresis for the high-resolution separation of reducing saccharides labelled with the fluorophore 8-aminonaphthalene-1,3,6-trisulphonic acid. Detection of picomolar quantities by an imaging system based on a cooled charge-coupled device. *Biochem J*. 270:705-713.

Jackson, P. 1994. The analysis of fluorophore-labeled glycans by high-resolution polyacrylamide gel electrophoresis. *Anal Biochem*. 216:243-252.

Jacobs, C., L.J. Huang, E. Bartowsky, S. Normark, and J.T. Park. 1994. Bacterial cell wall recycling provides cytosolic muropeptides as effectors for β-lactamase induction. *EMBO J.* 13:4684-4694.

Jacobs, C., B. Joris, M. Jamin, K. Klarsov, J. Van Beeumen, D. Mengin-Lecreulx, J. van Heijenoort, J.T. Park, S. Normark, and J.M. Frere. 1995. AmpD, essential for both β-lactamase regulation and cell wall recycling, is a novel cytosolic *N*-acetylmuramyl-L-alanine amidase. *Mol Microbiol.* 15:553-559.

Jaeger, T., M. Arsic, and C. Mayer. 2005. Scission of the lactyl ether bond of *N*-acetylmuramic acid by *Escherichia coli* "etherase". *J Biol Chem.* 280:30100-30106.

Jaeger, T., and C. Mayer. 2008a. *N*-acetylmuramic acid 6-phosphate lyases (MurNAc etherases): role in cell wall metabolism, distribution, structure, and mechanism. *Cell Mol Life Sci.* 65:928-939.

Jaeger, T., and C. Mayer. 2008b. The transcriptional factors MurR and catabolite activator protein regulate *N*-acetylmuramic acid catabolism in *Escherichia coli*. *J Bacteriol.* 190:6598-6608.

Jenkins, J., L. Lo Leggio, G. Harris, and R. Pickersgill. 1995. B-glucosidase, β-galactosidase, family A cellulases, family F xylanases and two barley glycanases form a superfamily of enzymes with 8-fold β/α architecture and with two conserved glutamates near the carboxy-terminal ends of β-strands four and seven. *FEBS Lett.* 362:281-285.

Jolly, L., P. Ferrari, D. Blanot, J. Van Heijenoort, F. Fassy, and D. Mengin-Lecreulx. 1999. Reaction mechanism of phosphoglucosamine mutase from *Escherichia coli*. *Eur J Biochem.* 262:202-210.

Jones, L.J., R. Carballido-Lopez, and J. Errington. 2001. Control of cell shape in bacteria: helical, actin-like filaments in *Bacillus subtilis*. *Cell.* 104:913-922.

Kabsch, W. 1993. Automatic processing of rotation diffraction data from crystals of initially unknown symmetry and cell constants. *J of Applied Crystallography.* 26:795-800.

Kern, T., S. Hediger, P. Muller, C. Giustini, B. Joris, C. Bougault, W. Vollmer, and J.P. Simorre. 2008. Toward the characterization of peptidoglycan structure and protein-peptidoglycan interactions by solid-state NMR spectroscopy. *J Am Chem Soc.* 130:5618-5619.

Kobayashi, K., S.D. Ehrlich, A. Albertini, G. Amati, K.K. Andersen, M. Arnaud, K. Asai, S. Ashikaga, S. Aymerich, P. Bessieres, F. Boland, S.C. Brignell, S. Bron, K. Bunai, J. Chapuis, L.C. Christiansen, A. Danchin, M. Debarbouille, E. Dervyn, E. Deuerling, K. Devine, S.K. Devine, O. Dreesen, J. Errington, S. Fillinger, S.J. Foster, Y. Fujita, A. Galizzi, R. Gardan, C. Eschevins, T. Fukushima, K. Haga, C.R. Harwood, M. Hecker, D. Hosoya, M.F. Hullo, H. Kakeshita, D. Karamata, Y. Kasahara, F. Kawamura, K. Koga, P. Koski, R. Kuwana, D. Imamura, M. Ishimaru, S. Ishikawa, I. Ishio, D. Le Coq, A. Masson, C. Mauel, R. Meima, R.P. Mellado, A. Moir, S. Moriya, E. Nagakawa, H. Nanamiya, S. Nakai, P. Nygaard, M. Ogura, T. Ohanan, M. O'Reilly, M. O'Rourke, Z. Pragai, H.M. Pooley, G. Rapoport, J.P. Rawlins, L.A. Rivas, C.

Rivolta, A. Sadaie, Y. Sadaie, M. Sarvas, T. Sato, H.H. Saxild, E. Scanlan, W. Schumann, J.F. Seegers, J. Sekiguchi, A. Sekowska, S.J. Seror, M. Simon, P. Stragier, R. Studer, H. Takamatsu, T. Tanaka, M. Takeuchi, H.B. Thomaides, V. Vagner, J.M. van Dijl, K. Watabe, A. Wipat, H. Yamamoto, M. Yamamoto, Y. Yamamoto, K. Yamane, K. Yata, K. Yoshida, H. Yoshikawa, U. Zuber, and N. Ogasawara. 2003. Essential *Bacillus subtilis* genes. *Proc Natl Acad Sci U S A*. 100:4678-4683.

Koch, A.L. 1985. How bacteria grow and divide in spite of internal hydrostatic pressure. *Can J Microbiol*. 31:1071-1084.

Koch, A.L. 1988. Biophysics of bacterial walls viewed as stress-bearing fabric. *Microbiol Rev*. 52:337-353.

Koch, A.L. 1998. Orientation of the peptidoglycan chains in the sacculus of *Escherichia coli*. *Res Microbiol*. 149:689-701.

Koch, A.L. 2006. The exocytoskeleton. *J Mol Microbiol Biotechnol*. 11:115-125.

Koch, A.L., and R.J. Doyle. 1985. Inside-to-outside growth and turnover of the wall of Gram-positive rods. *J Theor Biol*. 117:137-157.

Koch, A.L., M.L. Higgins, and R.J. Doyle. 1981. Surface tension-like forces determine bacterial shapes: *Streptococcus faecium*. *J Gen Microbiol*. 123:151-161.

Koch, A.L., M.L. Higgins, and R.J. Doyle. 1982. The role of surface stress in the morphology of microbes. *J Gen Microbiol*. 128:927-945.

Koch, A.L., and S. Woeste. 1992. Elasticity of the sacculus of *Escherichia coli*. *J Bacteriol*. 174:4811-4819.

Koraimann, G. 2003. Lytic transglycosylases in macromolecular transport systems of Gram-negative bacteria. *Cell Mol Life Sci*. 60:2371-2388.

Kunst, F., N. Ogasawara, I. Moszer, A.M. Albertini, G. Alloni, V. Azevedo, M.G. Bertero, P. Bessieres, A. Bolotin, S. Borchert, R. Borriss, L. Boursier, A. Brans, M. Braun, S.C. Brignell, S. Bron, S. Brouillet, C.V. Bruschi, B. Caldwell, V. Capuano, N.M. Carter, S.K. Choi, J.J. Codani, I.F. Connerton, A. Danchin, and et al. 1997. The complete genome sequence of the Gram-positive bacterium *Bacillus subtilis*. *Nature*. 390:249-256.

Kuroda, A., Y. Asami, and J. Sekiguchi. 1993. Molecular cloning of a sporulation-specific cell wall hydrolase gene of *Bacillus subtilis*. *J Bacteriol*. 175:6260-6268.

Kuroda, A., and J. Sekiguchi. 1990. Cloning, sequencing and genetic mapping of a *Bacillus subtilis* cell wall hydrolase gene. *J Gen Microbiol*. 136:2209-2216.

Kuroda, A., and J. Sekiguchi. 1991. Molecular cloning and sequencing of a major *Bacillus subtilis* autolysin gene. *J Bacteriol*. 173:7304-7312.

Labischinski, H., G. Barnickel, H. Bradaczek, and P. Giesbrecht. 1979. On the secondary and tertiary structure of murein. Low and medium-angle X-ray evidence against chitin-based conformations of bacterial peptidoglycan. *Eur J Biochem*. 95:147-155.

Labischinski, H., G. Barnickel, D. Naumann, and P. Keller. 1985. Conformational and topological aspects of the three-dimensional architecture of bacterial peptidoglycan. *Ann Inst Pasteur Microbiol*. 136:45-50.

Labischinski, H., E.W. Goodell, A. Goodell, and M.L. Hochberg. 1991. Direct proof of a "more-than-single-layered" peptidoglycan architecture of *Escherichia coli* W7: a neutron small-angle scattering study. *J Bacteriol*. 173:751-756.

Lazarevic, V., P. Margot, B. Soldo, and D. Karamata. 1992. Sequencing and analysis of the *Bacillus subtilis lytRABC* divergon: a regulatory unit encompassing the structural genes of the *N*-acetylmuramoyl-L-alanine amidase and its modifier. *J Gen Microbiol*. 138:1949-1961.

Lengeler, J.W., K. Jahreis, and U.F. Wehmeier. 1994. Enzymes II of the phosphoenol pyruvate-dependent phosphotransferase systems: their structure and function in carbohydrate transport. *Biochim Biophys Acta*. 1188:1-28.

Leps, B., H. Labischinski, and H. Bradaczek. 1987. Conformational behavior of the polysaccharide backbone of murein. *Biopolymers*. 26:1391-1406.

Leutgeb, W., and W. Weidel. 1963. [on a Glycogen Trapped in *E. coli* Cell Wall Preparations.]. *Z Naturforsch B*. 18:1060-1062.

Li, H., G. Zhao, H. Miyake, H. Umekawa, T. Kimura, K. Ohmiya, and K. Sakka. 2006. Identification of a catalytic residue of *Clostridium paraputrificum N*-acetyl-β-D-glucosaminidase Nag3A by site-directed mutagenesis. *Biosci Biotechnol Biochem*. 70:1127-1133.

Li, S.Y., J.V. Höltje, and K.D. Young. 2004. Comparison of high-performance liquid chromatography and fluorophore-assisted carbohydrate electrophoresis methods for analyzing peptidoglycan composition of *Escherichia coli*. *Anal Biochem*. 326:1-12.

Li, Y.K., J. Chir, S. Tanaka, and F.Y. Chen. 2002. Identification of the general acid/base catalyst of a family 3 β-glucosidase from *Flavobacterium meningosepticum*. *Biochemistry*. 41:2751-2759.

Litzinger, S., and C. Mayer. 2009. The murein sacculus. *In: König H., Claus H., Varma A. (eds) Prokaryotic cell wall compounds-Structure and biochemistry. Springer, Heidelberg, Berlin, New York, submitted.*

Lommatzsch, J., M.F. Templin, A.R. Kraft, W. Vollmer, and J.V. Höltje. 1997. Outer membrane localization of murein hydrolases: MltA, a third lipoprotein lytic transglycosylase in *Escherichia coli*. *J Bacteriol*. 179:5465-5470.

Londono-Vallejo, J.A., C. Frehel, and P. Stragier. 1997. *spoIIQ*, a forespore-expressed gene required for engulfment in *Bacillus subtilis*. *Mol Microbiol*. 24:29-39.

Longchamp, P.F., C. Mauel, and D. Karamata. 1994. Lytic enzymes associated with defective prophages of *Bacillus subtilis*: sequencing and characterization of the region comprising the *N*-acetylmuramoyl-L-alanine amidase gene of prophage PBSX. *Microbiology*. 140:1855-1867.

Lovell, S.C., I.W. Davis, W.B. Arendall, 3rd, P.I. de Bakker, J.M. Word, M.G. Prisant, J.S. Richardson, and D.C. Richardson. 2003. Structure validation by Calpha geometry: phi,psi and Cbeta deviation. *Proteins*. 50:437-450.

Lovering, A.L., L.H. de Castro, D. Lim, and N.C. Strynadka. 2007. Structural insight into the transglycosylation step of bacterial cell-wall biosynthesis. *Science*. 315:1402-1405.

Ludwig, R. 2001. Water: From Clusters to the Bulk. *Angew Chem Int Ed Engl*. 40:1808-1827.

Margot, P., and D. Karamata. 1992. Identification of the structural genes for *N*-acetylmuramoyl-L-alanine amidase and its modifier in *Bacillus subtilis* 168: inactivation of these genes by insertional mutagenesis has no effect on growth or cell separation. *Mol Gen Genet*. 232:359-366.

Margot, P., C. Mauel, and D. Karamata. 1994. The gene of the *N*-acetylglucosaminidase, a *Bacillus subtilis* 168 cell wall hydrolase not involved in vegetative cell autolysis. *Mol Microbiol*. 12:535-545.

Margot, P., M. Pagni, and D. Karamata. 1999. Bacillus subtilis 168 gene *lytF* encodes a γ-D-glutamate-*meso*-diaminopimelate muropeptidase expressed by the alternative vegetative sigma factor, σ^D. *Microbiology*. 145:57-65.

Margot, P., M. Wahlen, A. Gholamhoseinian, P. Piggot, and D. Karamata. 1998. The *lytE* gene of *Bacillus subtilis* 168 encodes a cell wall hydrolase. *J Bacteriol*. 180:749-752.

Mark, B.L., D.J. Vocadlo, S. Knapp, B.L. Triggs-Raine, S.G. Withers, and M.N. James. 2001. Crystallographic evidence for substrate-assisted catalysis in a bacterial β-hexosaminidase. *J Biol Chem*. 276:10330-10337.

Markley, J.L., and W.M. Westler. 1996. Protonation-state dependence of hydrogen bond strengths and exchange rates in a serine protease catalytic triad: bovine chymotrypsinogen A. *Biochemistry*. 35:11092-11097.

Markovic-Housley, Z., G. Miglierini, L. Soldatova, P.J. Rizkallah, U. Muller, and T. Schirmer. 2000. Crystal structure of hyaluronidase, a major allergen of bee venom. *Structure*. 8:1025-1035.

Massova, I., and S. Mobashery. 1998. Kinship and diversification of bacterial penicillin-binding proteins and β-lactamases. *Antimicrob Agents Chemother*. 42:1-17.

Mauck, J., L. Chan, and L. Glaser. 1971. Turnover of the cell wall of Gram-positive bacteria. *J Biol Chem*. 246:1820-1827.

Mauck, J., and L. Glaser. 1970. Turnover of the cell wall of *Bacillus subtilis* W-23 during logarithmic growth. *Biochem Biophys Res Commun*. 39:699-706.

Mayer, C., D.J. Vocadlo, M. Mah, K. Rupitz, D. Stoll, R.A. Warren, and S.G. Withers. 2006. Characterization of a β-*N*-acetylhexosaminidase and a β-*N*-acetylglucosaminidase/β-glucosidase from *Cellulomonas fimi*. *FEBS J.* 273:2929-2941.

Mayer, C., D.J. Vocadlo, and S.G. Withers. 2000a. β-*N*-acetylglucosaminidases: two enzyme families, two mechanisms. *Advan. Chitin Sci. (Peter, M.G., Domard, A. and Muzzarelli, R.A.A., eds.* 4:612-619.

Mayer, C., D.L. Zechel, S.P. Reid, R.A. Warren, and S.G. Withers. 2000b. The E358S mutant of *Agrobacterium sp.* β-glucosidase is a greatly improved glycosynthase. *FEBS Lett.* 466:40-44.

Mengin-Lecreulx, D., and J. van Heijenoort. 1993. Identification of the *glmU* gene encoding *N*-acetylglucosamine-1-phosphate uridyltransferase in *Escherichia coli*. *J Bacteriol.* 175:6150-6157.

Mengin-Lecreulx, D., and J. van Heijenoort. 1994. Copurification of glucosamine-1-phosphate acetyltransferase and *N*-acetylglucosamine-1-phosphate uridyltransferase activities of *Escherichia coli*: characterization of the *glmU* gene product as a bifunctional enzyme catalyzing two subsequent steps in the pathway for UDP-*N*-acetylglucosamine synthesis. *J Bacteriol.* 176:5788-5795.

Mengin-Lecreulx, D., and J. van Heijenoort. 1996. Characterization of the essential gene *glmM* encoding phosphoglucosamine mutase in *Escherichia coli*. *J Biol Chem.* 271:32-39.

Mengin-Lecreulx, D., J. van Heijenoort, and J.T. Park. 1996. Identification of the *mpl* gene encoding UDP-*N*-acetylmuramate: L-alanyl-γ-D-glutamyl-*meso*-diaminopimelate ligase in *Escherichia coli* and its role in recycling of cell wall peptidoglycan. *J Bacteriol.* 178:5347-5352.

Meroueh, S.O., K.Z. Bencze, D. Hesek, M. Lee, J.F. Fisher, T.L. Stemmler, and S. Mobashery. 2006. Three-dimensional structure of the bacterial cell wall peptidoglycan. *Proc Natl Acad Sci U S A.* 103:4404-4409.

Mignon, P., J. Steyaert, R. Loris, P. Geerlings, and S. Loverix. 2002. A nucleophile activation dyad in ribonucleases. A combined X-ray crystallographic/ab initio quantum chemical study. *J Biol Chem.* 277:36770-36774.

Moriyama, R., A. Hattori, S. Miyata, S. Kudoh, and S. Makino. 1996. A gene (s*leB*) encoding a spore cortex-lytic enzyme from *Bacillus subtilis* and response of the enzyme to L-alanine-mediated germination. *J Bacteriol.* 178:6059-6063.

Morris, R.J., A. Perrakis, and V.S. Lamzin. 2002. ARP/wARP's model-building algorithms. I. The main chain. *Acta Crystallogr D Biol Crystallogr.* 58:968-975.

Murshudov, G.N., A.A. Vagin, and E.J. Dodson. 1997. Refinement of macromolecular structures by the maximum-likelihood method. *Acta Crystallogr D Biol Crystallogr.* 53:240-255.

N, C.C.P. 1994. The CCP suite: programs for protein crystallography. *Acta Crystallogr D Biol Crystallogr*. D50:760-763.

Navarre, W.W., and O. Schneewind. 1999. Surface proteins of Gram-positive bacteria and mechanisms of their targeting to the cell wall envelope. *Microbiol Mol Biol Rev*. 63:174-229.

Nugroho, F.A., H. Yamamoto, Y. Kobayashi, and J. Sekiguchi. 1999. Characterization of a new sigma-K-dependent peptidoglycan hydrolase gene that plays a role in *Bacillus subtilis* mother cell lysis. *J Bacteriol*. 181:6230-6237.

Ohnishi, R., S. Ishikawa, and J. Sekiguchi. 1999. Peptidoglycan hydrolase LytF plays a role in cell separation with CwlF during vegetative growth of *Bacillus subtilis*. *J Bacteriol*. 181:3178-3184.

Ortiz, J.M., J.B. Gillespie, and R.C. Berkeley. 1972. An exo-β-*N*-acetylglucosaminidase from *Bacillus subtilis* B; extraction and purification. *Biochim Biophys Acta*. 289:174-186.

Paal, K., M. Ito, and S.G. Withers. 2004. *Paenibacillus sp.* TS12 glucosylceramidase: kinetic studies of a novel sub-family of family 3 glycosidases and identification of the catalytic residues. *Biochem J*. 378:141-149.

Park, J.T. 1993. Turnover and recycling of the murein sacculus in oligopeptide permease-negative strains of *Escherichia coli*: indirect evidence for an alternative permease system and for a monolayered sacculus. *J Bacteriol*. 175:7-11.

Park, J.T. 2001. Identification of a dedicated recycling pathway for anhydro-*N*-acetylmuramic acid and *N*-acetylglucosamine derived from *Escherichia coli* cell wall murein. *J Bacteriol*. 183:3842-3847.

Park, J.T., D. Raychaudhuri, H. Li, S. Normark, and D. Mengin-Lecreulx. 1998. MppA, a periplasmic binding protein essential for import of the bacterial cell wall peptide L-alanyl-γ-D-glutamyl-*meso*-diaminopimelate. *J Bacteriol*. 180:1215-1223.

Park, J.T., and T. Uehara. 2008. How bacteria consume their own exoskeletons (turnover and recycling of cell wall peptidoglycan). *Microbiol Mol Biol Rev*. 72:211-227.

Park, W., and M. Matsuhashi. 1984. *Staphylococcus aureus* and *Micrococcus luteus* peptidoglycan transglycosylases that are not penicillin-binding proteins. *J Bacteriol*. 157:538-544.

Phillips, D.C. 1967. The hen egg white lysozyme molecule. *Proceedings of the National Academy od Sciences of the United States of America*. 57:416-436.

Plumbridge, J. 2009. An alternative route for recycling of *N*-acetylglucosamine from peptidoglycan involves the *N*-acetylglucosamine phosphotransferase system in *Escherichia coli*. *J Bacteriol*. 191:5641-5647.

Plumbridge, J.A. 1989. Sequence of the *nagBACD* operon in *Escherichia coli* K12 and pattern of transcription within the nag regulon. *Mol Microbiol*. 3:505-515.

Pooley, H.M. 1976. Turnover and spreading of old wall during surface growth of *Bacillus subtilis*. *J Bacteriol*. 125:1127-1138.

Popham, D.L., J. Helin, C.E. Costello, and P. Setlow. 1996. Muramic lactam in peptidoglycan of *Bacillus subtilis* spores is required for spore outgrowth but not for spore dehydration or heat resistance. *Proc Natl Acad Sci U S A*. 93:15405-15410.

Priyadarshini, R., D.L. Popham, and K.D. Young. 2006. Daughter cell separation by penicillin-binding proteins and peptidoglycan amidases in *Escherichia coli*. *J Bacteriol*. 188:5345-5355.

Quintela, J.C., M. Caparros, and M.A. de Pedro. 1995. Variability of peptidoglycan structural parameters in Gram-negative bacteria. *FEMS Microbiol Lett*. 125:95-100.

Quirk, D.J., C. Park, J.E. Thompson, and R.T. Raines. 1998. His...Asp catalytic dyad of ribonuclease A: conformational stability of the wild-type, D121N, D121A, and H119A enzymes. *Biochemistry*. 37:17958-17964.

Quirk, D.J., and R.T. Raines. 1999. His ... Asp catalytic dyad of ribonuclease A: histidine pKa values in the wild-type, D121N, and D121A enzymes. *Biophys J*. 76:1571-1579.

Rashid, M.H., M. Mori, and J. Sekiguchi. 1995. Glucosaminidase of *Bacillus subtilis*: cloning, regulation, primary structure and biochemical characterization. *Microbiology*. 141:2391-2404.

Read, R.J. 2001. Pushing the boundaries of molecular replacement with maximum likelihood. *Acta Crystallogr D Biol Crystallogr*. 57:1373-1382.

Regamey, A., and D. Karamata. 1998. The *N*-acetylmuramoyl-L-alanine amidase encoded by the *Bacillus subtilis* 168 prophage SP *β*. *Microbiology*. 144:885-893.

Rogers, H.J., H.M. Pooley, P.F. Thurman, and C. Taylor. 1974. Wall and membrane growth in bacilli and their mutants. *Ann Microbiol (Paris)*. 125:135-147.

Rogers, H.J., C. Taylor, S. Rayter, and J.B. Ward. 1984. Purification and properties of autolytic endo-β-*N*-acetylglucosaminidase and the *N*-acetylmuramyl-L-alanine amidase from *Bacillus subtilis* strain 168. *J Gen Microbiol*. 130:2395-2402.

Romeis, T., and J.V. Höltje. 1994a. Penicillin-binding protein 7/8 of *Escherichia coli* is a DD-endopeptidase. *Eur J Biochem*. 224:597-604.

Romeis, T., and J.V. Höltje. 1994b. Specific interaction of penicillin-binding proteins 3 and 7/8 with soluble lytic transglycosylase in *Escherichia coli*. *J Biol Chem*. 269:21603-21607.

Rothfield, L.I., and S.S. Justice. 1997. Bacterial cell division: the cycle of the ring. *Cell*. 88:581-584.

Ruiz, N. 2008. Bioinformatics identification of MurJ (MviN) as the peptidoglycan lipid II flippase in *Escherichia coli*. *Proc Natl Acad Sci U S A*. 105:15553-15557.

Rye, C.S., and S.G. Withers. 2000. Glycosidase mechanisms. *Curr Opin Chem Biol*. 4:573-580.

Sauvage, E., F. Kerff, M. Terrak, J.A. Ayala, and P. Charlier. 2008. The penicillin-binding proteins: structure and role in peptidoglycan biosynthesis. *FEMS Microbiol Rev*. 32:234-258.

Scheffers, D.J., and J. Errington. 2004. PBP1 is a component of the *Bacillus subtilis* cell division machinery. *J Bacteriol*. 186:5153-5156.

Scheffers, D.J., and M.G. Pinho. 2005. Bacterial cell wall synthesis: new insights from localization studies. *Microbiol Mol Biol Rev*. 69:585-607.

Scheurwater, E., C.W. Reid, and A.J. Clarke. 2008. Lytic transglycosylases: bacterial space-making autolysins. *Int J Biochem Cell Biol*. 40:586-591.

Schleifer, K.H., and O. Kandler. 1972. Peptidoglycan types of bacterial cell walls and their taxonomic implications. *Bacteriol Rev*. 36:407-477.

Schmidt, D.M., B.K. Hubbard, and J.A. Gerlt. 2001. Evolution of enzymatic activities in the enolase superfamily: functional assignment of unknown proteins in *Bacillus subtilis* and *Escherichia coli* as L-Ala-D/L-Glu epimerases. *Biochemistry*. 40:15707-15715.

Schrag, J.D., Y.G. Li, S. Wu, and M. Cygler. 1991. Ser-His-Glu triad forms the catalytic site of the lipase from *Geotrichum candidum*. *Nature*. 351:761-764.

Schroeder, U., B. Henrich, J. Fink, and R. Plapp. 1994. Peptidase D of *Escherichia coli* K-12, a metallopeptidase of low substrate specificity. *FEMS Microbiol Lett*. 123:153-159.

Schultz, L.W., D.J. Quirk, and R.T. Raines. 1998. His...Asp catalytic dyad of ribonuclease A: structure and function of the wild-type, D121N, and D121A enzymes. *Biochemistry*. 37:8886-8898.

Sekiguchi, J., K. Akeo, H. Yamamoto, F.K. Khasanov, J.C. Alonso, and A. Kuroda. 1995. Nucleotide sequence and regulation of a new putative cell wall hydrolase gene, *cwlD*, which affects germination in *Bacillus subtilis*. *J Bacteriol*. 177:5582-5589.

Seltmann, G., and O. Holst. 2002. Periplasmic Space and Rigid Layer. *In: Seltmann G, Holst O (eds) The Bacterial Cell Wall. Springer-Verlag, Berlin*:103-132.

Shockman, G.D., and J.F. Barrett. 1983. Structure, function, and assembly of cell walls of Gram-positive bacteria. *Annu Rev Microbiol*. 37:501-527.

Smith, T.J., S.A. Blackman, and S.J. Foster. 2000. Autolysins of *Bacillus subtilis*: multiple enzymes with multiple functions. *Microbiology*. 146:249-262.

Smith, T.J., and S.J. Foster. 1995. Characterization of the involvement of two compensatory autolysins in mother cell lysis during sporulation of *Bacillus subtilis* 168. *J Bacteriol*. 177:3855-3862.

Spratt, B.G. 1975. Distinct penicillin binding proteins involved in the division, elongation, and shape of *Escherichia coli* K12. *Proc Natl Acad Sci U S A*. 72:2999-3003.

Spratt, B.G., and V. Jobanputra. 1977. Mutants of *Escherichia coli* which lack a component of penicillin-binding protein 1 are viable. *FEBS Lett*. 79:374-378.

Stack, R.J., and M.T. Sullivan. 1992. Electrophoretic resolution and fluorescence detection of N-linked glycoprotein oligosaccharides after reductive amination with 8-aminonaphthalene-1,3,6-trisulphonic acid. *Glycobiology*. 2:85-92.

Storoni, L.C., A.J. McCoy, and R.J. Read. 2004. Likelihood-enhanced fast rotation functions. *Acta Crystallogr D Biol Crystallogr*. 60:432-438.

Stubbs, K.A., M. Balcewich, B.L. Mark, and D.J. Vocadlo. 2007. Small molecule inhibitors of a glycoside hydrolase attenuate inducible AmpC-mediated β-lactam resistance. *J Biol Chem*. 282:21382-21391.

Studier, F.W., and B.A. Moffatt. 1986. Use of bacteriophage T7 RNA polymerase to direct selective high-level expression of cloned genes. *J Mol Biol*. 189:113-130.

Suzuki, H., Y. Nishimura, and Y. Hirota. 1978. On the process of cellular division in *Escherichia coli*: a series of mutants of *E. coli* altered in the penicillin-binding proteins. *Proc Natl Acad Sci U S A*. 75:664-668.

Templin, M.F., A. Ursinus, and J.V. Höltje. 1999. A defect in cell wall recycling triggers autolysis during the stationary growth phase of *Escherichia coli*. *EMBO J*. 18:4108-4117.

Terrak, M., T.K. Ghosh, J. van Heijenoort, J. Van Beeumen, M. Lampilas, J. Aszodi, J.A. Ayala, J.M. Ghuysen, and M. Nguyen-Disteche. 1999. The catalytic, glycosyl transferase and acyl transferase modules of the cell wall peptidoglycan-polymerizing penicillin-binding protein 1b of *Escherichia coli*. *Mol Microbiol*. 34:350-364.

Terwilliger, T.C. 2000. Maximum-likelihood density modification. *Acta Crystallogr D Biol Crystallogr*. 56:965-972.

Terwilliger, T.C. 2002. Automated structure solution, density modification and model building. *Acta Crystallogr D Biol Crystallogr*. 58:1937-1940.

Tews, I., A. Perrakis, A. Oppenheim, Z. Dauter, K.S. Wilson, and C.E. Vorgias. 1996. Bacterial chitobiase structure provides insight into catalytic mechanism and the basis of Tay-Sachs disease. *Nat Struct Biol*. 3:638-648.

Uehara, T., and J.T. Park. 2003. Identification of MpaA, an amidase in *Escherichia* coli that hydrolyzes the γ-D-glutamyl-*meso*-diaminopimelate bond in murein peptides. *J Bacteriol*. 185:679-682.

Uehara, T., and J.T. Park. 2004. The *N*-acetyl-D-glucosamine kinase of *Escherichia coli* and its role in murein recycling. *J Bacteriol*. 186:7273-7279.

Uehara, T., and J.T. Park. 2007. An anhydro-*N*-acetylmuramyl-L-alanine amidase with broad specificity tethered to the outer membrane of *Escherichia coli*. *J Bacteriol*. 189:5634-5641.

Uehara, T., K. Suefuji, T. Jaeger, C. Mayer, and J.T. Park. 2006. MurQ Etherase is required by *Escherichia coli* in order to metabolize anhydro-*N*-acetylmuramic acid obtained either from the environment or from its own cell wall. *J Bacteriol*. 188:1660-1662.

Uehara, T., K. Suefuji, N. Valbuena, B. Meehan, M. Donegan, and J.T. Park. 2005. Recycling of the anhydro-*N*-acetylmuramic acid derived from cell wall murein involves a two-step conversion to *N*-acetylglucosamine-phosphate. *J Bacteriol*. 187:3643-3649.

Vagin, A., and A. Teplyakov. 1997. MOLREP: an automated program for molecular replacement. *J of Applied Crystallography*. 30:1022-1025.

Vaguine, A.A., J. Richelle, and S.J. Wodak. 1999. SFCHECK: a unified set of procedures for evaluating the quality of macromolecular structure-factor data and their agreement with the atomic model. *Acta Crystallogr D Biol Crystallogr*. 55:191-205.

van Aalten, D.M., D. Komander, B. Synstad, S. Gaseidnes, M.G. Peter, and V.G. Eijsink. 2001. Structural insights into the catalytic mechanism of a family 18 exo-chitinase. *Proc Natl Acad Sci U S A*. 98:8979-8984.

van Dam, V., R. Sijbrandi, M. Kol, E. Swiezewska, B. de Kruijff, and E. Breukink. 2007. Transmembrane transport of peptidoglycan precursors across model and bacterial membranes. *Mol Microbiol*. 64:1105-1114.

van Heijenoort, J. 1998. Assembly of the monomer unit of bacterial peptidoglycan. *Cell Mol Life Sci*. 54:300-304.

van Heijenoort, J. 2001a. Formation of the glycan chains in the synthesis of bacterial peptidoglycan. *Glycobiology*. 11:25-36.

van Heijenoort, J. 2001b. Recent advances in the formation of the bacterial peptidoglycan monomer unit. *Nat Prod Rep*. 18:503-519.

van Heijenoort, J. 2007. Lipid intermediates in the biosynthesis of bacterial peptidoglycan. *Microbiol Mol Biol Rev*. 71:620-635.

Varghese, J.N., M. Hrmova, and G.B. Fincher. 1999. Three-dimensional structure of a barley β-D-glucan exohydrolase, a family 3 glycosyl hydrolase. *Structure*. 7:179-190.

Vocadlo, D.J., G.J. Davies, R. Laine, and S.G. Withers. 2001. Catalysis by hen egg-white lysozyme proceeds via a covalent intermediate. *Nature*. 412:835-838.

Vocadlo, D.J., C. Mayer, S. He, and S.G. Withers. 2000. Mechanism of action and identification of Asp242 as the catalytic nucleophile of Vibrio furnisii *N*-acetyl-β-D-glucosaminidase using 2-acetamido-2-deoxy-5-fluoro-alpha-L-idopyranosyl fluoride. *Biochemistry*. 39:117-126.

Vocadlo, D.J., and S.G. Withers. 2005. Detailed comparative analysis of the catalytic mechanisms of β-*N*-acetylglucosaminidases from families 3 and 20 of glycoside hydrolases. *Biochemistry*. 44:12809-12818.

Vollmer, W. 2008. Structural variation in the glycan strands of bacterial peptidoglycan. *FEMS Microbiol Rev*. 32:287-306.

Vollmer, W., and U. Bertsche. 2008. Murein (peptidoglycan) structure, architecture and biosynthesis in *Escherichia coli*. *Biochim Biophys Acta*. 1778:1714-1734.

Vollmer, W., D. Blanot, and M.A. de Pedro. 2008. Peptidoglycan structure and architecture. *FEMS Microbiol Rev*. 32:149-167.

Vollmer, W., and J.V. Höltje. 2001. Morphogenesis of *Escherichia coli*. *Curr Opin Microbiol*. 4:625-633.

Vollmer, W., and J.V. Höltje. 2004. The architecture of the murein (peptidoglycan) in Gram-negative bacteria: vertical scaffold or horizontal layer(s)? *J Bacteriol*. 186:5978-5987.

Vollmer, W., M. von Rechenberg, and J.V. Höltje. 1999. Demonstration of molecular interactions between the murein polymerase PBP1B, the lytic transglycosylase MltA, and the scaffolding protein MipA of *Escherichia coli*. *J Biol Chem*. 274:6726-6734.

von Rechenberg, M., A. Ursinus, and J.V. Höltje. 1996. Affinity chromatography as a means to study multienzyme complexes involved in murein synthesis. *Microb Drug Resist*. 2:155-157.

Vötsch, W., and M.F. Templin. 2000. Characterization of a β-*N*-acetylglucosaminidase of *Escherichia coli* and elucidation of its role in muropeptide recycling and β-lactamase induction. *J Biol Chem*. 275:39032-39038.

Ward, J.B. 1973. The chain length of the glycans in bacterial cell walls. *Biochem J*. 133:395-398.

Watts, A.G., I. Damager, M.L. Amaya, A. Buschiazzo, P. Alzari, A.C. Frasch, and S.G. Withers. 2003. *Trypanosoma cruzi* trans-sialidase operates through a covalent sialyl-enzyme intermediate: tyrosine is the catalytic nucleophile. *J Am Chem Soc*. 125:7532-7533.

Watts, A.G., P. Oppezzo, S.G. Withers, P.M. Alzari, and A. Buschiazzo. 2006. Structural and kinetic analysis of two covalent sialosyl-enzyme intermediates on *Trypanosoma rangeli* sialidase. *J Biol Chem*. 281:4149-4155.

Weidel, W., and H. Pelzer. 1964. Bagshaped Macromolecules-a New Outlook on Bacterial Cell Walls. *Adv Enzymol Relat Areas Mol Biol*. 26:193-232.

White, R.J. 1968. Control of amino sugar metabolism in *Escherichia coli* and isolation of mutants unable to degrade amino sugars. *Biochem J*. 106:847-858.

Wolfenden, R. 1976. Transition state analog inhibitors and enzyme catalysis. *Annu Rev Biophys Bioeng*. 5:271-306.

Wright, J., and J.E. Heckels. 1975. The teichuronic acid of cell walls of *Bacillus subtilis* W23 grown in a chemostat under phosphate limitation. *Biochem J*. 147:187-189.

Yem, D.W., and H.C. Wu. 1976a. Isolation of *Escherichia coli* K-12 mutants with altered level of β-*N*-acetylglucosaminidase. *J Bacteriol*. 125:372-373.

Yem, D.W., and H.C. Wu. 1976b. Purification and properties of β-*N*-acetylglucosaminidase from *Escherichia coli*. *J Bacteriol*. 125:324-331.

Yokoyama, K., T. Miyashita, Y. Araki, and E. Ito. 1986. Structure and functions of linkage unit intermediates in the biosynthesis of ribitol teichoic acids in *Staphylococcus aureus* H and *Bacillus subtilis* W23. *Eur J Biochem*. 161:479-489.

Young, K.D. 1996. A simple gel electrophoretic method for analyzing the muropeptide composition of bacterial peptidoglycan. *J Bacteriol*. 178:3962-3966.

Yuan, Y., D. Barrett, Y. Zhang, D. Kahne, P. Sliz, and S. Walker. 2007. Crystal structure of a peptidoglycan glycosyltransferase suggests a model for processive glycan chain synthesis. *Proc Natl Acad Sci U S A*. 104:5348-5353.

Zahrl, D., M. Wagner, K. Bischof, M. Bayer, B. Zavecz, A. Beranek, C. Ruckenstuhl, G.E. Zarfel, and G. Koraimann. 2005. Peptidoglycan degradation by specialized lytic transglycosylases associated with type III and type IV secretion systems. *Microbiology*. 151:3455-3467.

Zechel, D.L., and S.G. Withers. 2000. Glycosidase mechanisms: anatomy of a finely tuned catalyst. *Acc Chem Res*. 33:11-18.

DECLARATION OF AUTHOR CONTRIBUTION

Unless otherwise mentioned all results described in this thesis were obtained by myself.

CHAPTER 1:

Ulrike Dahl constructed the plasmid pET16b-*Bs*NagZ. Katja Nitzsche constructed the plasmid pASK-IBA32-*Bs*AmiE and also performed the protein overexpression and purification of the enzyme. Christian Risinger (University of Konstanz, Bioorganic and Organic Chemistry, Arbeitsgruppe Prof. Dr. Wittmann, Department of Chemistry) carried out the mass spectrometry analysis (MALDI-TOF) of the muropeptides and synthesized the substrate 4-methylumbelliferyl-β-D-acetylglucosamine (4-Mu-β-$GlcNH_2$). Dr. Christoph Mayer measured the kinetic activity of *Bs*NagZ with pNP-β-GlcNAc.

CHAPTER 2:

Crystallization of *Bs*NagZ was performed together with Stefanie Fischer (University of Konstanz, Structural Biology, Arbeitsgruppe Prof. Dr. Welte, Department of Biology). Crystallography was done by Stefanie Fischer and Patrick Polzer (Max-Planck-Institute of Quantum Optics, Garching). The mass spectrometry analysis of the trapped glycosyl-enzyme intermediate was performed by Jocelyne Fiaux (ZMBH, University of Heidelberg).

APPENDIX

Abbreviations

Å	Ångstrom; $1Å = 10^{-10}$m
AcCoA	acetyl-coenzyme-A
anhMurNAc	1,6-anhydro-*N*-acetylmuramic acid
Amp^r	ampicillin resistant
ANTS	8-aminonaphthalene-1,3,6-trisulfonic acid
APS	ammonium persulfate
Da	Dalton; 1 Da = 1 g x mol^{-1}
DMSO	dimethyl sulfoxide
EP	endopeptidase
ESI-MS	electrospray ionisation-time-of-flight mass spectrometry
FACE	fluorophore-assisted carbohydrate electrophoresis
FPLC	fast protein liquid chromatography
GFP	green fluorescent protein
GlcNAc	*N*-acetylglucosamine (2-acetamido-2-deoxy-β-D-glucopyranose)
GlcNAc-6-P	*N*-acetylglucosamine-6-phosphate
GroP	poly-glycerol-phosphate
GT	glycosyl transferase
HMW	high-molecular weight
IPTG	isopropyl-β-D-thiogalactopyranoside
Kan^r	kanamycin resistant
K_M	Michaelis-Menten constant
LB	Luria-Bertani
LMW	low-molecular weight
LT	lytic transglycosylase
m-DAP	*meso*-diaminopimelic acid
MALDI-TOF	matrix-assisted laser desorption/ionisation-time of flight
4-Mu-β-GlcNAc	4-methylumbelliferyl-β-*N*-acetyl-D-glucosaminide
MurNAc	*N*-acetylmuramic acid (2-acetamido-2-deoxy-3-*O*-[(R)-1-carboxyethyl]-D-glucopyranose)

MurNAc-6-P	*N*-acetylmuramic acid-6-phosphate
OD	optical density
PBP	penicillin-binding protein
PEG	polyethylene glycol
PEP	phosphoenolpyruvate
pNP-β-GlcNAc	4-nitrophenyl-*N*-acetyl-β-D-glucosaminide
PUGNAc	*O*-(2-Acetamido-2-deoxy-D-glucopyranosylidene) amino-*N*-phenylcarbamate
RboP	poly-ribitol-phosphate
RP-HPLC	reversed-phase high performance liquid chromatography
SDS-PAGE	sodium dodecylsulfate polyacrylamide gelelectrophoresis
TP	transpeptidase
UDP	undecaprenyl-pyrophosphate

Amino Acids

A	Ala	alanine	M	Met	methionine
B	Asx	Asn *or* Asp	N	Asn	asparagine
C	Cys	cysteine	P	Pro	proline
D	Asp	aspartate	Q	Gln	glutamine
E	Glu	glutamate	R	Arg	arginine
F	Phe	phenylalanine	S	Ser	serine
G	Gly	glycine	T	Thr	threonine
H	His	histidine	V	Val	valine
I	Ile	isoleucine	W	Trp	tryptophan
K	Lys	lysine	Y	Tyr	tyrosine
L	Leu	leucine	Z	Glx	Gln *or* Glu

Conference Posters

1. Litzinger, S. and Mayer, C. (2005): Identification of a gene cluster of *Bacillus subtilis* involved in a novel pathway of Gram-positive cell wall recycling. Annual Conference of the DGHM and VAAM in Göttingen, 25.-28.09.2005
2. Litzinger, S., Traub, S. and Mayer, C. (2006): Analysis of bacterial call wall recycling using an immunological assay for peptidoglycan fragments. Annual Conference of the VAAM in Jena, 19.-22.03.2006
3. Litzinger, S., Diehl, S. and Mayer, C. (2007): Cell wall recycling of *Bacillus subtilis*. Annual Conference of the VAAM in Osnabrück, 01.-04.04.2008
4. Litzinger, S., Diehl, S., Diederichs, K., Welte, W. and Mayer, C. (2008): Peptidoglycan recycling of *Bacillus subtilis*. Annual Conference of the VAAM in Frankfurt, 09.-11.03.2008
5. Litzinger, S., Fischer, S., Diederichs, K., Welte, W. and Mayer, C (2008): Characterization and structural elucidation of a cell wall recycling muramidase of *Bacillus subtilis*. Gordon Research Conference on Bacterial Cell Surfaces at Colby-Sawyer College in New London, NH United States, 06/22/2008-06/27/2008.
6. Litzinger, S., Fischer, S., Diederichs, K., Welte, W. and Mayer, C. (2009): An Asp-His catalytic dyad is the general acid/base catalyst of bacterial cell wall recycling β-*N*-acetylglucosaminidases. Annual Conference of the VAAM in Bochum, 08.-11.03.2009

ACKNOWLEDGEMENTS

This PhD thesis was carried out in the laboratory of PD Dr. Christoph Mayer.

A very special thank you to my supervisor PD Dr. Christoph Mayer for:

- always having time for me and my requests
- never-ending discussions, good ideas and the very good team work in an unforgettable atmosphere
- sharing “Westerwälder Kümmel” etc. to help through bad times and to digest the “however”

Many thanks go to Prof. Dr. Winfried Boos for providing the expertise and having time for discussions. His opinion was always very important to me.

I thank Prof. Dr. Iwona Adamska for providing the second expertise and being always ready to party.

Thank you to Stefanie Fischer and Christian Risinger for good cooperation.

I thank Prof. Dr. David Vocadlo from the Simon-Fraser University, Burnaby, Canada, for providing PUGNAc inhibitor and Jocelyne Fiaux for measuring ESI-MS.

I also thank the *Landesgraduiertenförderung Baden-Württemberg* and the *Frauenförderung der Universität Konstanz* for giving me a scholarship.

Especial thanks also go to:

- Dr. Jutta Nesper for the many valuable suggestions, many discussions and trips in the building supplies stores
- my previous and present colleagues at the Mayer lab for the nice atmosphere and hot discussions: Tina Jaeger, Jan Schleider, Ines Schütze, Alexander Schneider, Katja Nitzsche, Michael Joos, Amanda Duckworth and also our lab guest Myriam Weckenmann
- my colleagues at the Deuerling lab for the concerted literature and research seminars
- my friends, *Lustige Biologen* and *Villa Gabelsberg*, especially Birte, Eva, Kathrin, Nina, Sonja Ratte and Sonja Schaf for many funny events during our happy years of study and work
- Chrissi for her friendship and especially for her accompaniment to the flea market
- Uli for her affectionate care in good and bad times and having fun together especially at *Weinfest*, *Fasnet*, Christmas market and drinking Caipis in the *Klimperkasten*
- my best friends since childhood, *Little Hill* and *Resi*, for "holding the line" in good and bad times
- the Warken family, Christian and Michael, my *Gothi* Wiltrud, my *Pat* Walter and Uta and the *Jules-Club* members for always encouraging me during my time at home

Most of all I thank my parents and my brother Sven for their endless love, security, energy and good nerves during all my life and for the surety, that they are present for me all the time. You have ever believed in me!